The influence of the wave height distribution on the stability of single layer concrete armour units

Master of Science Thesis

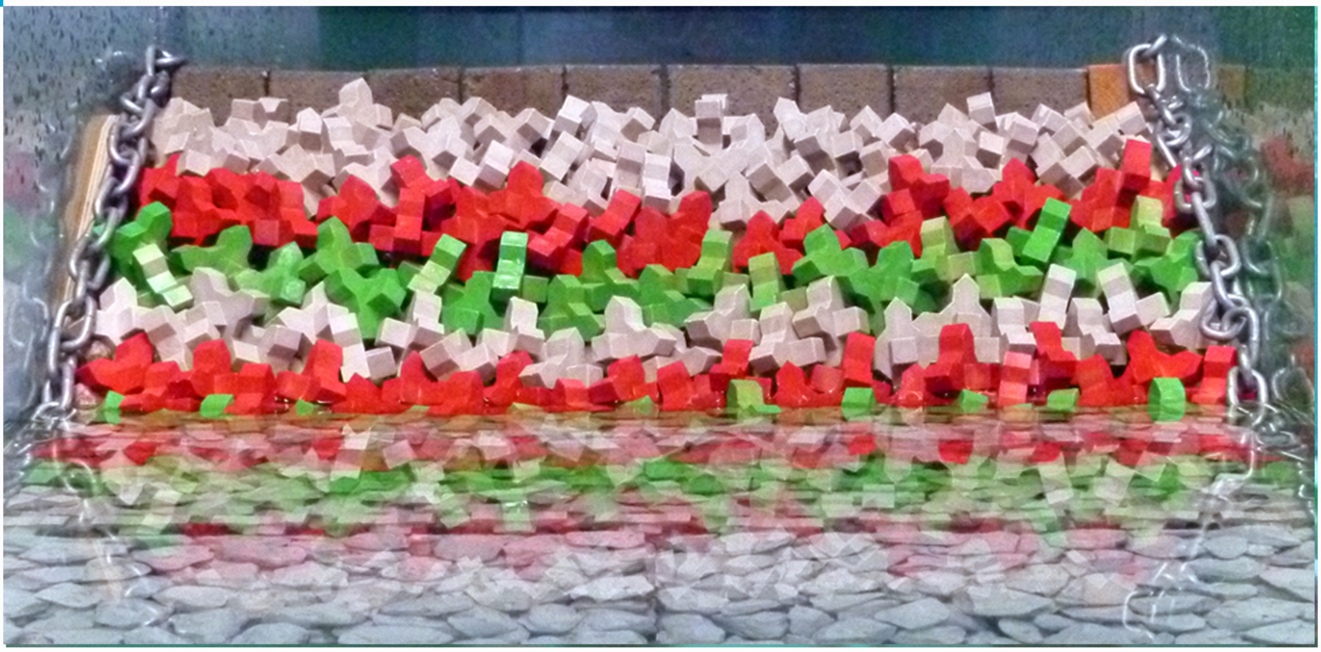

Author:
S.A.A. Zwanenburg

Supervisors:
Prof.dr.ir. W.S.J. Uijttewaal
Dr.ir. G.Ph. van Vledder
Ir. H.J. Verhagen
Ir. E. ten Oever

Delft University of Technology
Faculty of Civil Engineering and Geosciences
Department of Hydraulic Engineering

Delta Marine Consultants
Department Coastal Engineering

The influence of the wave height distribution on the stability of single layer concrete armour units

Preface

This is the final report of my masters thesis, which I performed to obtain the degree of Master of Science at Delft University of Technology in the field of Coastal Engineering. This thesis describes the research I performed on the influence of the wave height distribution on rocking of an Xbloc armour layer.

This thesis was supervised by the members of my graduation commitee: Prof. Dr. Ir. W.S.J Uijttewaal, Dr. Ir. G.Ph. van Vledder and Ir. H.J. Verhagen of Delft University of Technology and Ir. E. ten Oever of Delta Marine Consultants / BAM Infraconsult. I would like to thank the members of my graduation committee for their advise during the research and their supervision writing this report.

Secondly I would like to thank Delta Marine Consultants for giving me the opportunity to do this research. For giving me an inspiring working environment in Gouda and give me all freedom to perform the physical model tests the wave flume in Utrecht. In particular I want to thank Markus Muttray for his help with programming the wave maker and writing the abstract for ICE resulting from this research. I also want to thank Bart van Zwicht and Michiel Muilwijk for their expertise in the wave flume.

Finally I want to thank my parents for their support throughout my entire study and also my boyfriend, Alex, for his editorial contribution and his support.

Suzanna Zwanenburg
Delft, September 2012

Abstract

The dimensions of single layer concrete armour units (interlocking armour units) are calculated with a similar stability relation as the stability relation for quarry stone. In these design formulas an 'average/significant' wave load is used (H_s). Since quarry stone gains its stability only from gravity, this type of armour unit is constructed in a double layer and therefore some damage development is allowed. Interlocking armour units are constructed in a single layer and the design should be based on zero damage.

This research investigates whether this different approach to damage leads to a different characteristic design wave load which will increase the accuracy of the design method for interlocking armour units. It is focussed on the influence of the wave height distribution on the stability of single layer concrete armour units in general and Xbloc in particular.

For Xbloc, zero damage is defined as a criterion for rocking of the armour units: during design conditions *"not more than 2% of the units are allowed to move during more than 2% of the waves"*. To find a stability relation based on this criterion, the stability of Xbloc is investigated according to rocking of armour units contrary to the conventionally approach to stability based on the number of displaced units from the armour layer.

To find the relation between waves and rocking, physical model tests are performed. In these tests a model breakwater is loaded by wave series with different wave height distributions, wave steepness and groupiness. It resulted that every wave has a certain probability of causing rocking of an armour unit. This probability of rocking is mainly dependent on the height of individual waves and to a lesser extent on the groupiness of the wave series. The steepness of the waves appeared to have a negligible small influence.

When the found rocking probability relation is combined with the criterion for rocking, it appears that $H_{2\%}$ is mathematically a better fitting parameter for a stability relation according to rocking. A new stability relation for Xbloc is derived based on $H_{2\%}$.

Additionally, it is found that very extreme wave heights can dislodge an armour unit in such a way that this armour unit does not interlock anymore. Because it is undesirable that armour units do not interlock anymore, dislodgement of armour units should be accounted for in the stability calculations. Therefore, also a stability relation based on dislodgement of units is provided.

Summary

The focus of this research is the influence of the wave height distribution on the stability of single layer concrete armour units in general and Xbloc in particular. In this study it is investigated whether the application of a characteristic wave height with a smaller probability of exceedance than the present parameter for the wave height in Xbloc design (H_s) will increase the accuracy of the design formula.

An armour layer of Xbloc is tested in the wave flume for the rocking criterion *"not more than 2% of the units are allowed to move (rotate) during more than 2% of the waves"*. The hypothesis for rocking (rotational movement of the units) is that:

> There is a kind of 'boundary wave' for rocking: higher waves cause movement, lower waves do not.

In accordance with the rocking criterion and the concept 'boundary wave' the following hypothesis is set for the characteristic wave height in the design formula:

> $H_{2\%}$ is better characteristic parameter. It will give a more accurate design formula than the conventional one.

These hypotheses are tested and if needed adapted according to a literature study, an analysis of existing model tests by DMC and newly performed model tests.

Literature about wave loads and their effect on an armour layer of a breakwater supports these hypotheses. The evaluation of forces on an armour unit indicates that there is a 'boundary velocity' for the onset of instability of an armour unit. This 'boundary velocity' is expected to be mainly dependent on the wave height for a steep armour slope. Since waves breaking on a breakwater are very turbulent and the velocities are depending on very small scale effects, no analytical methods to describe run-up, run-down and the associated velocities in run-up and run-down have been developed yet and this evaluation is based on oversimplifications. Therefore, stability calculation methods should be found empirically.

Although it is expected that the stability criterion for Xbloc is mainly dependent on the wave height, other wave properties are also expected to have some influence. So the groupiness, shape of the waves and wave steepness should also be taken into account in the model tests. Because, when only the wave height will be evaluated while the other wave properties are ignored, the obtained relation between rocking and wave height can be 'polluted' with the influences of

other wave properties.

To analyse the influence of the wave height distribution empirically, the data of model tests performed by DMC are first analysed. This analysis showed, like the literature, that the wave height is the main influencing factor on the stability of single layer armour units. The parameter $H_{2\%}$ appears to be a better fitting design wave height than H_s for armour units with this rocking criterion. The other wave properties have minor influence compared to the wave height, but it appeared that the influence of groupiness and shape of the waves can not be omitted. The steepness of the waves seems of no influence, in contradiction to the expected small influence in chapter 3.

On the basis of literature and the analysis of existing model tests a research programme is made and new model tests are performed. To investigate purely the influence of the wave height on stability, the wave load is chosen in such a way that the shape of the waves does not influence the stability of the armour layer. The other properties of the wave series defining the wave load are chosen in such a way that the influence of the wave height distribution, steepness of the waves and groupiness of the waves can be separated in the analysis of the model tests.

From these model tests it followed that the hypothesis of a 'boundary wave' for rocking needs to be more specified. There appeared to be 3 categories of 'boundary waves' for rocking:

1. A 'boundary wave height' for rocking as described in the original hypothesis (the mean value is approximately $120mm$ during the model tests).
2. A 'boundary wave height' for dislodgement of units (the value is larger than $185mm$ during the model tests).
3. A 'boundary wave height' for rocking of dislodged units (the mean value is approximately $70mm$ during the model tests).

The concept 'boundary wave' itself needs to be nuanced too. The overlap between waves which cause rocking and which does not is quite wide, every wave height has a certain probability of causing rocking of a unit. It followed that the concept 'boundary wave' does not exist due to the following mechanism:

> Every wave loads the armour layer of the breakwater. This causes (very small) disturbances of the placement of the units. The larger the wave load, the larger the disturbance. Because the first under layer is not smooth and homogeneous, the settlements of the units due to a certain load will differ. Uneven settlements influence the interlocking between the units. A unit will start rocking when the unloaded position of the unit differs from the position where it is kept in place by neighbouring units. In other words, the unit rocks when there is some space for rotation of the unit before it touches the neighbouring units. Uneven settlements of the armour layer will increase or decrease the space which allows for rocking. Besides the rotational space between the units the settlements also influence the position of a unit on the under layer. Since the under layer is not

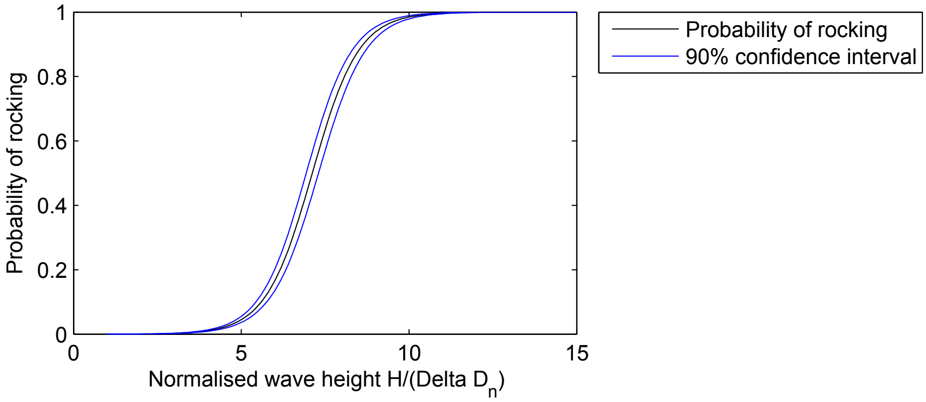

Figure 1: Probability of rocking of a single unit for the normalised wave height and mean group length of the Jonswap spectrum (1.4)

> smooth and homogeneous, the units can have a different stability at different positions. Whether a certain wave load causes rocking is dependent on the settlements caused by the previous waves.

This rocking stability mechanism holds until a large wave of category 2 dislodges a unit. Then the following mechanism dominates:

> This wave height causes very large disturbances, which distorts the placement of the armour layers in such a way that units are dislodged and do not interlock any more. When the position on the first under layer has changed in a negative way as well, these units are rocking for practically every wave afterwards.

The analysis of rocking probability showed also that the wave height is the main parameter for the stability criterion. The groupiness of the waves appeared to have some influence and the influence of the other parameters of the waves are negligible. It resulted in a probability density function for the rocking of an individual Xbloc as given in figure 1 for waves with a groupiness of the Jonswap spectrum.

The rocking criterion prescribes that *"not more than 2% of the units are allowed to move during more than 2% of the waves"*. Translating this in terms of the rocking probability it can be concluded that the probability of rocking for $H_{2\%}$ should not be larger than 0.02. This means that for waves smaller than $H_{2\%}$ it is expected that less than 2% of the units are rocking (since the probability is smaller than 0.02). It is expected than for waves higher than $H_{2\%}$ more than 2% of the units will rock. This is exactly the largest amount of movement accepted by the rocking criterion. The size of the Xbloc should be chosen such that the rocking probability for $H_{2\%}$ is smaller than or equal to 0.02. To derive a conservative design formula the upper bound of the confidence interval is used. This results in the following stability relation according to rocking:

$$\frac{H_{2\%}}{\Delta D_n} \leq 4.26 \tag{1}$$

The analysis of waves which can dislodge units resulted in the following stability criterion:

$$\frac{H_{0.1\%}}{\Delta D_n} \leq 5.12 \tag{2}$$

For shallow water however, the current design formula prescribes larger Xblocs than the new formulas. In shallow water, especially with a steep foreshore, waves become asymmetric. Asymmetry of waves has an adverse influence on the stability of armour units. Since the influence of the shape of the waves is omitted during this research by using only sinusoidal waves, the new design formula will underestimate the required Xbloc size in this case.

Therefore, it is advised to use the largest calculated Xbloc size from equation 1 (rocking based design formula), equation 2 (dislodgement based design formula) and equation 3 (current design formula).

$$\frac{H_s}{\Delta D_n} \leq 2.77 \tag{3}$$

Contents

List of symbols

A_d	area of armour unit exposed to shear	[m^2]
A_l	area of armour unit exposed to pressure differences	[m^2]
C	correction factors for the Xbloc design formula	[$-$]
C_d	empirical constant for drag force	[$-$]
C_l	empirical constant for lift force	[$-$]
C_m	empirical constant for acceleration force	[$-$]
D	diameter of Xbloc	[m]
D_n	nominal diameter of Xbloc (cubic root of Xbloc volume)	[m]
D_{n15}	15% of rocks in a grading has a smaller diameter than D_{n15}	[m]
D_{n50}	50% of rocks in a grading has a smaller diameter than D_{n50}	[m]
D_{n85}	85% of rocks in a grading has a smaller diameter than D_{n85}	[m]
D_x	horizontal distance between the centre of two Xblocs of an armour layer	[m]
D_y	vertical distance between the centre of two rows of the armour layer	[m]
E	wave energy	[J/m^2]
$F()$	cumulative distribution function	[ ]
F_a	acceleration force on an armour unit	[N]
F_d	drag force on an armour unit	[N]
F_l	lift force on an armour unit	[N]
F_z	gravity force on an armour unit	[N]
K_D	empirical derived parameter in Hudson formula	[$-$]
H	wave height	[m]
$H_{1/3}$	average of the 1/3 highest waves in the time series of the waves	[m]
H_1	scale parameter of composed Weibull distribution	[m]
H_2	scale parameter of composed Weibull distribution	[m]
$H_{0.1\%}$	wave height with a probability of exceedance of 0.1%	[m]
$H_{2\%}$	wave height with a probability of exceedance of 2%	[m]
$H_{50\%}$	wave height with a probability of exceedance of 50%	[m]
H_{m0}	significant wave height calculated from $m0$	[m]
H_{max}	maximum wave height	[m]
H_{rms}	root-mean-squared wave height	[m]
H_s	significant wave height $H_{1/3}$	[m]
H_{tr}	transitional wave height of composed Weibull distribution	[m]
L	wave length	[m]
L_x	horizontal distance of an armour layer	[m]
L_y	vertical distance of an armour layer	[m]
N	number of waves in van der Meer formula	[$-$]
N_{od}	relative number of displaced units	[$-$]
N_x	number of units in a row of Xblocs of the armour layer	[$-$]

N_y	number of rows of Xblocs of the armour layer	$[-]$
P	permeability of the core in van der Meer formula	$[-]$
RPD	relative packing density	$[\%]$
S	damage level in van der Meer formula	$[-]$
T	wave period	$[s]$
V	volume of Xbloc	$[m^3]$
$V:H$	slope of the foreshore or breakwater	$[-]$
W_{15}	15% of rocks in a grading has a smaller weight than W_{15}	$[m]$
W_{50}	50% of rocks in a grading has a smaller weight than W_{50}	$[m]$
W_{85}	85% of rocks in a grading has a smaller weight than W_{85}	$[m]$
W_{Xbloc}	weight of Xbloc	$[kg]$
		$[\ ]$
a	wave amplitude	$[m]$
a_d	arm of moment due to the drag force	$[m]$
a_l	arm of moment due to the lift force	$[m]$
a_z	arm of moment due to the gravity force	$[m]$
d	water depth	$[m]$
f	frequency of the wave	$[Hz]$
$f()$	probability density function	$[\ ]$
$f_{rocking}$	probability density of rocking	$[\ ]$
g	gravitational acceleration	$[m/s^2]$
$\bar{j}$	mean group length	$[-]$
k	wave number	$[rad/m]$
k_1	constant of composed Weibull distribution	$[-]$
k_2	constant of composed Weibull distribution	$[-]$
$m0$	zero-order moment of the wave spectrum	$[m^2]$
s	wave steepness	$[-]$
t	time	$[s]$
u	flow velocity	$[m/s]$
$z_{2\%}$	run-up	$[m]$
		$[\ ]$
Δ	relative density	$[-]$
		$[\ ]$
α	slope angle of the foreshore or breakwater	$[^\circ]$
β_i	constant of logistic regression function	$[-]$
γ	correction factors for run-up	$[-]$
η	water level elevation	$[m]$
κ	spectral narrowness parameter	$[\ ]$
ρ_s	density of armour unit	$[kg/m^3]$
ρ_w	density of water	$[kg/m^3]$
σ_i	standard deviation of β_i	$[-]$
θ	slope angle of the breakwater	$[^\circ]$
φ	phase of the wave	$[rad]$
φ_{wm}	phase of the wave at the location of the wave maker	$[rad]$
φ_{bw}	phase of the wave at the location of the breakwater	$[rad]$
ξ	Iribarren number	$[-]$
ω	radian frequency of the wave	$[rad/s]$
		$[\ ]$
$\mathcal{L}$	likelihood	$[\ ]$

Chapter 1

Introduction

The focus of this research is the influence of the wave height distribution on the stability of single layer concrete armour units. With a short introduction of breakwaters and their properties, the meaning of this will be explained in the first section of this chapter. Thereafter the motivation and goal of this research will be given in terms of the problem description and the objective of this research.

1.1 Breakwaters

The area of interest of this study is the armour layer of statically stable rubble mound breakwaters. The meaning of this will be briefly described below. Breakwaters provide a sheltered area from wave action and currents. They are mainly used to protect port facilities and provide a calm berth for vessels. Breakwaters can also be used to protect a valuable habitat, to protect beaches from erosion or to reduce siltation of navigation channels. A breakwater is designed to withstand the loads during the design conditions. Design conditions are related to an event with a certain probability of occurrence and are defined in terms of wave loads, water levels and loads due to currents. There are many types of breakwaters, which can be divided into categories according to their structural features. A rubble mound is one of the ways to construct a breakwater and basically is a mound of loose elements. Other types of breakwaters are monolithic breakwaters (the structure acts as a solid block), composite breakwaters (a combination of a rubble mound and a monolithic structure) and special types like floating or pneumatic breakwaters. A rubble mound breakwater can be statically or dynamically stable. A statically stable breakwater has a fixed shape. The shape of the cross section of a dynamically stable breakwater changes in time due to wave action, but the volume of the cross section stays the same. A typical cross section of a statically stable rubble mound breakwater is given in figure 1.1.

This type of breakwater consists of a core of fine material like quarry run. The armour layer provides the stability of the breakwater, it dissipates and reflects the wave energy and limits the wave run-up. The filter layer(s) between core and armour layer protect the core from washing out. The toe supports the armour layer whereas the underlying filter layer(s) protect the seabed from

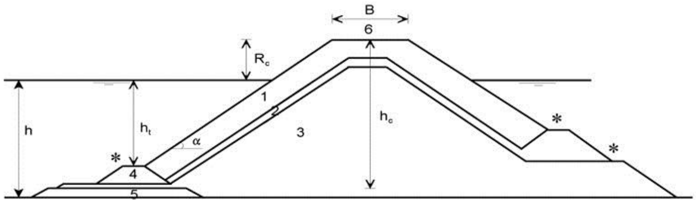

1. Armour layer
2. First under layer
3. Core
4. Toe
5. Filter
6. Crest

R_c Freeboard

Figure 1.1: Cross section of a typical rubble mound breakwater. [Verhagen et al.(2009)Verhagen, d'Angremond, and van Roode]

washing out. Additionally elements like a crown wall to limit overtopping and/or a road on top of the breakwater can be added.

The armour layer

An armour layer can be constructed from quarry stones or concrete units. The choice of armour unit is dependent on both the wave conditions and the available construction material. The stability of quarry stone is gravity based. The stability of concrete armour units can also be gravity based or based on a combination of gravity and interlocking. Gravity based stability means that the weight of the unit is enough to keep the armour unit in place during the design conditions. Interlocking units gain stability as well as from their own weight, from the weight of neighbouring units. This means that interlocking units can be lighter than non-interlocking units under the same design conditions. In general, armour units which only gain stability from gravity are placed in a double layer to allow some damage. Most interlocking armour units have better interlocking in a single layer and are therefore placed in a single layer. Because a displaced armour unit will decrease the interlocking between the units, this type of armour should be designed for zero-damage. For the few unit types with a better interlocking in a double layer, it also holds that the interlocking decreases when units are displaced from the slope. These units should also be designed for zero-damage. Some examples of concrete armour units which gain stability from gravity and which gain stability from both gravity and interlocking are given in figure 1.2.

Stability from:	Gravity	Interlocking and gravity
Placed in a double layer	 *Cube* *Antifer cube* *Tetrapod*	 *Dolos*
Placed in a single layer	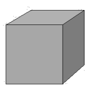 *Cube*	 *Accropode®* *Core-loc®* *Xbloc®*

Figure 1.2: Examples of armour units. [Verhagen et al.(2009)Verhagen, d'Angremond, and van Roode]

This research is focused on the stability of interlocking single layer concrete armour units in general and Xbloc in particular.

1.2 Problem description

The dimensions of single layer concrete armour units (interlocking armour units) are calculated with a similar stability relation as the stability relation for quarry stone. In these design formulas an 'average/significant' wave load is used (H_s). The waves of the design conditions have a wave height probability distribution. The H_s is the average of the 1/3 highest waves. Since quarry stone gains its stability only from gravity, this type of armour unit is constructed in a double layer and therefore some damage development is allowed. As mentioned in the previous section, contrary to quarry stone, interlocking armour units are constructed in a single layer and the design should be based on zero damage. For a design where some damage development is allowed, designing with an average extreme load is a logical choice. But if zero damage is allowed, a maximum extreme load seems more applicable. It would therefore make sense to design interlocking units for the maximum expected wave load (H_{max}) in the lifetime of the structure instead of the significant wave height (H_s) of the design conditions. This statement is supported by the following 3 examples: the failure of the breakwater at port Sines, the correction factors in the design method of Xbloc and other zero-damage based design methods.

Breakwater at port Sines

In 1974 the construction of a huge breakwater started at Sines (Portugal). The breakwater is a dual-purpose structure, supporting oil pipelines as well as providing shelter from the Atlantic Ocean for the port. The location at Sines was in particular very suitable for this harbour because of the deep water very near to the coast. The water depth at the location of the breakwater extended down to a depth of 50 meters. This breakwater was the first which was constructed in such deep water. When the construction of the breakwater was almost completed, a severe storm (February 26, 1978) caused major damage and failure of the breakwater. Figure 1.3 shows the cross section of the breakwater and a top view of the port.

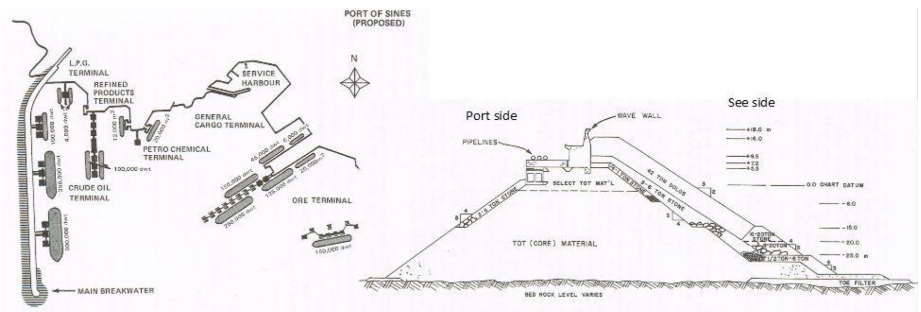

Figure 1.3: Top view of the port at Sines and cross section of the breakwater. [Sin(1982)]

Although the armour layer was constructed of a double layer of Dolos elements, this example is also representative for single layer interlocking armour units, because Dolos should also be designed for zero-damage. Figure 1.4 shows pictures of the breakwater after the storm. It can be clearly seen that the armour layer was not sufficiently stable to withstand the wave load.

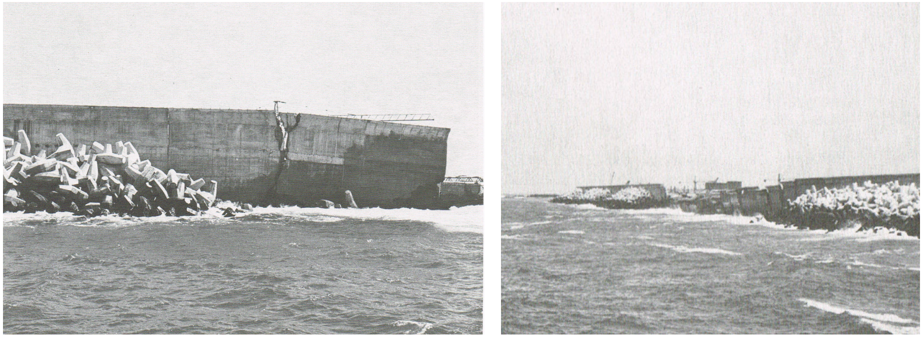

Figure 1.4: Pictures of the breakwater at port Sines after the storm of February 26 1978. [Sin(1982)]

The Official Portuguese Investigation Team, which investigated the cause of failure, found a number of plausible causes. These causes were related to the execution of the breakwater, the structural reliability of the armour units as well as the design wave conditions. The fact that the breakwater was still under construction was not the cause of failure, because the failed parts of the breakwater were all completed and the part under construction was the lowest loaded part. The Official Portuguese Investigation Team wrote the following about the causes of failure related to the design wave conditions:

> "The failure scenario was subsequently: rocking of the Dolos units, fracture of the rocking Dolos and displacement of the fractured units from the armour layer. Hereafter the armour layer failed, the first under layer started to wash out and the concrete structure on top of the breakwater became unstable and fractured.
> The design wave height was a significant wave height of 11 meter. The breakwater was tested with a model loaded by regular waves with a height of the design wave height. The armour layer was stable during these model tests.
> The significant wave height of the storm of February 26 was 9 to 10 meter. According to the model tests the armour layer of the breakwater should be stable in this wave load. The particularly damaging effect of the waves should be sought in the largest waves of this storm. Because of the large water depth in front of the breakwater, the largest waves in the wave field could reach the structure without being reduced due to wave breaking. The effect of these large waves cannot be described by the significant wave height alone; model tests at an appropriate scale reproducing realistic prototype waves in deep water are essential. With a probable incident wave height (H_s) during the peak of the storm of 9 to 10 m, maximum incident wave heights af 14 to 17 m must have occurred. Due to refraction

> the significant wave height was locally increased to 11-12 m and the corresponding maximum wave height 17 to 20 m. Refraction was not accounted for in the model tests." [Sin(1982)]

During the storm of February 26 the significant wave height (H_s) did not exceed the design H_s. Although the highest waves in the wave field were almost 2 times higher than H_s in deep water. Since in shallow water the highest waves are in the order of 1.3 times H_s due to wave breaking and this was the first breakwater in such deep water, other breakwaters did not show this much damage after the design storm. This illustrates that there is probably a better characteristic wave height than H_s.

Design of Xbloc

At the moment Delta Marine Consultants (DMC) applies correction factors to fit the design formulas based on H_s for the design of Xbloc. The correction factors are derived empirically in model tests and are related to both the geometry of the breakwater (curve, low crest, mild armour slope) and the foreshore (slope and relative water depth). The correction factors related to the foreshore are actually corrections for the wave load, since the wave conditions in front of the structure depend on a combination of offshore wave conditions and the wave damping properties of the foreshore (which accounts for the distribution of individual wave heights). The inequality between maximum wave load and significant wave load is assumed to be the largest contribution to the need for correction factors related to the foreshore. Based on the above DMC assumes that there is a better parameter than H_s to predict the stability of a single layer armour. Chapter 3 describes this design method in more detail.

Other structures designed for zero-damage

A clear example of the difference in the design wave height for a structure designed for zero-damage and design of a structure where some damage is allowed in found in the *the Rock Manual* for the design of a breakwater of the type 'caisson on riprap foundation':

> "The design of the caisson stability is determined by an extreme wave height - wave period combination, while the instability of the toe is linked to the occurrence of a design storm, characterised by a significant wave height, usually combined with a low water level. This difference is due ot the fact that a single extreme wave condition may cause the caisson failure, in contrast to the more gradual process of hydraulic damage to a mound of stone. Different probabilities of exceedance will thus be applied in defining the single design wave height, $H_{d,c}$, for the caisson and the significant wave height, H_s, for design of the toe." [RM(2007)]

Similar to this can be found in the *Coastal Engineering Manual* for the design wave height of a monolithic breakwater:

> "The design wave height is defined as the highest wave in the design state at a location just in front of the breakwater. If seaward of a surfzone, *Goda (1985)* recommends for practical design a value of 1.8

times H_s to be used corresponding to the 0.15% exceedance value for Rayleigh distributed wave heights." [CEM(2004)]

This illustrates that for constructions designed for zero-damage a maximum extreme wave height should be used, because the ratio between H_s and the extreme wave height is not constant (i.e. at the offshore side of the surf zone it is approximately 1.8 times H_s, beyond the surf zone this ratio decreases further to the coast). Other examples of this design philosophy can also be found in other manuals like the *Brittish Standard* and *Shore Protection Manual* for numerous af hydraulic structures designed for zero-damage like walls, piles and coffer dams. [RM(2007)] [CEM(2004)] [BS(2000)] [SPM(1984)]

1.3 Objective of this research

The present parameter for the design of single layer concrete armour units is H_s. As suggested in the problem description H_{max} will be a better parameter for the wave height according to a zero-damage criterion. Although the term H_{max} should be used and read with care, since the statistical meaning is a wave height with zero probability of exceedance, but it can also mean the maximum wave which occurred in a time record or the maximum expected wave in a design storm. Also the term zero-damage needs to be described in more detail.
This study will investigate whether the application of a wave height with a smaller probability of exceedance will increase the accuracy in designing single layer concrete armour, what the influence of the wave height distribution is and which wave height is better to include in the design formula.
The best fitting wave height for the design formula will be based on the definition of zero-damage (in terms of movement, displacement and fracture) of Xbloc.

1.4 Approach

To find if H_{max} can better be used than H_s when an armour layer is designed for zero-damage, first the terms zero-damage and H_{max} need to be defined. Hereafter a first expectation of the influence of the wave height and its distribution will be made based on literature. Also the method to find a wave height with a certain probability of exceedance will be provided from literature. Thereafter existing model tests by DMC will be analysed according to their wave height distribution and stability of the armour layer. The expectations based on literature will be compared to the analysis of existing model tests. On the basis of literature and the analysis of existing model tests a research programme will be made and new model tests will be performed. This will give the right data to analyse the influence of the wave height distribution in detail and conclude which wave height is best to include in the design formula for single layer concrete armour units.

Chapter 2

Definitions

The research question contains two concepts which need a more detailed definition: zero damage and H_{max}. These concepts will be described in section 2.1 and 2.2. The significant wave height H_s has two different definitions. The definition which will be used in this report is described in section 2.3.

2.1 Zero damage

According to DMC a unit which is visibly moving (rocking) due to more than 2% of the waves of the design conditions in a model test has an unacceptable risk of fracturing in the prototype. Visible movement is a rotational movement of more than 5 degrees of the armour unit. Rocking of more than 2% of the units decreases the interlocking between the units, which can cause displacements. Therefore DMC provides the criterion that during the design conditions in a model test not more than 2% of the units are allowed to move during more than 2% of the waves. An other type of movement is settlement. Settlement is defined as a small displacement of a unit to a location with better interlocking. In practice this settlement occurs soon after the placement of the unit, whereafter the unit is stable for the remaining lifetime. In model tests small settlement should not be counted as damage. Displacements of units are not allowed during design wave conditions. Designing an armour layer for zero damage means that the mentioned criteria must be met during the design conditions in the model test. During overload conditions (a more severe wave load than the design conditions) more rocking than the criterion is allowed. If no movement at all occurs during overload conditions the design is probably conservative (and probably too expensive). Displacements of units out of the slope and settlements which decreases the interlocking are not allowed at all in the design conditions nor in the overload conditions.

2.2 Maximum wave height H_{max}

As mentioned in section 2.1 rocking is allowed during 2% of the waves of the design conditions; these waves are assumed to be the 2% highest waves. Displacement of a unit is not allowed. But because the criterion for rocking is quite strict, displacement will not happen before damage by rocking occurs. Wave heights are distributed with a certain probability of exceedance. As mentioned in section 1.2, the ratio between H_s and H_{max} differs for deep and shallow water. Even with the highest possible H_{max}/H_s ratio, the rocking criterion is normative for damage. So designing a unit for zero damage should be focused on rocking. Basically, this means that the $s\%$ worst interlocking units should be designed in such a way that it will not be moving during 98% of the waves. Assuming that the uncertainties in interlocking are provided in the factor of the design formula, the only parameter which should be looked at is the wave height. From this point of view, the wave height which is exceeded by 2% of the waves is a kind of 'boundary wave' in the most efficient design: higher waves cause movement, lower waves do not. Designing with this 'boundary wave' would be a logical choice. Following from the above, the hypothesis is that the H_{max} in the research question can be best defined as $H_{2\%}$ (the wave height, exceeded by 2% of the waves).

2.3 Significant wave height H_s

The significant wave height has two different definitions. The significant wave height from the time series of the wave heights (see section 3.1.1) is the mean of the 1/3 highest waves ($H_{1/3}$). The significant wave height from the wave spectrum (see section 3.1.1) is the wave height following from the zero-order moment of the spectrum (H_{m0}). In deep water $H_{1/3}$ and H_{m0} are practically the same. The shallower the water is, the more these wave heights diverge. Since breakwaters are generally build in shallow water, it is important to define which one of the definitions of H_s is referred to in this report. In the design formula for Xbloc, described and explained in chapter 3, the largest of the two significant wave heights is used. $H_{1/3}$ is in general larger than H_{m0}. Also, from the point of view of this research, $H_{1/3}$ is a more useful definition, since the focus of this research is on the wave height distribution. And therefore more on the time series of the waves than the wave spectrum. When the significant wave height H_s is used from now on in this report, it will refer to the significant wave height from the time series of the waves $H_{1/3}$.

Chapter 3

Literature study

In this chapter the stability of single layer concrete armour units is considered based on a literature study and the current design of Xblocs. In accordance with the research question special attention is given to the influence of wave height distribution. To understand the influence of wave the height distribution on the different components of the design method, first the waves and the wave load itself are regarded. Thereafter the derivation of the design formula for Xbloc is given and explained. Based on the literature study, an initial conclusion regarding the objective of this research will be made.

3.1 Wave load on breakwaters

Wind generated waves cause the main wave load on breakwaters. Waves will therefore refer to wind waves in the rest of this report. This waves have a typical period of 1 to 30 seconds. The wave load by tides, seiches, tsunamis and all other types of waves are not considered in this research. To understand the wave action on structures better, a brief introduction about the main concepts of waves will be given first.

3.1.1 Ocean waves

A wave is the profile of the sea surface elevation between two successive downward zero-crossings (zero = mean of surface elevations). A wave has a height, length and period as illustrated in figure 3.1. The left panel shows the surface

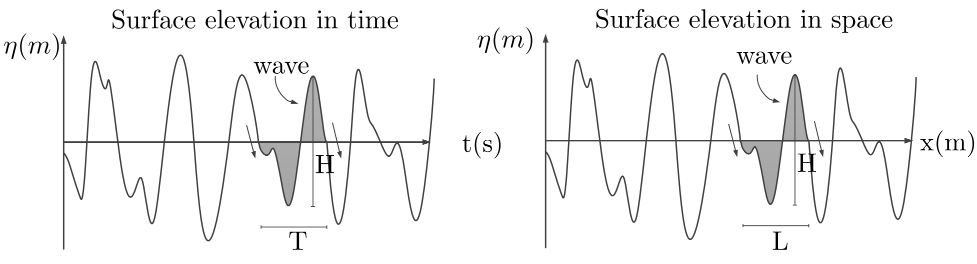

Figure 3.1: Illustration of the definition of a wave, the wave height (H), the period (T) of a wave and the length (L) of a wave. [Holthuijsen(2008)]

elevation at a fixed location as a function of time. The time series of the wave heights are calculated from the time series of the water level elevation. The right panel shows the surface elevation at a fixed time as a function of the location. Wind waves are also called surface gravity waves, because gravity dominates the propagation of this type of waves. In the generation area (where the wind blows) wind waves are irregular and short crested. This is called wind sea. When the waves are not longer influenced by the wind, the waves become more regular the further they travel. These waves are called swell. On a short time scale the wind can be considered stationary and homogeneous; the gradual growth and decay of the wave field can be neglected. Here the waves can be described as a superposition of an infinite number of propagating waves, each with its own amplitude (a), radian frequency (ω), wave number (k) and phase (φ) (equation 3.1).

$$\eta(t) = \sum_{i=1}^{\infty} a_i \, sin(\omega_i \, t - k_i \, x + \varphi_i) \tag{3.1}$$

This superposition of harmonics can be presented in a variance density spectrum, which shows how the variance of the sea surface elevation is distributed over the frequencies. A wind sea has a large variation in frequencies and therefore a wide spectrum. Swell has less variation in frequencies and therefore a narrow spectrum. Two examples of a time series with corresponding wave spectrum are given in figure 3.2.

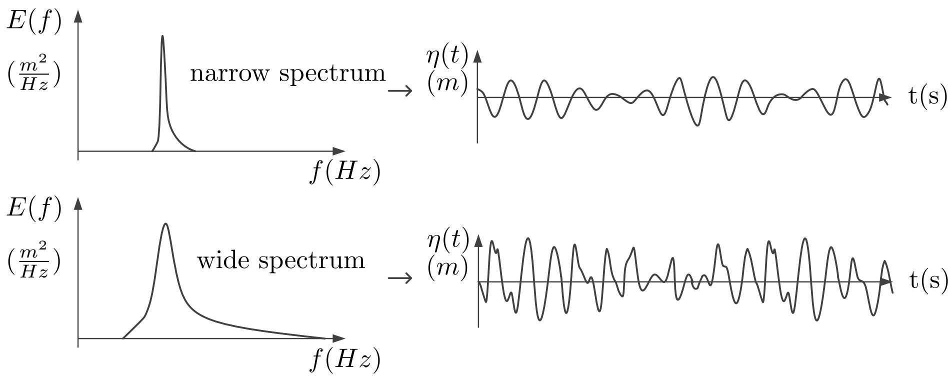

Figure 3.2: Illustration of a wide and a narrow spectrum with corresponding time series. [Holthuijsen(2008)]

A wave spectrum describes infinitely different time series of waves with the same statistical characteristics. This means that the sequence of waves in a time series is not predictable, but the statistical characteristics of all possible time series of a spectrum are the same. A commonly used statistical characteristic of a spectrum is the H_{m0} (see section 2.3). Because in deep water H_{m0} is practically the same as H_s and the wave heights are Rayleigh distributed, other wave characteristics like $H_{2\%}$ (wave height with a probability of exceedance of 2%) can be calculated from this H_{m0}.

On long time scale the wave conditions can be seen as time series with numerous different wave spectra which follow each other up. The characteristics of these wave spectra, like (H_{m0}), have a probability distribution. This way, design wave conditions can be found with a certain probability of exceedance.

Whether it is a wind sea spectrum, a swell spectrum or a combination of these spectra, is location dependent. [Holthuijsen(2008)]

Design wave conditions and wave load

The wave field of the design wave conditions are the main interest for the wave load on a breakwater. This design wave condition is usually given in terms of a deep water wave spectrum. The characteristics of this spectrum are calculated from the long term probability distribution, according to the required safety of the design (for example a once in a 100 year probability of exceedance). This wave spectrum can describe infinitely different time series of waves, because a time series is a realisation of a stochastic process. For a given spectrum, the probability of occurrence of a certain wave height in a corresponding time series can be calculated. Therefore the statistics of the design wave spectrum are used in design methods. Commonly used design wave heights in a design method are $H_{2\%}$ and H_s. An other property of the design wave conditions which can influence the wave load is the wave length. The length (L) of the waves is in general considered relative to the significant wave height, as an average wave steepness (s), as described in equation 3.2.

$$L = \frac{2\pi}{gT^2} \quad , \quad s = \frac{H_s}{L} \quad \rightarrow \quad s = \frac{2\pi H_s}{gT^2} \tag{3.2}$$

Two other properties of a wave series are the shape of the waves (skewness, see section 3.1.2) and the groupiness of the waves. Groupiness is the mean number of consecutive waves larger than H_s (a wave train) in a time series of waves. To investigate the influence of wave height and its distribution on a breakwater and the part of it in the total wave load the other wave properties can not be ignored. Therefore also the other properties of waves will be evaluated in this chapter. [Holthuijsen(2008)]

3.1.2 Deep and shallow water effects in relation to the wave properties

Waves in deep water are not influenced by the bathymetry of the seabed. The properties of a stationary wave field, like significant wave height, steepness and groupiness, can all be calculated from the spectrum.

When the water is becoming shallower, the motion of the waves will reach the bottom. Now the bathymetry of the sea bed will influence the waves. A combination of the shallow water wave effects breaking, shoaling and refraction influences the wave heights, wave height distribution, wave lengths and shape of the waves. The way in which these shallow water wave effects influence the properties of the waves will be briefly described below.

Shoaling is the effect of the shallower water on the propagation speed of the waves. Due to a decrease of the group velocity the wave energy propagation slows also down, resulting in 'energy bunching '. This causes an increase in wave amplitude. Because all waves are influenced by shoaling the wave height distribution shifts a bit to higher amplitudes, but parameters like the ratio between $H_{2\%}$ and H_s stay the same.

In (very) shallow water linear wave theory (the wave theory described in 3.1.1) no longer holds. The relative water depth starts to differ significantly

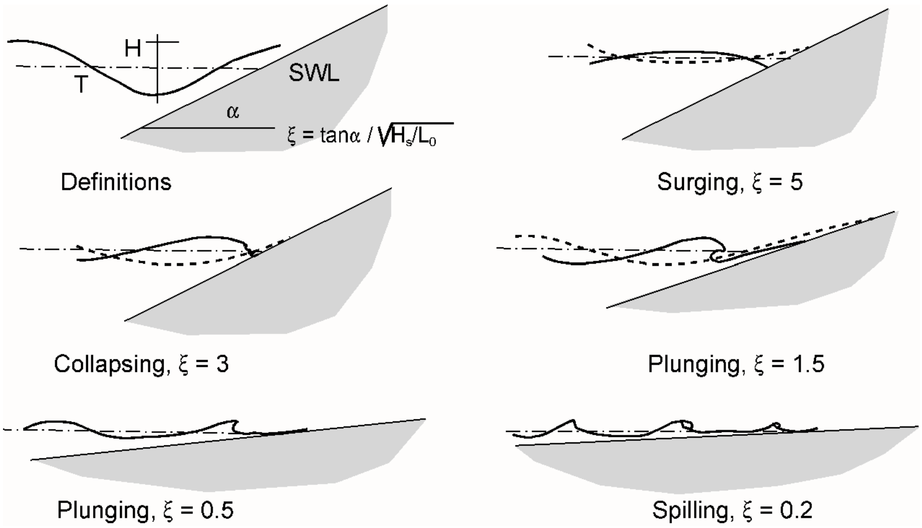

Figure 3.3: Illustration of breaker types of the waves. [Schiereck(2001)]

between the top and the trough of the wave. This results in a different propagation speed of the trough and top of the wave and subsequently the waves are not sinusoidal anymore. The peaks become narrower, the troughs wider and less deep and the waves become asymmetric.

When the water depth becomes too low, the waves become so steep that the highest waves will break. Resulting in a maximum wave height in shallow water between 0.5-1.5 times the water depth, depending on the bottom slope, wave steepness offshore, wind etc. In general 0.75 times the water depth (d) will give a good estimate of the maximum wave height, that can exist is shallow water (equation 3.3).

$$H_{max,shallowwater} \approx 0.75 * d \tag{3.3}$$

Wave breaking is the main effect in shallow water which changes the wave height distribution. Because the highest waves break and their wave heights decrease, parameters like the ratio between $H_{2\%}$ and H_s decrease too. There are different types of wave breaking, depending on the steepness of the waves and the steepness of the foreshore. The Iribarren number (equation 3.4) gives an indication of the type of wave breaking illustrated in figure 3.3.

$$\xi = \frac{tan(\alpha)}{\sqrt{s}} \tag{3.4}$$

Refraction is the influence of the shallower water on the propagation direction of the waves. It affects the direction of the propagation of wave crests into the direction of the depth contours of the seabed. If the depth contours of the seabed are not straight lines, the wave propagation concentrates to a headland and diverges in a bay. Therefore wave heights increase at a headland and decrease in a bay. The influence of refraction on the wave heights is a 3-dimensional effect.

Diffraction is the turning of waves towards areas with lower amplitudes due to amplitude changes along the wave crest. This is particularly strong in areas behind the shadow line of obstacles such as islands and breakwaters. Since the area behind shadow lines is not particularly the heaviest loaded part of a breakwater, diffraction effects fall outside the scope of this research. [Holthuijsen(2008)]

The influence of shallow water on the wave height and its distribution

The wave heights in deep water are Rayleigh distributed (equation 3.5). The shape of this distribution is related to the significant wave height, which can be estimated from the zero order moment (m0) of the spectrum (equation 3.6).

$$P(\underline{H} > H) = e^{(-2(\frac{H}{H_s})^2)} \tag{3.5}$$

$$H_s = H_{m0} = 4\sqrt{m0} \tag{3.6}$$

In shallow water shoaling and refraction affects the shape of this Rayleigh distribution, since these phenomena affect all wave heights. Wave breaking is the main cause that the wave height distribution in shallow water deviates from the Rayleigh distribution. In shallow water the $H_{2\%}/H_s$ ratio depends on the slope and water depth of the foreshore. The influence of shallow water on the wave height distribution can be clearly seen in figure 3.4. The probability of exceedance of the wave heights is plotted on Rayleigh scale and the line is the Rayleigh distributed offshore wave height. For shallow water a number of wave height distributions is plotted for three different relative water depths. It can be seen that for smaller relative water depths, the extreme wave heights (for example $H_{2\%}$) decrease much and wave heights like $H_{50\%}$ do not change.

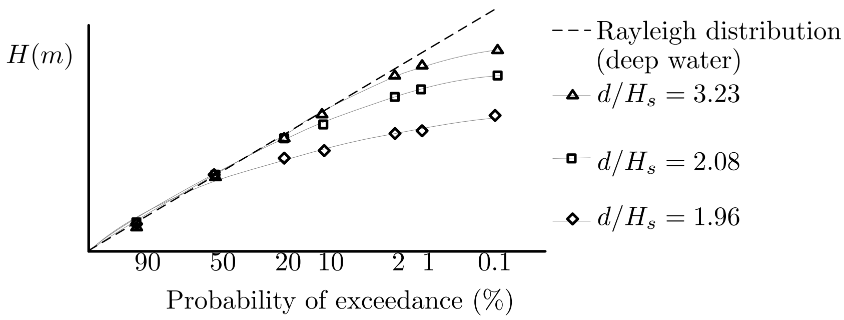

Figure 3.4: Shallow water wave height distributions on Rayleigh scale [Groenendijk(1998)]

The influence of shallow water on the wave steepness

The decreased propagation speed due to shoaling results in a smaller wave length. Together with increased wave heights due to shoaling and refraction the steepness of the waves will also increase. Where the wave height decreases due to refraction (in a bay), the steepness decreases or increases depending on the magnitude of the influence of both shallow water effects. When the waves become asymmetric the local steepness of the wave between trough and top differs from the steepness between top and trough, but the average steepness (described with equation 3.2) remains the same.

The influence of shallow water on the shape of the waves

As described above, in shallow water the waves become asymmetric due to non-linear effects. The waves become asymmetric and peaked (a narrow top and a wide trough). The peakedness and asymmetry of the waves together is called skewness of the waves and is illustrated in figure 3.5. The skewness of waves can be expressed in different parameters, one of these parameters is the ratio between L_1 and L_2 as illustrated in figure 3.5. For sinusoidal waves, this ratio is 1.

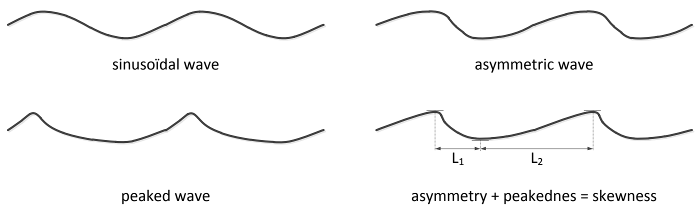

Figure 3.5: Illustration of non-linear wave forms

The influence of shallow water on the groupiness of the waves

For Rayleigh distributed waves the groupiness of waves is related to the spectral narrowness parameter κ, which can be calculated from the wave spectrum. A narrow spectrum gives wave series with a larger groupiness than a wide spectrum.

When the waves enter shallower water, the spectrum becomes slightly more peaked in shoaling waves while the wave heights are still Rayleigh distributed. [Holthuijsen(2008)]

This indicates that the waves will become slightly more grouped in shoaling waves. When the waves arrive in such shallow water that the highest waves start to break, the wave heights are no longer Rayleigh distributed. The effect of shallow water on groupiness is not known. More detailed information about groupiness and the groupiness parameter for Rayleigh distributed waves can be found in [van Vledder(1983)], [van Vledder(1992)] and [Stam(1988)].

3.1.3 Loads on armour units

The wave load on an armour layer results from the flow velocity and the acceleration of the flow in run-up respectively run-down. The shear between the water and an armour unit and the pressure differences in the flow over an armour unit cause shear stresses and normal stresses. These stresses result in a drag force (F_d) and a lift force (F_l), dependent on the flow velocity. Also the acceleration of the water causes a force on the armour unit, the acceleration force (F_a). The gravity force (F_z) on the unit resists movement due to the wave load. Interlocking units also gain stability from neighbouring units. Because the flow velocity and acceleration vary in both time and space and the roughness of the under layer causes a variation in stability, the first unit which tends to move is held in place by more stable neighbouring units. This force interaction between units is called interlocking and makes the armour layer as a whole much more stable than when the units are not interlocking. The forces on armour units due to the wave load, gravity and the interaction with the under layer (F_N and F_W) are illustrated in figure 3.6. The forces due to the wave load and gravity can be described with the following formulas:

$$\begin{aligned} F_l &= 0.5 * C_l * \rho_w * u^2 * A_l \\ F_d &= 0.5 * C_d * \rho_w * u^2 * A_d \\ F_a &= C_m * \rho_w * V * \tfrac{d\,u}{d\,t} \\ F_z &= (\rho_s - \rho_w) * V * g \end{aligned} \tag{3.7}$$

With:
F_l = Lift force $[N]$
F_d = Drag force $[N]$
F_a = Acceleration force $[N]$
F_z = Unit weight $[N]$
C_l, C_d, C_m = empirically found constants $[-]$
A_l, A_d = area of armour unit exposed to the shear or pressure differences $[m^2]$
u = flow velocity in run-up or run-down $[m/s]$
ρ_s, ρ_w = density of the armour unit and density of water $[kg/m^3]$

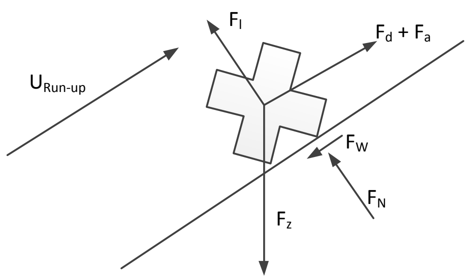

Figure 3.6: Forces on an armour unit during run-up

The units are stable when the moment due to the gravity is larger than the moment due to the wave load (see section 3.1.4). If the wave load increases and the moment due to the wave load becomes larger than the moment due to gravity the unit starts to rotate. Because the flow velocity is also very dynamic in time this overload can be very short. The unit rotates back to its previous position when the load decreases. This is called rocking. When the overload is too large, the unit does not rotate back to its previous position and displaces from the slope. To calculate the forces on the armour units the velocities in run-up and respectively, run-down are needed. But since the waves breaking on a breakwater are very turbulent and the velocities are depending on very small scale effects, no analytical methods to describe run-up, run-down and the associated velocities in run-up and run-down have been developed yet. Calculation of the actual forces on armour and the stability of the units is therefore not possible with this analytical approach. So the formulas of equation 3.7 are only useful for general understanding of wave loads and stability of armour. Stability calculation methods should be found empirically. The flow velocity and acceleration are dependent on the wave properties and the way the waves break. [RM(2007)]

3.1.4 Loads on armour units in relation to the wave properties

Based on the theory of the previous sections a rough estimate of the influence of the different wave properties is made.

For sinusoidal waves, the velocity is zero when the acceleration is maximum and vice versa. The load resulting from the velocity is larger than the load resulting from the acceleration. Therefore only the forces due to the velocity will be considered. At the time of maximum velocity, equation 3.8 holds for rotation of a unit. The left part of this equation is the momentum of the forces related to the velocity and the right part is the momentum related to the gravity around the rotation point. When the momentum resulting from the lift force and drag force on the unit is larger than the momentum resulting from the unit weight, the unit starts to move.

$$0.5 * C_d * \rho_w * u^2 * A_d * a_d + 0.5 * C_l * \rho_w * u^2 * A_l * a_l > (\rho_s - \rho_w) * V * g * a_g \tag{3.8}$$

In this equation, a_g, a_d and a_l are the arms of the forces. See figure 3.7.

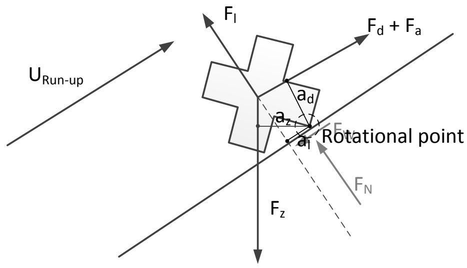

Figure 3.7: Forces on an armour unit during run-up

This equation can be rewritten to equation 3.9. Here, the left part (only the velocity) is wave and time dependent. The right part is dependent on the geometry of the armour units and the density of the water and the units, it is not dependent on the wave properties and time. A velocity larger than the root of the right part of the equation causes movement.

$$u^2 > \frac{(\rho_s - \rho_w) * V * g * a_g}{0.5 * C_d * \rho_w * A_d * a_d + 0.5 * C_l * \rho_w * A_l * a_l} \tag{3.9}$$

As mentioned in the previous section, the flow velocity can not be found analytically. But using the (empirical) formulas for wave run-up, a rough estimate of the dependency of the flow velocity on the different wave properties can be illustrated. The run-up depends on the way the waves break. The run-up relation for spilling and plunging breakers differs from the run-up relation for collapsing and surging breakers. Equation 3.10 gives both run-up relations depending on the Iribarren number (equation 3.4), the wave height and different correction factors (γ) for the roughness of the slope, the permeability, the angle of the waves etc. according to [TAW(2002)].

$$\begin{aligned} z_{2\%} &= \gamma * 1.75 * \xi * H_{m0} & for\, \xi < 1.77 \\ z_{2\%} &= \gamma * (4.3 - \tfrac{1.6}{\sqrt{\xi}}) * H_{m0} & for\, \xi > 1.77 \end{aligned} \tag{3.10}$$

Considering the run-up (left part of figure 3.8) as a box shaped volume of water stretching out over the slope (right part of figure 3.8) the dependency of the velocity on the different properties of waves can be estimated using the equations for wave run-up. The volume in the run-up (volume B) is considered to be the volume of water in the wave (volume A), the breakwater is considered impermeable. For both run-up equations the dependent parameters for the velocity are estimated in equation 3.11.

Step 1 calculates an expression for the height (D) of the box-shaped run-up, following from water volume A and B. All wave independent parameters and constants are combined in parameter c_i. Step 2 describes the run-up velocity during one wave, assumed that the velocity is homogeneous in the box-shaped run-up. The height of the box is assumed to be constant (D) and the run-up changes according to the volume of water which arrives at the breakwater (water volume A in time). Step 3 combines the found expression for D with the equation of the run-up velocity. This gives an indication of the dependency of the maximum water velocity on the properties (wave height and period) of the waves.

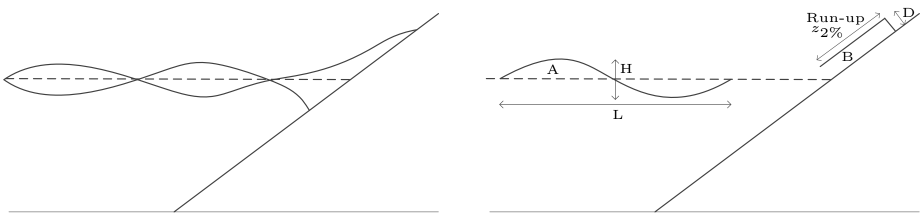

Figure 3.8: Illustration of simplifications run-up

$$\begin{array}{lll}
 & for\, \xi < 1.77 & for\, \xi > 1.77 \\
1 & B \sim A & B \sim A \\
 & z_{2\%} * D \sim \int_0^{\frac{1}{2}L} \frac{1}{2} H_{m0}\, sin(\frac{2*\pi}{g*T^2} x) dx & z_{2\%} * D \sim 2 \int_0^{\frac{1}{2}L} \frac{1}{2} H_{m0}\, sin(\frac{2*\pi}{g*T^2} x) dx \\
 & D * c1 * \sqrt{H} * T \sim \frac{H*g*T^2}{2\pi^2} & D * (c2 * H - c3 * \frac{H^1.25}{\sqrt{T}}) \sim \frac{H*g*T^2}{2\pi^2} \\
 & D \sim \frac{c_4*H*T^2}{c1*\sqrt{H}*T} & D \sim \frac{c_5*H*T^2}{c2*H - c3*\frac{H^1.25}{\sqrt{T}}} \\
2 & \frac{dz_{2\%}}{dt} \sim -\frac{c_4*H*T^2}{D} cos(\frac{2*\pi}{g*T^2} x) & \frac{dz_{2\%}}{dt} \sim -\frac{c_4*H*T^2}{D} cos(\frac{2*\pi}{g*T^2} x) \\
 & \frac{dz_{2\%}}{dt}_{max} \sim -\frac{c_4*H*T^2}{D} & \frac{dz_{2\%}}{dt}_{max} \sim -\frac{c_4*H*T^2}{D} \\
3 & u_{max} \sim c_6 * \sqrt{H} * T & u_{max} \sim c_7 * H - c_8 * \frac{H^1.25}{\sqrt{T}}
\end{array} \tag{3.11}$$

It appears that for plunging and spilling breakers (for $\xi < 1.77$), the period of the waves (and therefore the steepness of the waves) has more influence on the magnitude of maximum velocity than for other breaker types. For the other breaker types the wave height mainly influences the magnitude of the velocity.

It should be kept in mind that this estimate is based on some oversimplifications and not all wave properties are evaluated in this estimate.

Forces on armour units in relation to the wave height and its distribution

Since breakwaters with interlocking concrete armour units are typically constructed with steep slopes (up to 3V:4H), the Iribarren parameter varies between approximately 2.7 and 4.5. Corresponding with this large Iribarren parameter, the wave height will be the main influence on maximum velocity. Because higher waves cause larger forces, the highest waves will determine the stability of the armour units. A wave series corresponding to a wave height distribution with a large $H_{2\%}/H_s$ is expected to cause more rocking than a wave series with a small $H_{2\%}/H_s$.

Forces on armour units in relation to the wave steepness

For an armour layer of quarry stone (riprap) the wave steepness influences the stability. Waves with a smaller steepness (longer waves) cause more damage than steeper waves. Also the wave steepness in combination with the slope of the breakwater influences the stability of riprap. Damage occurs during run-down for surging waves and during run-up for plunging waves. [van der Meer(1988)] [Hovestad(2005)]

Since a breakwater with a riprap armour layer has a more gentle slope than a breakwater with interlocking armour units, the typical Iribarren number is between 1.4 and 3. For this type of armour the steepness of the waves will also influence the stability according to the calculation from section 3.1.4. As mentioned in section 3.1.4, the Iribarren parameter for a breakwater with interlocking armour units is larger than for a breakwater with a riprap armour layer and, according to the calculations of section 3.1.4, the steepness of the waves will have minor influence. In line with the damage of riprap armour, it would be expected that movement of interlocking armour units will occur during run-down (large Iribarren number indicates surging waves). But it is imaginable that the interlocking between the units is stronger for a downward rotation than an upward rotation. Therefore the movement of an interlocking armour unit is expected during run-up.

Forces on armour units in relation to the shape of the waves

The shape of the waves is not included in the run-up formula, so its influence can not be estimated with the calculations above. But this does not mean that the shape of the waves does not influence the wave load.

Evaluating the velocity and the acceleration of the water due to sinusoidal waves and waves with a large skewness the following can be concluded. For sinusoidal waves it turns out that the phase shift between the velocity and the acceleration of the waves is $\frac{1}{2}\pi$. This means that at the time of maximum velocity the acceleration is zero and at the time of maximum acceleration the velocity is zero. The forces on armour units resulting from the flow velocity are larger than the forces due to the acceleration. For armour units loaded by sinusoidal waves the acceleration forces can be omitted. But in case of waves with a large skewness, the velocity and the acceleration of the water particles are not sinusoidal any more and the phase shift is smaller than $\frac{1}{2}\pi$. The result is that at the time of maximum velocity the acceleration is still zero, but at the time of maximum acceleration the velocity is almost maximal. This is illustrated in figure 3.9.

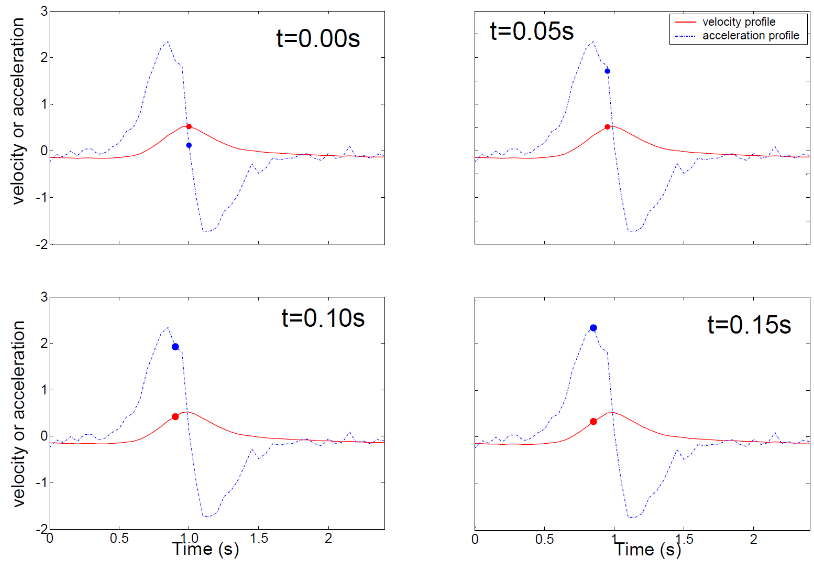

Figure 3.9: The velocity and acceleration of an asymmetric wave [Tromp(2004)]

In this case the acceleration cannot be omitted in the stability calculation of the armour. This means that not only the frequency domain, but also the time domain of the waves should be considered to find the maximum loads on the armour layer. [Dessens(2004)] [Mertens(2007)] [Tromp(2004)] [Verhagen et al.(2006)Verhagen, Reedijk, and Muttray]

As mentioned in paragraph 3.1.2 waves are not sinusoidal any more in shallow water, but peaked and asymmetric. Especially for steep foreshores this effect is significant and also the acceleration will influence the stability of armour units.

Forces on armour units in relation to the groupiness of the waves

The groupiness of the waves is also not included in the run-up formula. So an indication of the influence of groupiness can not be given using the approach of the calculation of equation 3.11. The groupiness of waves is also not included in different design formulas for an armour layer. This seems to imply that the groupiness does not influence the stability of armour units. Although during model testing several researchers noticed that wave trains (a series of high waves) caused more damage than a single wave with the same wave height. For example the research of *Johnson et al. (1978)* showed more damage due to wave series with a large groupiness than wave series with a small groupiness for both quarry stone and interlocking concrete armour units (Damage was here defined as the number of displaced armour units instead of a rocking criterion used in this research). The suggested explanation by *Johnson et al. (1978)*)

of this phenomena was as follows: The first wave in the wave train destabilises the armour unit, the second wave lifts it out of the slope and the third wave displaces it from the slope. Also during model tests with Xbloc DMC noticed a relation between wave trains and rocking. Some suggestions of the explanation for the influence of groupiness on rocking are: Waves influence the water level in the core of the breakwater. During a wave train of high waves not all the water can flow out of the core resulting in an increase in the average water level in the core. This results in a water pressure difference over the armour layer, also at the moment of maximum load by the flow velocity, and subsequently an extra force on the armour units. An other explanation is that a high wave moves an armour unit to a less stable position, lower subsequent waves allows the unit to settle back in its original position, high subsequent waves keep the unit rocking.

3.2 Computation of the shallow water wave height distribution

The wave conditions offshore are homogeneous over a large area. Near shore, the wave conditions are highly location dependent due to shallow water effects on the waves. Wave data collected near shore is therefore only applicable on that specific location. To determine the design wave conditions, long term statistics are needed. To determine long term statistics of wave conditions, measurements of the wave conditions of a long time are needed. Because the location dependency of the wave conditions near shore, the fact that not on every location wave conditions are already measured for many years and that it is not useful to first measure the wave conditions for (for example) 50 years before building a breakwater, only offshore design wave conditions are in general available.

3.2.1 Calculation of H_{m0} in shallow water

Near shore wave data can be determined from offshore wave data using numeric wave transformation models like *SWAN(ONE)* and *MIKE21 SW*. To illustrate the calculation method of these kind of models, the calculation method of $SWAN$ will be described briefly. Other models work in a similar way. $SWAN$ is based on the transformation of wave energy. The shallow water wave effects shoaling, refraction and water depth induces wave breaking are properly accounted for in the model. Diffraction is only approximately included. Also the effects of currents, wind, reflection against and transmission trough obstacles are included in the model. The $SWAN$ model is based on the wave action balance equation, which describes the evolution of the wave spectrum in time and space due to wind, currents and depth effects. In the $SWAN$ model, the wave field is represented by means of an action density spectrum. This is the energy density spectrum (wave spectrum of section 3.1.1) relative to the current. Instead of the absolute radian frequency (ω), the relative radian frequency (σ) is used.

In every grid point it is calculated how the action density spectrum changes in that grid point over time and space (x and y). The output of $SWAN$ form a lot of data at every location, like a mean period, mean direction and significant height (H_{m0}) of the waves, the wind velocity and the bottom level. The main parameter of interest for this research is the significant wave height (H_{m0}).

SWAN can calculate the significant wave height from the spectrum (H_{m0}) at every location. Other wave height related parameters, like $H_{2\%}$, cannot be calculated by *SWAN*. [Holthuijsen(2008)] [SWA(2006)]

3.2.2 Shallow water wave height distribution

Since the wave height distribution in shallow water is depending on foreshore characteristics, other parameters like $H_{2\%}$ and $H_{0.1\%}$ cannot be calculated by multiplying H_s with a simple factor. To calculate these other parameters a conversion formula is needed; a formula to describe the shallow water wave height distribution. *Rattanapitikon (2010)* describes and compares several of these conversion formulas. It resulted that the formulas which include a transition for wave breaking are much more accurate than the formulas without transition for wave breaking. The most accurate conversion formula appeared to be the composed Weibull distribution of *Battjes and Groenendijk (2000)*. This conversion formula consists of a Weibull distribution for the lowest waves. From a certain transitional wave height (H_{tr}) the wave height distribution is described with a Weibull distribution with a different exponent mainly to take into account wave breaking. The cumulative distribution functions and probability density functions of the composed Weibull distribution are given in equation 3.12 and 3.13.

$$F(H) = \begin{cases} 1 - exp[-(\frac{H}{H_1})^{k_1}] & \text{for } H \leq H_{tr} \\ 1 - exp[-(\frac{H}{H_2})^{k_2}] & \text{for } H \geq H_{tr} \end{cases} \tag{3.12}$$

$$f(H) = \begin{cases} \frac{k_1 H^{k_1 - 1}}{H_1^{k_1}} exp[-(\frac{H}{H_1})^{k_1}] & \text{for } H \leq H_{tr} \\ \frac{k_2 H^{k_2 - 1}}{H_2^{k_2}} exp[-(\frac{H}{H_2})^{k_2}] & \text{for } H \geq H_{tr} \end{cases} \tag{3.13}$$

$$H_{tr} = 0.36d \tag{3.14}$$

The parameter H_{tr} is dependent on the water depth (d) as described in equation 3.14. The parameters H_1 and H_2 can be calculated from the properties of a cumulative distribution function and a probability density function. The cumulative distribution function should be continuous, which means that $H = H_{tr}$ should be equal for both equations to prevent a jump in the cumulative distribution function. The integral over the probability density function should be 1. *Groenendijk (1998)* provided a table (see A) to find these parameters corresponding to the transitional wave height, normalized to the root-mean-squared wave height (H_{rms}). H_{rms} can be calculated from H_{m0}. The parameters k_1 and k_2 are constants, which should be found empirically. *Groenendijk (1998)* found $k_1 = 2$, which makes this Weibull distribution a Rayleigh distribution and indicates that the lowest waves are still distributed like deep water waves. For k_2 he found 3.6.

An example of the composed Weibull distribution of *Groenendijk and Battjes(2000)* compared with the deep water Rayleigh distribution is shown in figure 3.10. It can be seen that for waves with a smaller probability of exceedance than the probability of exceedance of H_{tr}, the wave heights start to deviate from the Rayleigh distribution. The smaller the probability of exceedance of the wave height, the more the wave height deviates from the Rayleigh distribution. When this figure is compared with figure 3.4, it can be seen that the shape of the composed Weibull distribution is much like the shape of the measured shallow water wave height distribution.

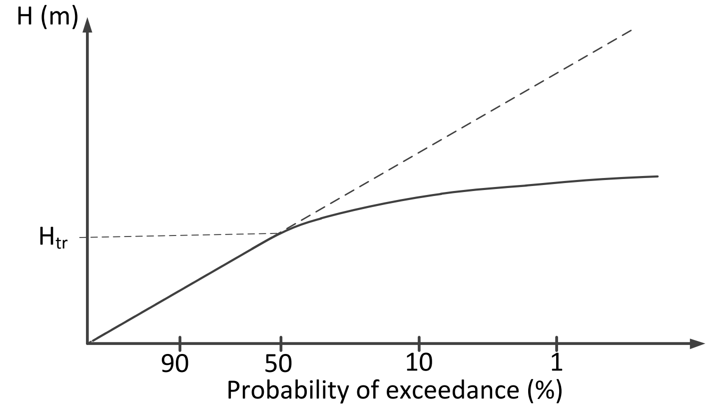

Figure 3.10: Example of the composed Weibull distribution on Rayleigh scale [Groenendijk(1998)]

Rattanapitikon (2010) collected a large amount of data from small scale model tests, large scale model tests and field experiments. He examined the conversion formulas and calibrated the constants with this data. He found that, when the transitional wave height is described by the wave breaking criterion of *Goda (1970)* instead of equation 3.14, the composed Weibull distribution becomes more accurate. The wave breaking criterion of *Goda (1970)* is given in equation 3.15.

$$\tilde{H_{tr}} = \frac{1.1}{H_{rms}} 0.1 L_0 \left(1 - exp\left(-1.5 \frac{\pi d}{L_0} (1 + 15 m^{\frac{4}{3}}) \right) \right) \tag{3.15}$$

In this equation L_0 indicates the deep water wave length related to T_p and m indicates the slope of the foreshore. For the corresponding constants of the composed Weibull distribution he found: $k_1 = 2.2$ and $k_2 = 3.4$. The constants H_1 and H_2 can still be calculated using the table of *Groenendijk (1998)* (see table A.1). More detailed information about the composed Weibull distribution can be found in appendix A. [Rattanapitikon(2010)] [Groenendijk(1998)] [Battjes and Groenendijk(2000)]

3.2.3 Calculation method of shallow water wave hight ($H_{x\%}$)

A wave height with a certain probability of exceedance ($H_{x\%}$) in shallow water can be found with the following method:

1. Calculate H_{m0}, using a numeric transformation model like *SWAN* or *MIKE21*.

2. Calculate H_{rms} using equation 3.16.

$$H_{rms} = \sqrt{8 m_0}, \quad H_{m0} = 4\sqrt{m_0} \;\rightarrow\; H_{rms} = \sqrt{0.5}\, H_{m0} \tag{3.16}$$

3. Calculate the normalised transitional wave height $\tilde{H_{tr}}$ using equation 3.15. The deep water wave length L_0 can be calculated using equation 3.2 with period T_m. For the water depth (d) and the slope of the foreshore (m) the values at the location of interest should be used.

4. From table A follow the values of $\tilde{H_1}$ and $\tilde{H_2}$ corresponding to $\tilde{H_{tr}}$. H_1 can be calculated by multiplying $\tilde{H_1}$ with H_{rms} and H_2 can be calculated by multiplying $\tilde{H_2}$ with H_{rms}.

5. The wave height distribution at the location of interest is described by equation 3.12 with the found H_1 and H_2. $k_1 = 2.2$ and $k_2 = 3.4$.

6. To calculate the height of a wave with a probability of exceedance of x%, equation 3.12 can be rewritten as:

$$H_{x\%} = H_1 * (-ln(1 - \frac{x}{100}))^{k_1} \quad for\ H \leq H_{tr} \tag{3.17}$$

$$H_{x\%} = H_2 * (-ln(1 - \frac{x}{100}))^{k_2} \quad for\ H \geq H_{tr} \tag{3.18}$$

7. First calculate the wave height with equation 3.17. When the calculated wave height is larger than H_{tr}, recalculate the wave height with equation 3.18.

3.3 Design of an armour layer with Xblocs

As mentioned in section 1.2, the design formula for single layer armour units is based on the design of an armour layer of quarry run. This design formula is adapted with several correction factors to account for unfavourable effects of the geometry of the breakwater (curve, low crest, mild armour slope) and the foreshore (slope and relative water depth). This section describes the derivation of the design formula by DMC for the hydraulic stability of Xbloc. Thereafter the design formula for Xbloc will be compared with other design formulas. In the last part of this section the design formula for Xbloc will be evaluated in relation to the wave load and shallow water effects in particular.

3.3.1 Properties of Xbloc

The shape and dimensions of Xbloc are illustrated in figure 3.11. Xblocs are interlocking armour units and gain their stability from both gravity of the unit itself and interlocking between neighbouring units. The stability due to gravity increases as the slope angle of the armour layer decreases. For interlocking the opposite occurs, the stability increases as the slope angle increases. This gives an optimal slope of the armour layer. In case of Xblocs, and other interlocking armour units, the most favourable slope for stability due to the combination of gravity and interlocking is between 3V:4H and 2V:3H. Usually a slope of 3V:4H is applied, since for a steeper slope less material is required. In earthquake sensitive area a somewhat milder slope of 2V:3H can be more favourable.

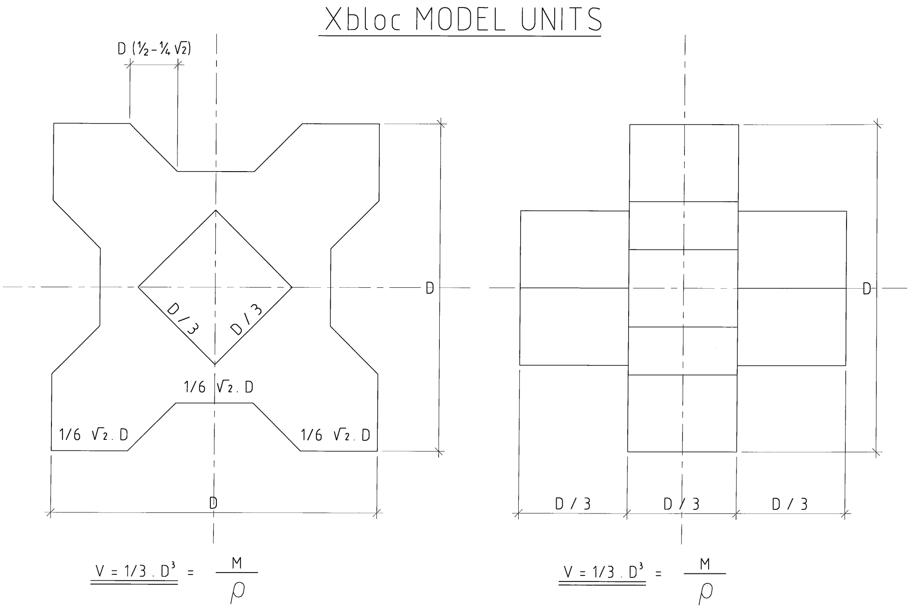

Figure 3.11: Dimensions of Xbloc

3.3.2 Model tests for the development of the Xbloc design formula

To study the hydraulic stability of Xbloc, DMC performed 2-D hydraulic model tests with irregular waves and shallow and intermediate water depths (where the wave heights are not Rayleigh distributed). The wave height, wave length and water depth varied over the different tests. The tests programme consisted of 7 test series consisting of $5-12$ tests. For the test series 2 different water depths, 3 different wave steepnesses and 2 different placements (random and regular) were used, as described in table 3.1. The slope of the foreshore was 1:30 for every test series. For every test series the structure was loaded by 1000 waves derived from a Jonswap spectrum with an increased H_s for the following test until the structure failed or the maximum wave height of the wavemaker was reached.

In these tests the following definitions were used:

Settlement is the downward movement of units along the slope without loss of the interlocking function.

Damage is the displacement of a unit out of the grid while the function of the armour layer keeps intact.

Failure is the loss of the function of the armour layer; the start of damage of the first under layer.

The amount of damage is expressed by N_{od}, the relative number of displaced units.

The stability parameter is the wave height relative to the seize of the armour unit, $H_s/\Delta D_n$.

Table 3.1: Summary of the test programme used for the development of the Xbloc design formula

Test series	Water depth at the toe (m)	Wave steepness (-)	Placement
1	0.40	0.02	random
2	0.35	0.06	random
3	0.35	0.02	random
4	0.35	0.04	random
5	0.40	0.06	random
6	0.35	0.02	regular
7	0.40	0.06	random

During the tests no progressive failure mechanism was observed that started directly after the displacement of a very limited number of units, which was (contrary to these tests) observed during model tests with other single layer armour units. After a unit displaced, the first under layer remained stable in the gap. It was observed that the units above the gap gradually settled till the gap was completely filled. This settlement continued up to the crest of the breakwater and resulted in a protection of the damaged section while the overall packing density decreased. Only after failure of the armour layer, the first under layer became damaged. This self healing behaviour is due to the large number of interlocking interfaces between adjacent Xblocs. The results of the tests in terms of relative number of displaced units versus the stability parameter for the 7 test series are shown in figure 3.12. The stability parameter is the significant wave height of the test, relative to the size of the used Xbloc. The figure shows how many Xblocs were removed from the slope relative to the total amount of units on the slope, by the wave series with a significant wave height according to the stability factor. A vertical line indicates failure of the armour layer.

From these results the following relations with the hydraulic stability were found:

The packing density influences both the start of damage as well as the wave height of failure. A larger packing density (more units per area) increases the wave height which causes damage and the wave height which causes failure. This can be seen in figure 3.12, since the packing density of test series 1, 2 and 3 is lower than 4, 5 and 7. The armour layer of test series 6 was regular placed while the others were randomly placed, so this test result can not be compared with the others related tot the packing density.

The placement of the units is not considered appropriate to make conclusions about, since the armour layer of only one of the test series was placed with a different pattern. In the test with a regular placement pattern no damage was observed. But since a regular placed armour layer might be very difficult to construct under water in a marine environment, this outweighs the advantage of a higher stability.

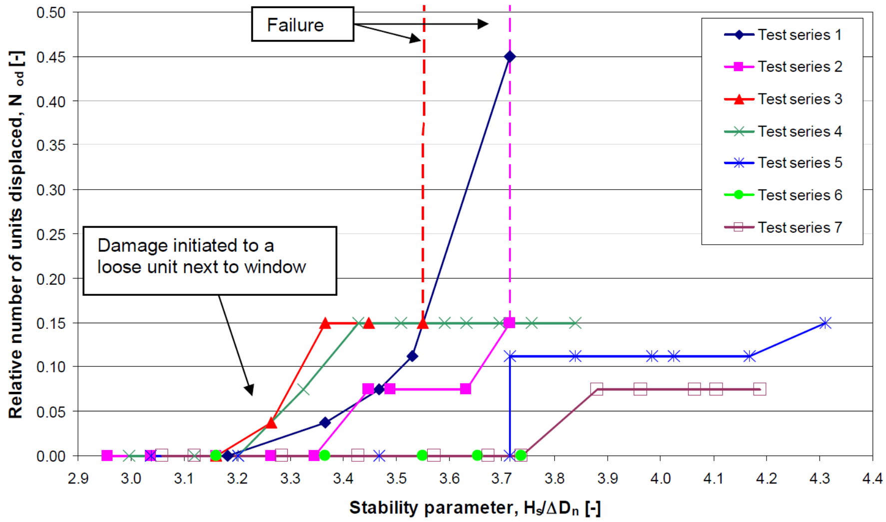

Figure 3.12: Hydraulic stability of Xbloc during the Xbloc development model tests [xbl(2003a)]

The influence of the wave steepness on the hydraulic stability can not be concluded from these test results. For the test series with a large wave steepness (2, 5 and 7) the Xblocs seem to be more stable than for the test series with a smaller wave steepness (1, 3 and 4). But since test series 5 and 7 had a larger packing density, only test 2 with a large steepness should be compared with the test series with a small steepness. Now the relation between wave steepness and stability vanishes and the number of tests compared is quite low for a proper conclusion.

The relative freeboard of test series 7 was larger than the relative freeboard of the other test series (relative freeboard is the crest level above the water level divided by the wave height). Despite of only one test with a large relative freeboard is performed, it seems quite clear that a larger relative freeboard increases the stability. The reason for this higher stability can be the increased downward pressure on the Xblocs due to the increased number of rows, which enhances the interlocking.

For test 1 and 3, the following annotation should be kept in mind. During these tests, damage started with units located at the sides of the flume. These units have less interlocking which results in a lower stability compared to the other units. [xbl(2003a)]

3.3.3 The design formula for Xblox

DMC used the results of these tests to create a design formula, which is universally applicable for the basic design of slopes with Xbloc armour units. Because exceedance of design waves might cause damage to the breakwater, but severe damage and failure should be prevented, the criteria of table 3.2 are taken into account while determining the design formula.

Table 3.2: Limiting wave conditions for design purpose

Wave height	Effect on Xbloc slope
$1.0 \quad H_{design}$	Slope is completely stable
$> \ 1.1 \quad H_{design}$	Start of rocking
$> \ 1.25 \quad H_{design}$	Start of damage (1 or more units displaced)
$> \ 1.3 \quad H_{design}$	Continues damage (further units displaced)
$> \ 1.4 \quad H_{design}$	Start of progressive failure

In table 3.2 also the effect rocking is mentioned. In the development tests for Xbloc, rocking is not considered as a major risk of failure. In projects with slender concrete armour units, it was found that rocking of units can cause partial or complete fracture of the unit, which reduces the function of the unit. Structural stability tests with Xbloc showed that Xbloc is not a slender armour unit and has a high structural stability. According to the model tests damage starts on average at a value of $H_s/\Delta D_n \simeq 3.5$ and varies between 3.25 and 3.85. Failure starts on average at a $H_s/\Delta D_n$ of 3.9 and varies between 3.61 and 4.31. To meet the criteria of table 3.2 the relation of equation 3.19 should be used for the preliminary design of Xbloc armour units:

$$H_s/\Delta D_n \leq 2.77 \tag{3.19}$$

The design formula is based on the average value before the start of damage. It should be noted that the derived formula is based on a limited amount of test series in which several parameters have been varied. Therefore it is always required to perform model tests of a design. Further model tests indicate the need of several correction factors to improve the accuracy of the design formula. This results in the currently used design formula, as given in equation 3.20. [xbl(2003a)] [xbl(2003b)] [xbl(2011)]

$$V = \left(\frac{H_s}{2.77 * \Delta}\right)^3 * C \tag{3.20}$$

With:
V = the volume of the Xbloc = D_n^3
H_s = significant wave height
$\Delta = \frac{\rho_c - \rho_w}{\rho_w}$ = relative density of the concrete
2.77 = empirically derived factor
C = correction factors

The influencing phenomena with related correction factors are given in table 3.3. When more than one correction factor is needed, C is the multiplication of the different correction factors from table 3.3.

3.3.4 Relation to other stability formula

The stability parameter ($H_s/\Delta\ D_n$) used to determine the design formula of Xbloc, is a commonly used stability parameter for breakwater design. The used parameter for the wave height(H_s) in this stability parameter is chosen in consistency with the wave height used in other design formulas for the armour

Table 3.3: Correction factors for the Xbloc design formula [xbl(2011)]

Phenomenon	Correction factor
Crest or curved section	1.25
Frequent near design wave conditions	1.25
Steep fore shore	1.1 for 1:30 < slope < 1:20 1.25 for 1:20 < slope < 1:15 1.5 for 1:15 < slope < 1:10 2 for 1:10 < slope
Low crested breakwater	2 for relative free-board < 0.5 1.5 for relative free-board < 1
Large water depth	1.5 for a water depth > 2.5 H_s 2 for a water depth > 3.5 H_s
Low core permeability	1.5 for a low core permeability 2 for an impermeable core
Mild armour slope	1.25 for a slope < 2:3 1.5 for a slope < 1:2

layer of a breakwater. The formula proposed by *Hudson (1953)* for armour layers of natural rock is much alike the design formula for Xbloc:

$$\frac{H_s}{\Delta D_{n50}} = \sqrt[3]{K_D \, cot(\theta)} \tag{3.21}$$

With:
D_{n50} = median nominal diameter of the rock
K_D = empirical derived factor
θ = angle of the slope of the breakwater

The only difference is the presence of the angle of the slope of the breakwater in the Hudson formula, which is excluded in the design formula for Xbloc. Since breakwaters with Xbloc are constructed with a typical slope of $3V : 4H$ it is not necessary to include this parameter. Moreover, the relation between slope angle and stability is different for interlocking armour units and quarry stone (for which stability is based on gravity instead of interlocking). Stability due to gravity increases for milder slopes; stability due to interlocking increases for steeper slopes. Combining $\sqrt[3]{K_D * cot(\theta)}$ in one constant, equation 3.19 and 3.21 are equal, with a constant of 2.77 for an Xbloc design and 1.74 - 2.41 for a design with natural rock (with a typical slope between $2V : 3H$ and $1V : 4H$ and a K_D of 3.5). An example of an other interlocking concrete armour unit is Accropode®. An armour layer with this type of armour units is designed with a similar formula, only the constant slightly differs.

$$H_s/\Delta D_n = 2.5 \tag{3.22}$$

An other design formula for armour layers of natural rock is the formula of *Van der Meer (1988)*. In this formula are, besides the parameters of the Hudson formula, also the wave steepness (included in Iribarren number) and the permeability of the core (P) included. The K_D factor is replaced by a constant and a parameter related to the allowed damage level($\frac{S}{\sqrt{N}}$), shown in equation 3.23.

$$\begin{aligned} \frac{H_s}{\Delta\, D_{n50}} &= 6.2P^{0.18}(\frac{S}{\sqrt{N}})^{0.2}\xi^{-0.5} \quad plunging\, breakers \\ \frac{H_s}{\Delta\, D_{n50}} &= 1.0P^{-0.13}(\frac{S}{\sqrt{N}})^{0.2}\xi^{P} \quad surging\, breakers \end{aligned} \tag{3.23}$$

When this design formula is compared with the design formula for Xbloc, one can see that the parameter for the permeability of the core, which is added by *Van der Meer (1988)* compared to the formula of *Hudson (1953)*, is also included in the design formula of Xbloc by a correction factor. Since the damage level in the formula of *Van der Meer (1988)* is related to the number of displaced units, and displacement of units is not allowed for single layer armour during design conditions, this parameter is not included by a correction factor for Xbloc. The steepness of the waves is also not included with a correction factor for the design using Xbloc, because during model tests no clear relation has been found between the stability of Xbloc and the steepness of the waves (section 3.3.2). According to the estimate of influence of the wave period (and therefore the steepness) compared to the wave height this minor influence is due to the type of breaking of the waves (as described in equation 3.11). When the formulas of *Van der Meer (1988)* are evaluated in the same way as the run-up formulas in section 3.1.4 it gives a similar estimate of dependency. If $H^{0.75}T^{0.5}$ is larger than a certain value, units are expected to be unstable for plunging waves. Instability by surging waves is related to $H^{1.4}T^{-0.4}$. The relations are not equal to the relations found in equation 3.11, but it also shows that the period is of less importance compared to the influence of the wave height for surging waves than for plunging waves.

3.3.5 Design formula in relation to the wave load

It can be clearly seen that the wave height influences the stability of Xbloc, since it is the main parameter related to the wave load, which is included in the design formula. But if, and in which way, the other wave load related parameters are included, the correction factors should be evaluated in more detail. These correction factors can be divided in two categories. Correction factors related to the environmental conditions and correction factors related to the geometry of the breakwater. The correction factors related to the geometry of the breakwater are the factors for curved sections, the crest, a low core permeability and a mild armour slope. These phenomena do not (or hardly) influence the wave load itself, but influence the impact a certain wave load has on the armour units. Therefore these phenomena are out of the scope of this research. The correction factors related to the ambient conditions are factors for frequently occurring near-design wave conditions, the steep foreshore and the large water depth. Only the slope of the foreshore and the water depth influence the wave load during design conditions. These phenomena are in the scope of this research and will be studied in more detail in relation with the parameters according to the wave load.

A steep foreshore influences the shape of the waves, which can lead to adverse wave impact against the armour layer, as described in section 3.1.4. The steepness of the foreshore is also included in the transitional wave height of the shallow water wave distribution of *Battjes and Groenendijk (2000)*, equation 3.12, 3.13 and 3.14. A steeper slope of the foreshore gives a larger transitional wave height, which gives a larger $H_{2\%}/H_s$.

A high water level at the toe of the breakwater results also in a larger transitional wave height, see equation 3.14. The higher the water level at the toe of the breakwater, the more the wave height distribution tends to the Rayleigh distribution and the larger $H_{2\%}/H_s$ is. As the largest waves in the spectrum cause the largest loads on the armour layer, the stability of the armour layer is reduced compared to breakwaters in lower water depth.

Design formula in relation to the wave height and its distribution

The design formula for Xbloc is based on tests in shallow water. So on wave series with a shallow water wave height distribution. Since for deeper water, with a larger $H_{2\%}/H_s$ than shallow water, a correction factor is proposed and it is also expected that $H_{2\%}$ is a better characteristic parameter for the stability relation of Xbloc, it is expected that both correction factors are related to the distribution of the wave height.

Design formula in relation to the wave steepness

The steepness of the waves is neither included in the design formula nor the correction factors for the design of Xbloc. From the development tests of Xbloc is expected that the wave steepness has no significant influence, see section 3.3.2. But it should be kept in mind that this expectation is based on a limited number of test results.

Design formula in relation to the shape of the waves

The correction factor for slope is besides the wave height distribution also related to the shape of the waves. The steepness of the foreshore mainly causes the asymmetry of the waves. When the armour layer is loaded by asymmetric waves, the acceleration force will also play a role in stability of the armour. The influence of the acceleration force is expected to be included by this correction factor.

Design formula in relation to the groupiness of the waves

The groupiness of the waves is neither included in the design formula for Xbloc nor in the correction factors. Although during model tests the damage due to wave trains was observed to be higher than the damage due to a single high wave with the same wave height. It is assumed that the groupiness of the waves influences the stability of Xbloc.

3.4 Summary

The objective of this research is to obtain a better design wave height than H_s for single layer concrete armour units. Section 2.2 suggests that $H_{2\%}$ will fit better as a design wave height according to the damage criteria of Xbloc. After studying the literature about wave loads and its effect on an armour layer of a breakwater this expectation still holds. The evaluation of forces on an armour unit of section 3.1.3 and 3.1.4 indicates that there is a 'boundary velocity' for the onset of instability of an armour unit. A higher velocity causes movement of a unit. This 'boundary velocity' is expected to be mainly dependent on the wave height for a steep armour slope, as described in equation 3.11. It should be kept in mind that this estimate is based on some oversimplifications and not all wave properties are evaluated with this estimate.

This implies that more research is required to reach the objective properly. As described in section 3.1.3 the relation between the wave load and rocking should be found empirically, viz. with physical model tests. Since it is expected that not only the wave height, but also the groupiness and shape of the waves determines the wave load and the influence of the wave steepness is uncertain, these wave properties should also be taken into account in the model tests. Because, when only the wave height will be evaluated while the other wave properties are ignored, the obtained relation between rocking and wave height can be 'polluted' with the influences of other wave properties.

Chapter 4

Evaluation of existing model tests

In this chapter the design of single layer armour units is focussed on the use of Xbloc. Previous designs of an Xbloc armour layer have been tested in a wave flume by DMC. The results of these tests will be used in this chapter to investigate rocking behaviour of Xbloc. The used data originates from four different projects of DMC. The according reports are not publicly available.

4.1 Available test data

The available wave data of the tests are the incoming time series of the water level elevation, the corresponding wave spectrum and the corresponding wave statistics. Furthermore the design specifications of the physical model and a qualitative description of the observed rocking are available. For some of the tests this description is quite detailed, for example:

> "One rocking element in the second row, fourth element from the left. The intensity of rocking reduces to zero movement at the end of the test. Multiple elements (4 to 5) start moving after 12 min. of testing."

Other descriptions are more brief, like:

> "1 unit rocking, some settlements"

With this data, the mean influence of the waves from a particular wave series can be evaluated. For example, it can be investigated whether the calculated dimensions of the Xbloc with $H_{2\%}$ fits the required Xbloc size according to the model tests better than calculations using H_s. However, the hypothesis of the 'boundary wave' from section 2.2 can not be confirmed nor rejected, because there is no wave specific rocking information available. The only information available are the overall observations of rocking for a whole test. The tested structures of the different model tests are distributed over a wide range of different foreshores and dimensions of the breakwater. There are wide differences in the water depth relative to the wave heights, the slope of the foreshore and the height of the breakwater relative to the waves. An overview of the available data can be found in appendix B. The following sections will evaluate the influence of the different wave properties based on the existing model tests.

4.2 Influence of the wave height and distribution

First the results from these model tests are analysed to determine whether there is a stronger relation between $H_{2\%}$ and stability than H_s and stability. The size of the tested Xbloc in the first model tests of each structure is calculated using the Xbloc design formula (equation 3.20) and (if needed) its additional correction factors. If the damage occurred which during the tests did not meet the requirements of the Xbloc design, as defined in section 2.1, the tests were repeated with a larger Xbloc until the stability of the armour layer was sufficient. The smallest Xbloc size which meets the requirements is the empirically found size for the design. This size (scaled to the waves of the prototype) is used for the construction of the real breakwater. In figure 4.1, the calculated and the empirically determined nominal diameter of the Xbloc are shown for the different tested structures. The line represents the ideal situation of a design formula which exactly gives the sufficient size according to the model tests. When a point is located above this line it means that the design formula is conservative; it gives a larger Xbloc size than needed for this particular design. When a point is located below the line it means that the design formula gave a too small Xbloc size. The more the points deviate from this line, the less accurate the design formula is in that particular case.

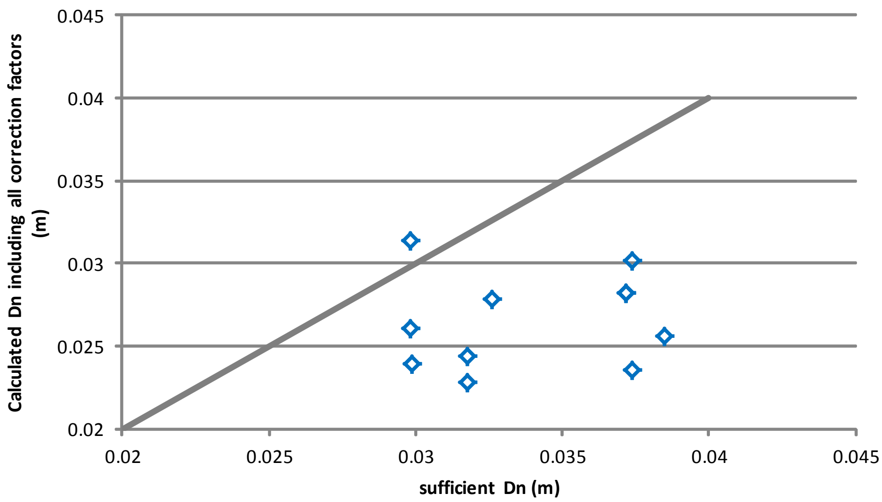

Figure 4.1: Calculated D_n with the design formula and needed correction factors versus the sufficient D_n following from model tests

It can be clearly seen that for most structures the sufficient Xbloc size appears to be larger than the calculated Xbloc size. It is also notable that the points are not crowded around the line, but have a large scatter. In other words, the graph shows that for the same calculated size there is a very wide spread in the sufficient size. This indicates that the significant wave height (H_s), as used in the calculation of the Xbloc size, might not be the right parameter for the wave height. The tests where the calculated size differs most from the sufficient size, were breakwaters in deep water. Since in deep water the ratio $H_{2\%}/H_s$ is larger than in shallow water (section 3.1.2), it seems plausible that the deviations between calculated and sufficient size will be reduced when a wave height with a smaller probability of exceedance is used in the design formula. However, it should be kept in mind that this scatter can also indicate that there are more parameters influencing the stability than included in the design formula. For instance, the steepness, the groupiness or the shape of the waves. To investigate if the use of $H_{2\%}$ would give a better fit for the design formula, the Xbloc sizes are recalculated with the design formula while H_s is replaced with the corresponding $H_{2\%}$. According to section 3.3.5, the correction factors for the foreshore and the relative water depth are assumed to compensate for, among others, a large $H_{2\%}/H_s$ ratio. When $H_{2\%}$ gives a better fit for the design formula, these correction factors are expected to be unnecessary. So when the Xbloc size is calculated with $H_{2\%}$ these correction factors should not be used. Naturally, the other correction factors should still be used. The results are plotted in figure 4.2 (in the same way as figure 4.1).

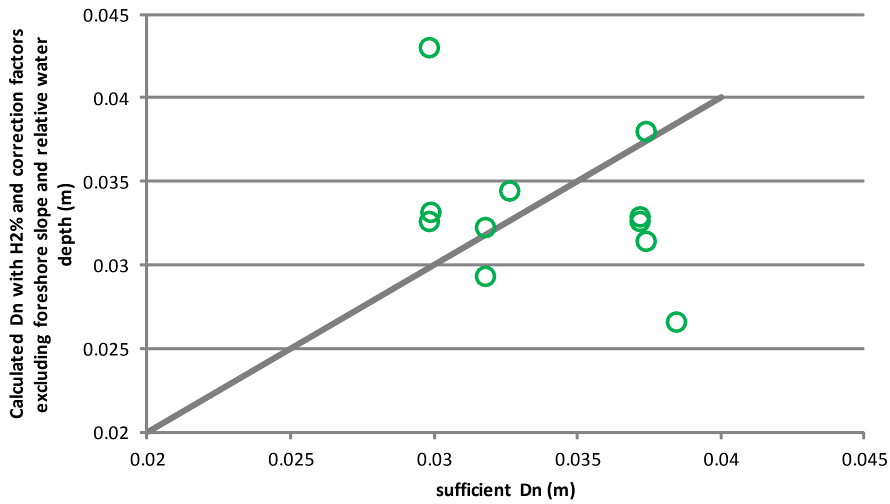

Figure 4.2: Calculated D_n with $H_{2\%}$ instead of H_s and excluding the correction for the slope of the foreshore and the relative water depth versus the sufficient D_n following from model tests

The points in figure 4.2 are more crowded around the line, which indicates that $H_{2\%}$ gives indeed a better fit for the design formula, even though there are still 2 points with a very large deviation from the line. Since the correction factor for the slope of the foreshore is expected to correct for both the shape of the waves and a large $H_{2\%}/H_s$ ratio, it might be not right that this factor is excluded in the calculations. Therefore, the Xbloc sizes are recalculated with the design formula adapted with $H_{2\%}$, while only the correction factor for the large water depth is excluded. The results are shown in figure 4.3.

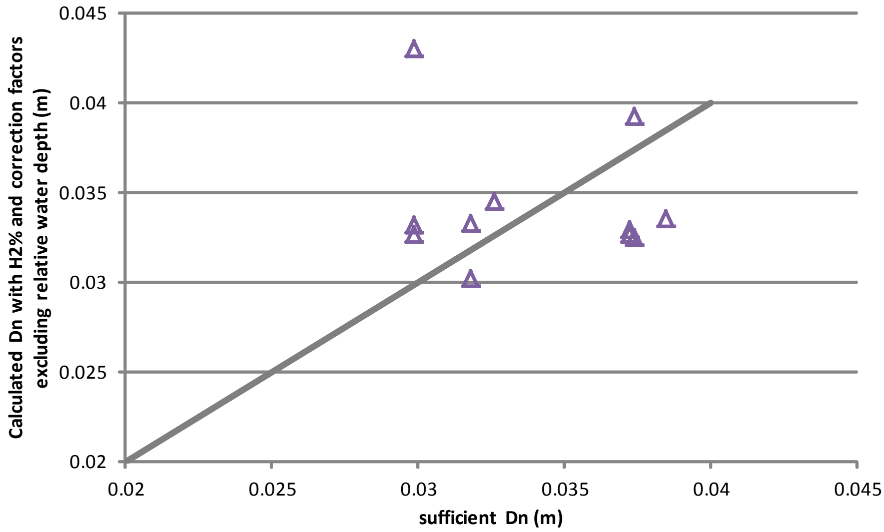

Figure 4.3: Calculated D_n with $H_{2\%}$ instead of H_s and excluding the correction for the relative water depth versus the sufficient D_n following from model tests

In this figure the data points are even more crowded around the line compared to figure 4.2. This indicates that the large scatter in figure 4.1 is most likely caused by the $H_{2\%}/H_s$ ratio. It follows that the $H_{2\%}$ is a better parameter to include in the design formula.

4.3 Influence of the steepness of the waves

There is still some scatter in the data of figure 4.3. As mentioned in section 4.2, the scatter can also be caused by the influence of other parameters, which are not included in the design formula. Therefore the other wave properties will also be evaluated. The wave steepness of the test series can be easily calculated from the available data. But since the steepness is not included in the design formula, the Xbloc size can not be recalculated as in section 4.2. The potential relation between stability and steepness can have many forms and the data set is too small for a proper regression fit. Therefore the data in figure 4.1 is coloured according to the steepness of the waves in the test series; blue for a mean wave steepness smaller than 0.047 and green for a mean wave steepness larger than 0.047. The steepness varies between 0.030 and 0.058. The tests are divided in two groups with an equal amount of data points. The result is shown in figure 4.4.

According to this figure the steepness of the waves seems to have no influence. There is no visible relation between a larger steepness and a smaller or larger stability. An other method to show a potential relation is to plot the steepness against the relative Xbloc size; the calculated size divided by the sufficient size. This is shown in figure 4.5 for the size calculated with H_s and with $H_{2\%}$.

This figure shows a very weak relation between steepness and stability. From this evaluation follows no clear relation between wave steepness and stability, but it does not clearly show that it is completely unrelated.

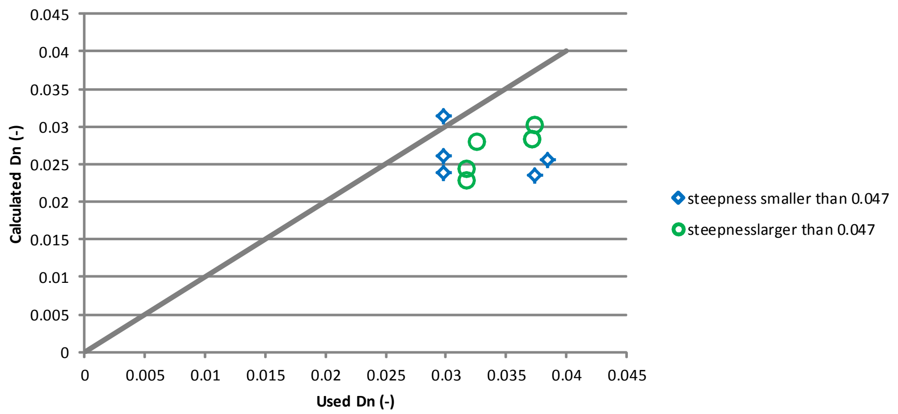

Figure 4.4: Calculated D_n with $H_{2\%}$ instead of H_s and excluding the correction for the relative water depth versus the sufficient D_n following from model tests

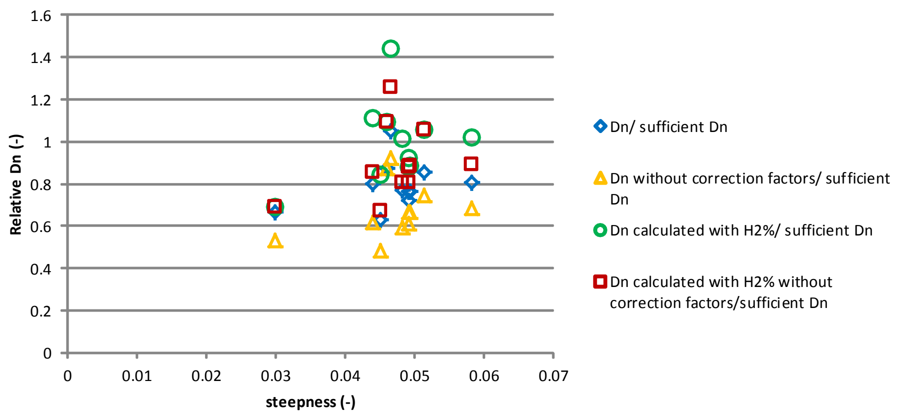

Figure 4.5: Calculated D_n with $H_{2\%}$ instead of H_s and excluding the correction for the relative water depth versus the sufficient D_n following from model tests

4.4 Influence of groupiness

The influence of the groupiness can not be evaluated from this data, because all tests use a Jonswap spectrum. Since all Jonswap spectra have the same spectral shape and the groupiness is calculated from the wave spectrum, the waves of these tests are expected to have the same spectral narrowness. Although it is observed by DMC that a wave train (consecutive high waves) causes more rocking than a single high wave, it is therefore expected that the groupiness of waves influences the stability of Xbloc.

4.5 Influence of the shape of the waves

The shape of the waves can not be evaluated with the data from the existing model tests. But since the calculation of the Xbloc size with $H_{2\%}$ without the correction for deep water gives better results than also without the correction factor related to the slope of the foreshore (section 4.2), it is expected that the shape of the waves has an influence on the stability of the Xblocs.

4.6 Conclusion

The results of the evaluation of the existing model tests are in line with the expectations from chapter 3. The wave height is the main influencing factor on the stability of single layer armour units. The parameter $H_{2\%}$ appears to be a better fitting design wave height than H_s for armour units with this rocking criterion. The other wave properties have minor influence compared to the wave height, but it seems that the influence of groupiness and shape of the waves can not be omitted. The steepness of the waves seems of no influence, in contradiction to the expected small influence in chapter 3.

Chapter 5

Research programme

5.1 Introduction

The focus of this study is to determine the influence of the wave height distribution on the stability of single layer concrete armour units (section 1.3). In particular, the influence of $H_{2\%}$ and the ratio $H_{2\%}/H_s$ (chapter 2). It is expected that $H_{2\%}$ is a better wave height to include in the design formula (equation 3.20) than H_s. As mentioned in paragraph 3.1.3 the stability of armour units should be found empirically. This also applies to the influence of the wave height distribution on the stability. Existing model tests confirmed the expected influence of $H_{2\%}$ (section 4.2). Although these test results support the hypothesis, a quantitative relation can not be found from this data because of the wide range of different geometries of the tested breakwaters. A new model test programme will provide a better basis for a quantitative analysis of the influence of the wave statistics on stability. This chapter describes this test programme, the used test facility and the design of the model geometry.

5.2 Wave flume

The model tests will be carried out at the DMC wave laboratory in Utrecht. The length of the flume is $25m$, the width is $0.6m$ and the height of the side walls is $1.0m$. The maximum allowed water depth is $70cm$ with a maximum individual wave height of $30cm$. A picture of the wave flume can be found in figure 5.1.

The wave flume is equipped with a fully absorbing piston type spectral wave maker. The surface elevation can be measured by 8 resistance wave gauges. For the purpose of reflection analysis 3 wave gauges at one location are needed. The reflection analysis is based on the method of *Mansard and Funke (1983)* for which the WaveLab software (Aalborg University) has been applied. For a reliable reflection analysis, the wave field at the 3 wave gauges should be homogeneous; not disturbed by e.g. bottom effects. In other words, the wave gauges should be placed at a location with a flat bed and with the right spacing (mostly $0.3m$ and $0.4m$). Time series of water level elevations will be recorded at a sampling frequency of 32 Hz.

For the design of the model breakwater, the limitations of the available

Wave flume

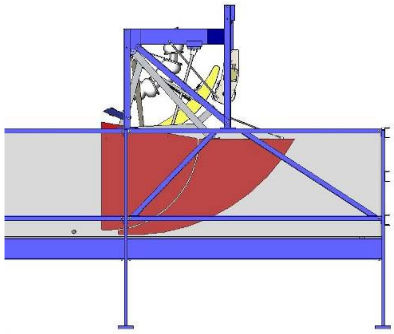

Piston type wave maker

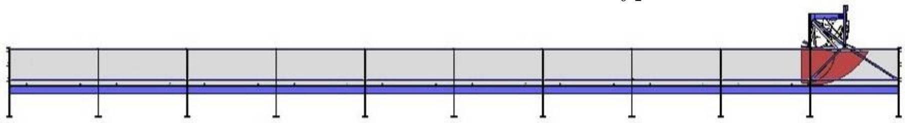

Wave flume longitudinal section

Figure 5.1: Wave flume facility at DMC laboratory in Utrecht [wav(2010)]

material in the laboratory should be taken into account. The gradings of the construction material are restricted by the characteristics of the sieve. This sieve enables the following gradings: $2-4mm$, $4-5.6mm$, $5.6-8mm$, $8-11.2mm$, $11.2-16mm$, $16-22.4mm$, $22.4-31.5mm$ and larger than $31.5mm$. [wav(2010)]

5.3 Fundamentals of the test program

To investigate whether $H_{2\%}$ is a better wave height to include in the design formula than H_s during model tests the breakwater should be loaded by wave series with the same H_s and a different $H_2\%$. Simply put, when the stability of the armour layer is equal for all wave series, H_s is the right parameter for the wave height in the design formula. If the armour layer is less stable for wave series with a larger $H_2\%$, this parameter would be a better fit for the design formula. However, in chapter 3 more wave properties are found which might influence the stability of an armour layer. To find the relation between the wave height and stability, it should be possible to separate the influence of the different properties of the waves. The parameters which influence the wave height (steepness of the foreshore and water depth at the toe), influence more than only the height of the waves and its distribution. The influence of the other parameters related to the wave statistics (wave steepness and groupiness) is unknown. Therefore, the following should be considered by designing the geometry of the model and making the test programme:

The wave height distribution of the wave series of a model test is usually modelled as the wave height distribution will be at the project location during design conditions. This means that the wavemaker produces a time series according to a Jonswap or a Pierson-Moskowitz (PM spectrum). This represents the offshore wave field at the project location. The foreshore of the project location is also scaled and built in the flume. Travelling onto the breakwater, the waves are influenced by the shallow water effects according to the foreshore. At the toe of the model breakwater, the wave height distribution is a shallow water wave height distribution like at the project location.

The foreshore in front of the structure influences, apart from the wave height distribution, also the shape of the waves (section 3.1.4). Because the research question is focused on a better fitting wave height for the design formula, it should be possible to distinguish the influence of the shape of the waves from the influence of the wave height distribution. Since both skewness and wave height distribution are dependent on the foreshore, the influence of both parameters can not be investigated separately for wave series from a Jonswap of PM spectrum. To prevent this contradiction, no Jonswap (or other commonly used) spectrum will be used, but a wave series composed of a summation of a limited number of sinusoidal waves. A summation of a limited number of sinusoids gives the opportunity to have full control over the wave height distribution. The time series of the waves can be calculated beforehand. They are fixed series of irregular waves; they are not the result of a stochastic process like the time series of a spectrum. In this way, the wave height distribution can be easily varied with a flat foreshore. Besides the advantage that the influence of the wave height distribution can be separated from the influence of the shape of the waves, the use of these wave series gives also the advantage that the wave series and wave height distribution can be made almost exactly as desired.

The wave steepness is not a parameter which can be omitted like the influence of the shape of the waves according to a steep foreshore by adjusting the waves, because waves have always a steepness. As described in chapter 3 and 4, it is expected that the steepness of the waves has minor influence on stability. But this expectation is quite uncertain so the steepness of the waves can not be neglected beforehand. Because the design formula and the correction factors do not account for wave steepness and that the method should be valid for all circumstances, different wave steepnesses should be tested. At least, to point out whether wave steepness influences stability and whether more research on this subject is needed.

For the groupiness of the waves , the same holds as for the influence of the wave steepness. It cannot simply be neglected and should be considered by setting up the test programme. Tests with a different groupiness will show whether only the wave height of the wave which causes rocking or also the hight of the previous wave influences the stability.

Table 3.3 gives more parameters for which a correction factor is needed, in other words more parameters which influence the stability, than only the wave height related slope of the foreshore and water depth at the toe. These parameters should be taken into account when designing the geometry of the breakwater for the model tests. They should be chosen in the range where no correction factor is needed, and exactly the same in all tests. Many test should be done, so that an inaccuracy due to placement variability of the phenomenon is of little influence. This will be described in detail in the next section.

5.4 Geometry of the breakwater

The layout of the breakwater for the model tests is dependent on the limitations of the wave flume, as described in section 5.2, and the remarks described in section 5.3. Normally, the layout of the breakwater is the layout of the prototype scaled to a size which fits in the flume. Because this research concerns no prototype, the model has not a fixed model scale. The model units with the most favourable properties for the armour layer of this research, are chosen. Some elements of the model breakwater need a model scale for design of it. This model scale results from the chosen model Xblocs and a commonly used size of Xbloc. The properties of the breakwater for the model are described below and shown in figure 5.2.

The foreshore should be flat for minor influence on the shape of the waves. A slope is not needed to create different wave height distributions since a hand-made wave series, based on the wave height distribution, will be used instead of a standard wave spectrum.

The front slope of the breakwater should be $3V : 4H$. For stability reasons the slope of the armour layer should be between $2V : 3H$ and $3V : 4H$. The most commonly used slope in practice is $3V : 4H$ (less material needed). Therefore this slope will be used in the model tests. [xbl(2008)]

The Xblocs are available in different sizes. For the model tests Xblocs of 49 gram are chosen, because these units have a small standard deviation of both the volume and the density of the units. This size is one of the smaller units, which is an advantage, because the wave height which causes rocking is lower and therefore the relative water depth is larger. This means less influence of the bottom on the waves. The disadvantage of small Xblocs over larger ones are scale effects. In general, it is better to use model units as large as possible to minimize the differences in viscous forces and prevent the need for Froude scaling (scaling for a characteristic pore velocity as described by *Burcharth et al. (1999)*). The 49 gram units are large enough for scale effects to be negligible. The Xblocs are also large enough for rocking to be visible and the design H_s is large enough to be measured accurately.

The required packing density of the armour layer is described in the design manual for Xbloc and is $1.2/D^2$. The distance between the centre of two units horizontally is $1.32D$ and the distance between the centre line of the rows is $0.63D$. A unit should make contact with two units of the previous row and with the slope. [xbl(2008)]

The relative water depth should be maximised to have the lowest influence of the bottom on the waves and keep the waves as sinusoidal as possible. The maximum water depth in the wave flume is $70cm$. For some water depths, including $70cm$, the wave generator is pre-configured. This means that the wave generation for these water depths is more accurate than for other water depths. Therefore a water depth of $70cm$ is the best choice.

The crest height of the breakwater should not be in the low-crested category. For a not-low-crested breakwater, the relative freeboard (ratio between freeboard and significant wave height) should be at least 1. For Xblocs of 49 grams in fresh water the design wave height H_s is 9.95 cm according to equation 3.20. This gives a freeboard of $10cm$. To include the possibility of overload an extra $5cm$ freeboard should be included. This gives a relative freeboard of 1.5 which is small enough for a realistic stability of the armour units. (A larger freeboard gives a larger stability of the armour units. In practice, breakwaters does not have a very large freeboard, so model tests with a very large freeboard give an unrealistic stability of the armour units.) This results in a breakwater with a crest height of $85cm$.

The crest should not influence the stability of the armour layer and will therefore be constructed with a crown wall.

The under layer under layer prevents the core from washing out due to wave action through the pores between the armour units. The grading of the material of the under layer should be chosen in such a way that it does not wash out though the pores of the armour layer itself and that the core material does not wash out through the pores of the under layer. To accomplish this, the under layer should be designed according to the following guidelines: the W_{85} of the under layer should be smaller or equal to 1/7 W_{Xbloc}; the W_{50} should be in-between 1/9 and 1/11 W_{Xbloc} and the W_{15} should be larger or equal to 1/15 W_{Xbloc}. The density of the available core material is $2650kg/m^2$. This results in a grading with a D_{n15} equal or larger than 10.7 mm, a D_{n50} between 12.3 and 12.7 mm and a D_{n85} equal to or larger than 13.8 mm. With the available gradings in the lab it is not possible to fulfil all requirements. The grading which fits best consists of 30% $8 - 11.2mm$ stones and 70% $11.2 - 16mm$ stones. This gives a grading with a D_{n15} of 9.6 mm, a D_{n50} of 12.6 mm and a D_{n85} of 15 mm. [xbl(2008)]

The core should have a representative permeability. It should have a comparable permeability to a prototype breakwater. Usually the grading of the core material in the prototype is determined on the basis of the available material with an acceptable permeability. From the grading of the core, the needed grading of the under layer(s) is calculated using the filter rules of *Terzaghi*. Since there is no prototype breakwater for this research and the filter rules of *Terzaghi* can not be used in the model scale because of scale effects, a representative prototype is chosen to scale the core. The geometrical scale of the armour layer compared with the model unit of 49 gram is calculated and the core of the prototype breakwater is scaled with Froude scaling to find the grading for the core of the model according to *Burchardt (1999)*. The chosen prototype breakwater is a breakwater with an armour unit of $2.5m^3$, from the Xbloc design manual. For the Froude scaling, the excel sheet for Froude scaling of DMC is used. A representative grading for the core is 5.6 - 8 mm.

The toe of the breakwater should have a minor influence on the waves and give a stable basis for the armour units. Since the maximum number of rows of armour units on the slope is 20, a toe of about $55cm$ would be needed for a water depth of $70cm$. The best way to provide a stable basis for the armour, with minimal influence on the waves in model tests, is a toe of gabions or elastocoast. Because of the convenience of constructing tiles of elastocoast, this type of toe construction is chosen. The tiles are made of stones with a grading of $22.4 - 31.5mm$. They are glued together with epoxy instead of elastocoast, because this works as good as elastocoast and was directly available. The grading of $22.4 - 31.5mm$ gives geometrically closed under layer of good permeability. The tiles should be supported at the bottom by a small toe of large stones (larger than $31.5mm$).

The rear slope must be stable, so it does not influence the stability of the front slope and the rest of the breakwater. Therefore the rear slope will be constructed of the same epoxy tiles as the toe. The slope will be $3V : 4H$. The tiles can be placed directly on the core material, because they are also geometrically closed for this grading of stones.

At the walls of the wave flume, the interlocking between the armour units is decreased and therefore the stability is decreased. Because this does not occur in the prototype, instability of the armour units at the walls should be prevented. Movement parallel to the slope will be prevented by filling the gaps with large stones and movement perpendicular to the slope will be prevented by placing a metal chain along the sides of the armour layer.

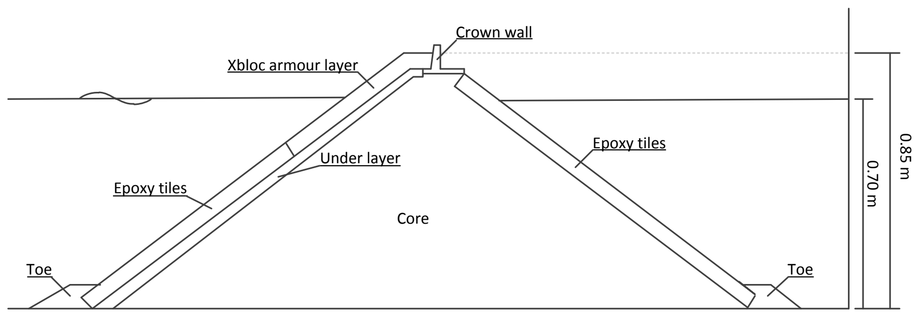

Figure 5.2: Model test breakwater lay-out

5.5 The wave load

The test programme will be focussed on wave series with different wave height distributions. But in accordance with the fundamentals of the test programme (section 5.3), the influence of wave steepness and groupiness of the waves should be included in the test programme to make it possible to separate the influence of these parameters from the influence of the wave height. Therefore, for every wave height distribution, wave series with two different steepnesses and two different groupinesses will be used to load the breakwater. To avoid the influence of the shape of the waves, the wave height distribution should be varied by handmade wave series. For the tests, 6 different wave height distributions are chosen based on the extreme and most common wave height distributions of existing model tests. The H_s of all wave series will be the design wave height of the 49 gram Xbloc calculated from equation 3.20, which is $9.95cm$. The target wave height distributions will be defined in terms of $H_{2\%}/H_s$ and $H_{0.1\%}/H_s$. Although the focus of this research is on the ratio between $H_{2\%}/H_s$, the $H_{0.1\%}$ is also considered generating the wave series. The ratio between $H_{0.1\%}$ and H_s is included, because the definition of H_{max} as $H_{2\%}$ is a hypothesis which should be proven or disproved. The results of tests with wave groups with the same $H_{2\%}/H_s$ and a different $H_{0.1\%}/H_s$ will show whether H_{max} is correctly defined. The highest waves in the spectrum are therefore also of influence and should be as realistic as possible.

The chosen ratios $H_{2\%}/H_s$ are the lowest occurring ratio of 1.15, the highest occurring ratio of 1.45 and the most common ratio of 1.35 in the existing model tests. The ratios $H_{0.1\%}/H_s$ are thereafter chosen based on the lowest and highest ratio regarding the model tests with the related $H_{2\%}/H_s$ ratio. Table 5.1 gives an overview of the target properties of the wave height distributions. To give an indication of the foreshore properties needed to affect a time series according to a Jonswap spectrum to this wave height distributions, the foreshore properties of the existing model test with an equivalent wave height distribution are given in table 5.1. It can be seen that particularly the relative water depth (ratio between water depth and significant wave height) influences the wave height distribution.

Table 5.1: Target wave height distributions for the wave series of the model tests and foreshore parameters of the existing model tests (e.m.t.) with an equivalent wave height distribution

target $H_{2\%}/H_s$	target $H_{0.1\%}/H_s$	slope fore shore equivalent e.m.t.	relative water depth equivalent e.m.t.
1.15	1.28	1:30	0.9
1.15	1.38	1:50	1.2
1.35	1.46	1:30	1.8
1.35	1.85	1:50	2.3
1.45	1.57	flat	3.4
1.45	2.03	1:60	4.5

After the target wave height distributions were determined from the wave height distributions of the existing model tests, wave series with the target wave height distribution in deep water were made. The method for making these wave series is described in the next section.

5.5.1 Method of making wave series

This section describes a practical way of creating time series with the desired wave height distribution.

The wave series used in the model tests are a summation of 5 to 8 sinusoids, because this is the minimum number of sinusoids needed to generate a cumulative wave height distribution with an acceptable smoothness (not stairs-like) and with the target ratios between the extreme wave heights. For the calculation of the wave height distribution a Matlab script is used. A combination of iterations and trial and error gave the needed wave series.

First, a kind of 'unit wave series' is created with the right wave height distribution. This unit wave series can be later modified with the right wave height and wave steepness. For each wave height distribution two different unit wave series are made: one with wave trains (to simulate a spectrum with a large groupiness) and one without wave trains (to simulate a spectrum with a small groupiness). The wave series without wave trains has no subsequent waves higher than H_s (and $H_{2\%}$), in other words, waves higher than H_s are followed up by a wave smaller than H_s. The wave series with wave trains have a mean wave train length (= group length) between 7 and 17 subsequent waves higher than H_s.

For the generation of the wave series some rules of thumb were found:

1. To generate a wave series with a smooth wave height distribution which includes waves with a smaller probability of exceedence than $H_{2\%}$ the wave series should contain around 1000 waves.

2. To provide a wave series of about 1000 waves with a large variation in wave height, the radian frequency should be chosen as a fraction of prime numbers close to the desired number of waves. For example $\frac{929}{1000}\ rad/s$ and $\frac{877}{1000}\ rad/s$. Because of the prime numbers, it just occurs once in a 1000 wave time record that all individual sinusoids have their top at exactly the same time and it occurs only once in a 1000 wave time record that the individual sinusoids have their troughs at exactly the same time. This makes the wave heights of the waves with a small probability of exceedance very diverse and manipulation of the wave height distribution becomes quite easy by only varying the amplitudes of the individual sinusoids. This makes it possible to generate wave series with a very specific wave height distribution for the highest waves.

3. A wave series with wave trains can be generated by subsequent prime numbers.

4. To generate a wave series without wave trains, the prime numbers should be chosen in groups of sequent prime numbers of which one group is much larger than the other. For example a group of prime numbers around 600, a group of prime numbers around 900 and a group of prime numbers around 1200.

5. With a phase of 0 for the sinusoids, the wave series starts with one of the highest waves. When the wave maker is starting up the waves are not exactly as prescribed. It takes about 5 waves to increase the movement of the wave maker to the prescribed movement. Because the focus of this research is on the highest waves it is important that these waves are as high as prescribed. Having the highest waves at the start is also not desirable for measurement purposes. So it is important that the wave series start with waves lower than H_s. This should be provided by the phase of the sinusoids.

6. The wave height distribution can be manipulated a bit by choosing the phase by including or excluding a specific part of the wave series. The best results are generated if the phases only make a time shift in the wave series. In that case, the phase of each sinusoid is the product of the time shift and the phase speed. Choosing different time shifts for the sinusoids will give lower ratios between $H_{2\%}$ and H_s, and between $H_{0.1\%}$ and H_s.

7. The main way to manipulate the wave height distribution is adjusting the individual amplitudes of the sinusoids.

When the 'unit wave series' is adjusted to the desired wave series at the toe of the breakwater, the corresponding wave series at the wave maker should be calculated. Because the water depth in the wave flume is not very shallow compared to the wave length, the waves with different phase speeds have different wave numbers. Therefore the time series of the wave group at the location of the wave maker differs from the time series at the toe of the breakwater. The individual sinusoidal waves can be described with the equation below, equation 5.1.

$$\eta(t,x) = a\, sin(\omega * t - k * x + \phi) \tag{5.1}$$

With:
η = water level elevation [m]
a = amplitude [m]
ω = radian frequency [rad/s]
t = time [s]
k = wave number [rad/m]
x = distance in propagation direction of the waves [m]
ϕ = phase [rad]

In this equation, the '$-k * x + \phi$' part is the location dependent phase of the sinusoid. To provide the desired wave height distribution at the toe of the breakwater, the wave numbers of the individual sinusoids are needed to calculate the phase of the individual sinusoids at the location of the wave maker. The wave number can be calculated from the linear dispersion relation, equation 5.2. [Holthuijsen(2008)]

$$\omega = \sqrt{k\, g\, tanh(k\, d)} \tag{5.2}$$

With:
ω = phase speed $[rad/s]$
k = wave number $[rad/m]$
d = water depth $[m]$
g = gravitation acceleration $[m/s^2]$

The specifications of the hand-made wave series can be found in appendix D. The wave series are described as a sum of 8 sinusoids (equation 5.3) with an amplitude vector (a), a radian frequency vector (ω), a phase vector at the location of the breakwater (φ_{bw}) and a phase vector at the location of the wave maker (φ_{wm}).

$$\eta(t, x = x_{wavemaker}\, or\, x_{breakwater}) = \sum_{1=1}^{8}(a_i\, sin(\omega_i\, t + \varphi_i)) \qquad (5.3)$$

5.6 Test programme

For every wave height distribution from table 5.1, four different wave series are made. Four different combinations of a wave steepness of 0.03 or 0.05 and with or without wave trains. To show to which extent the results from the tests with these wave series are comparable with a situation with wave series from a Jonswap spectrum, the test program will be extended with a deep water wave series from a Jonswap spectrum with both steepnesses. This results in a test programme of 26 different wave series. An overview of these test series can be found in table 5.2. The name of the wave series are given as the value of $H_{2\%}/H_s$ (for example 115128 means that $H_{2\%}/H_s$ = 1.15 and $H_{0.1\%}/H_s$ = 1.28), the value of $H_{0.1\%}/H_s$ (for example 115128 means that $H_{2\%}/H_s$ = 1.15 and $H_{0.1\%}/H_s$ = 1.28, the presence of wave trains (yes=g/no=ug) and the wave steepness. Further in this report these names will be used to refer to these wave series.

The specifications of these wave series are given in appendix D. A plot of the wave height distribution and time series of the different wave series can be found in appendix C.

The armour layer of the model has a quasi-random placement. Because for a quasi-random placement some variation in the stability of the units is expected, the test series will be repeated 4 times with a rebuild armour layer to gain an average stability of the units and increase the statistical reliability of the results. This results in a test programme of 104 wave series of 1000 waves. The (re)built armour layer will first be loaded by a series of small waves, smaller than H_s, to simulate the daily wave load and induce settlements of the armour units due to the daily wave load. The sequence of the wave series will be shuffled after every replacement of the armour layer to ensure that the sequence of testing does not influence the test results. During the tests, rocking will be marked manually, based on visual observations, with a pulse through one of the unused wave gauges. The signal of the pulse is recorded together with the signal of the wave gauges which measure the water level elevations. Which unit is rocking will be written down in a lab journal. This way, the waves which caused rocking can be analysed in detail afterwards. Because the individual waves will be analysed it is expected that the effects from the manually made wave series are comparable to the wave series of a Jonswap spectrum. It is important that this expectation is first verified before the test data can be used for further analysis.

Table 5.2: Properties of the wave series

Name wave series	$H_{2\%}/H_s$	$H_{0.1\%}/H_s$	wave trains (yes/no)	wave steepness
115128g3	1.15	1.28	yes	0.03
115138g3	1.15	1.38	yes	0.03
135146g3	1.35	1.46	yes	0.03
135185g3	1.35	1.85	yes	0.03
145157g3	1.45	1.57	yes	0.03
145203g3	1.45	2.03	yes	0.03
115128ug3	1.15	1.28	no	0.03
115138ug3	1.15	1.38	no	0.03
135146ug3	1.35	1.46	no	0.03
135185ug3	1.35	1.85	no	0.03
145157ug3	1.45	1.57	no	0.03
145203ug3	1.45	2.03	no	0.03
115128g5	1.15	1.28	yes	0.05
115138g5	1.15	1.38	yes	0.05
135146g5	1.35	1.46	yes	0.05
135185g5	1.35	1.85	yes	0.05
145157g5	1.45	1.57	yes	0.05
145203g5	1.45	2.03	yes	0.05
115128ug5	1.15	1.28	no	0.05
115138ug5	1.15	1.38	no	0.05
135146ug5	1.35	1.46	no	0.05
135185ug5	1.35	1.85	no	0.05
145157ug5	1.45	1.57	no	0.05
145203ug5	1.45	2.03	no	0.05
Jonswap3	1.48	1.94	yes	0.03
Jonswap5	1.40	1.85	yes	0.05

Chapter 6

Model tests

This chapter describes the execution of the model tests, the encountered problems and phenomena and the observations made during model testing.

6.1 Calibration of the wave generation

Before the wave groups can be used to load the model, the wavemaker should be calibrated in the flume. It should be tested whether the incident time series in the flume match the theoretical time series. The water level elevation will be measured with 3 wave gauges, because a reflection analysis is necessary to distinguish the incoming from the reflected waves. For this reflection analysis Wavelab is used. The calculations of this computer programme are based on the reflection theory of *Mansard and Funke (1983).* Because the wave gauges are positioned in a line parallel to the length of the flume, only waves in length direction of the flume will be found with the reflection analysis. Since the surface of an armour layer of a breakwater is quite rough, the waves will be reflected in more directions than only the direction of the length of the flume. This will cause an inaccuracy in the reflection analysis. When waves are generated in a flume without a structure the appearance of standing waves is very likely, also the reflections can be so large that the wave maker can not entirely absorb the reflected waves. Therefore the waves are first calibrated with a reflection sponge at the end of the flume. This sponge absorbs a part of the waves. The reflected part will be in length direction of the flume, like the incoming waves, because the sponge has a smooth surface. This ensures a much more accurate reflection analysis. The wavemaker is controlled with an input file, which contains a description of the force the wave maker should produce on the water. Since the same input file generates exactly the same time series at the wave maker, it is best to calibrate the waves without structure. For the measured waves in the flume a maximum deviation of 5% of the wave height distribution compared to the theoretical wave height distribution is allowed. Allowing a smaller deviation is not realistic since the reflection analysis has, even with a wave sponge, an error up to 5%.

The first tests gave time series which mismatched with both the theoretical time series and wave height distribution. To find the cause of this mismatch a number of conceivable causes were considered and tested. This is described in

Appendix C. The main cause of the deviations was found in the description of sinusoids and the rounding of frequencies by the control program of the wave maker. So the largest part of the deviations could be addressed by rewriting the control files, driving the wave maker. The final control files gave deviations in the order of 2%, which is more accurate than the expected highest attainable accuracy. The properties of the wave height distributions of the waves in the flume compared with the desired wave height distributions are given in table 6.1. Four of the wave series have a larger deviation than 5% for one or more parameters. In case of wave series 135185ug3, this deviation originates from a high location dependency of the highest waves. At small distance from the calculated location a jump occurred in the wave height distribution, $H_{2.1\%}$ still has the desired wave height, only $H_{2\%}$ has not. Because only one wave differs, this is no problem and this wave series can be used for model testing. The other three wave series deviate because the waves break on their way from wave maker to breakwater. This type of wave breaking is much like white capping. The cause of this white capping seems to be the large difference in propagation speed of the mutual harmonics. The waves seem to become too steep very locally by overtaking waves. The remedy for this white capping is decreasing the wave steepness or decreasing the differences in propagation speed of the individual waves. Both remedies will change the wave series in a wave series which already exists in the test programme; leaving the tests with white capping give wave height distributions which already exist in the test programme. These tests appear to be irrelevant and will not be used in the test programme.

6.2 Activities during model testing

After the calibration of the waves, the breakwater is built in the flume. The front toe of the breakwater is built at the location of the rear wave gauge during the calibration. Because the breakwater influences the waves and the reflection analysis needs a homogeneous wave field along the three wave gauges, it will make no sense to measure the waves in that location during the tests. Therefore the wave gauges will be placed one meter in front of the breakwater.

Placement of the armour layer

The placement procedure of the armour layer is as follows. The bottom row is regularly placed, all Xblocs have the same orientation, the nose is supported by the tile of elastocoast and two legs are supported by the first under layer. The distance between the centre of gravity of two neighbouring units is 1.3 times the width of the units. The units of the row on the top of the bottom row are placed in between two units of the bottom row. One of the legs of the unit should point down between the units underneath. The orientation of the units should be random. The rest of the units on the slope are placed like the second row. The mean distance between the centre lines of two rows should be 0.63 times the width of the units. The colour of the rows is varied to make the placement of the armour layer easier, to make rocking more visible and to make it easier to see which particular unit is rocking. The placement of a completed armour layer is shown in figure 6.1.

Near the walls of the flume the interlocking between the units is decreased.

Table 6.1: Properties of the wave series in the flume

wave trains, a wave steepness of 0.03 and an H_s of 99.5 mm							
desired		occurred			relative deviation		
$H_{2\%}/H_s$ $[-]$	$H_{0.1\%}/H_s$ $[-]$	H_s $[mm]$	$H_{2\%}/H_s$ $[-]$	$H_{0.1\%}/H_s$ $[-]$	H_s $[\%]$	$H_{2\%}/H_s$ $[\%]$	$H_{0.1\%}/H_s$ $[\%]$
1.15	1.28	98.69	1.12	1.25	-0.81%	-2.99%	-2.32%
1.15	1.38	97.69	1.17	1.39	-1.82%	1.39%	0.44%
1.35	1.46	99.75	1.37	1.48	0.25%	1.29%	1.35%
1.35	1.85	99.56	1.35	1.86	0.06%	0.37%	0.66%
1.45	1.57	98.2	1.46	1.59	-1.31%	0.78%	1.25%
1.45	2.03	101.9	1.44	1.98	0.90%	1.94%	-1.82%
no wave trains, a wave steepness of 0.03 and an H_s of 99.5 mm							
desired		occurred			relative deviation		
$H_{2\%}/H_s$ $[-]$	$H_{0.1\%}/H_s$ $[-]$	H_s $[mm]$	$H_{2\%}/H_s$ $[-]$	$H_{0.1\%}/H_s$ $[-]$	H_s $[\%]$	$H_{2\%}/H_s$ $[\%]$	$H_{0.1\%}/H_s$ $[\%]$
1.15	1.28	100.1	1.16	1.28	0.60%	0.94%	0.21%
1.15	1.38	99.76	1.17	1.37	0.26%	4.77%	-1.07%
1.35	1.46	101.6	1.36	1.44	0.25%	1.29%	1.35%
1.35	1.85	101.2	1.50	1.88	1.71%	11.11%	1.86%
1.45	1.57	97.04	1.44	1.46	-2.47%	-0.93%	-0.63%
1.45	2.03	100.4	1.48	1.99	0.90%	1.94%	-1.82%
wave trains, a wave steepness of 0.05 and an H_s of 99.5 mm							
desired		occurred			relative deviation		
$H_{2\%}/H_s$ $[-]$	$H_{0.1\%}/H_s$ $[-]$	H_s $[mm]$	$H_{2\%}/H_s$ $[-]$	$H_{0.1\%}/H_s$ $[-]$	H_s $[\%]$	$H_{2\%}/H_s$ $[\%]$	$H_{0.1\%}/H_s$ $[\%]$
1.15	1.28	102.1	1.15	1.30	2.61%	-0.01%	1.39%
1.15	1.35	102.8	1.18	1.42	3.32%	2.53%	2.84%
1.35	1.46	102.2	1.36	1.47	2.71%	0.89%	0.66%
1.35	1.85	100.9	1.37	1.86	1.41%	1.24%	0.72%
1.45	1.57	102.2	1.46	1.59	2.71%	0.55%	1.21%
1.45	2.03	102.4	1.42	2.01	2.91%	-2.34%	-0.76%
no wave trains, a wave steepness of 0.05 and an H_s of 99.5 mm							
desired		occurred			relative deviation		
$H_{2\%}/H_s$ $[-]$	$H_{0.1\%}/H_s$ $[-]$	H_s $[mm]$	$H_{2\%}/H_s$ $[-]$	$H_{0.1\%}/H_s$ $[-]$	H_s $[\%]$	$H_{2\%}/H_s$ $[\%]$	$H_{0.1\%}/H_s$ $[\%]$
1.15	1.28	100.5	1.14	1.30	1.01%	-0.58%	1.45%
1.15	1.38	103.9	1.24	1.40	4.42%	8.13%	1.20%
1.35	1.46	97.39	1.31	1.43	-2.12%	-2.80%	-2.17%
1.35	1.85	104.6	1.39	1.51	5.13%	3.11%	-18.14%
1.45	1.57	96.66	1.30	1.45	-2.85%	-10.03%	-7.94%
1.45	2.03	104.4	1.31	1.62	4.92%	-9.37%	-20.07%

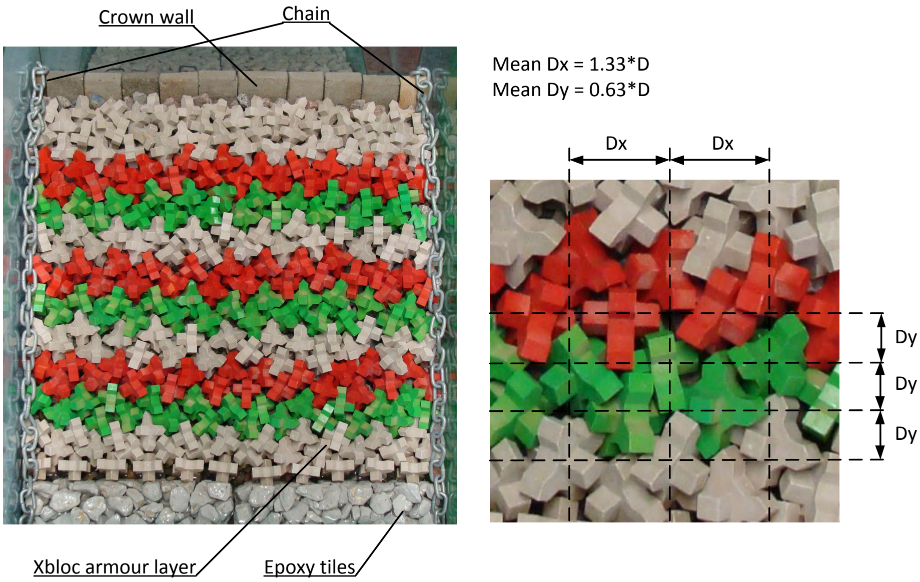

Figure 6.1: Placement of the armour layer

Therefore the gaps are filled with stones and covered with a metal chain to give the units at the side a comparable stability to the rest of the units.

Training

First the armour layer is built two times to practice the placement of Xbloc. These armour layers are also used to practice in noticing rocking. It needs some training to see every rocking unit. Thereafter the Xbloc armour layer is removed, the under layer is levelled and the armour layer is replaced.

Test procedure

Before the armour layer is loaded by the first wave series, the distance between the centre of the bottom layer and the 18th row (from the bottom) is measured to calculate the relative packing density. The relative packing density (RPD) is the packing density relative to the theoretical (required) packing density as can be calculated with equation 6.1.

$$RPD = \frac{(N_x - 1)(N_y - 1) * D_x * D_y * D^2}{L_x * L_y} * 100\% \tag{6.1}$$

with:
N = number of units in x respectively y direction
d = the distance between the centre points of the units in x/y direction relative to the width of the unit
D = width of the unit (figure 3.11)
L = Width of the slope in x respectively y direction

The armour layer is also photographed. The RPD and photographs can both be used to gain information about the settlements of the armour layer over a test. Thereafter the wave flume is filled with water. The breakwater will first be loaded by a wave series of 60% of the first test series. This is done to induce settlements which occur in daily wave conditions. After the test, the water level in the flume is decreased till just below the armour layer to photograph it and to measure the height of the armour layer. The wave flume is filled again and the breakwater is loaded by the first wave series. The test is recorded with two camera's, one at the top of the wave flume and one at the side. During the test every wave which caused rocking of one or more units is marked with a pulse signal recorded by one of the unused wave gauges for wave measuring. At the start of every test a marker is visible in front of the camera marked, to be able to synchronise the videos with the measured data. After the test, the water level is decreased again under the armour layer, the armour layer is photographed and the height of the armour layer is measured. Which units moved during the test is noted together with a short description of the observation. After filling the flume with water, the breakwater is loaded by the second wave series. This procedure is repeated till the breakwater is loaded by all 23 tests. When the breakwater is loaded by all wave series, the armour layer is removed. The first under layer, elastocoast tiles, toe, crown and crown wall are checked for damage and settlements. If needed, the breakwater is repaired. Thereafter, the first under layer is levelled and the armour layer is rebuilt. The test procedure is repeated for the rebuild armour layer. In total the breakwater is loaded 4 times with the 23 wave series of 1000 waves each on a rebuilt armour layer.

6.3 Observations during model testing

Low relative packing density

The first placed armour layer showed heavier rocking and more settlements than expected after the first 9 wave series. Additionally one of the units displaced from the armour layer during the wave series with the highest $H_{0.1\%}$. This can indicate that the armour layer was placed with an insufficient RPD. Since the calculated RPD was 99.9%, this should not have given any problems. The RPD might be not correctly calculated due to the use of an incorrect width of the armour unit in the formula. To check whether this is the cause of the heavy rocking and settlements in the first number of wave series or that this is just normal armour layer behaviour, the width (D) of the Xbloc is checked before the new armour layer is placed and loaded. It appeared that the width indeed slightly differed from the previously used width for the packing density determination of the first armour layer placed. The width appeared to be 39.55mm instead of 40.00mm, which results in an insufficient RPD of the first repetition of 97.6%. To ensure that the following armour layers are placed with a correct packing density in horizontal direction a wooden slat is placed between the armour units and the wall at one side, to slightly decrease the width of the wave flume. The next 3 repetitions are placed with the right relative packing density.

General observations

The visual observations and analyses of rocking of Xblocs without analysing the measured wave and displacement data will be described below.

Rocking occurs during run-up. The armour unit rotates up when the flow velocity is directed upward, during run-down the unit rotates back to its original position.

The 60% tests did not cause rocking or visible settlements.

Observing rocking is not possible above the 10th row from the bottom. Because the layer of water in the run-up and run-down above row 10 is very thin and the flow of a thin layer over a rough surface produces a lot of bubbles, rocking is simply not visible in that area.

Damage of the first under layer is only observed after the first repetition. When the armour layer was removed, a small erosion pit was visible at the location where a unit displaced from the slope. The material of the first under layer was not displaced from the slope, but spread over the slope. The other repetitions showed a smooth first under layer after the removal of the armour layer.

The elastocoast tiles showed no settlement, displacement or damage after the tests.

The crown wall did not show settlements, displacements or damage after the tests.

The core showed minor settlements after a test series, which was supplemented for the following test series with a replaced armour layer.

The self healing effect of an armour layer with Xbloc was clearly visible after the displacement of a unit during the first repetition (where the RPD was too low). The neighbouring units settled and the armour layer showed no further displacement of units during the following high waves.

A destructive test with waves of four times the design wave height was performed after all tests were completed. This showed that first a lot of units displaced from the middle of the armour layer. When a large gap in the armour layer arose, the first under layer started to wash out. When a large part of the first under layer and the core were washed out, the crown wall displaced and at last the elastocoast tiles displaced. From this it can be concluded that the model is correctly designed according to the target described in section 5.4 for designing the toe, rear slope and crown wall. Namely that the breakwater should be designed in such a way that instability of the armour layer is not caused by instability of one of the other parts of the breakwater. It also showed that the chain worked well to compensate for the reduced interlocking at the walls of the flume.

Chapter 7

Data analysis

The analysis of the measurement data of the model tests is described in this chapter. The hypothesis of a ‘boundary wave height’ for rocking will be evaluated according to the test results. This will show whether $H_{2\%}$ is indeed a better parameter for the wave height to include in the design formula. Also the influence of the steepness of the waves and the groupiness of the waves will be evaluated to find a clear relation between rocking and wave height. Thereafter, an advice to adjust the design formula will be given, if this is required according to the test results. Before the test data can be analysed, the data should be arranged and processed to make it useful. This is described in the first section of this chapter.

7.1 Processing the data for the analysis

As described in section 6.2, a lot of information is collected during the model tests. This data should be processed to make it useful for analysis.

The photo’s, notes and RPD

The photo’s of the armour layer after each test are combined with the noted observations of the test in a powerpoint sheet. In these photo’s, the units which moved are marked and the relative packing density (RPD) is calculated from the measured mean distance between the centre point of the units of the bottom row and the 18th row from the bottom with equation 6.1. Switching between the power point sheets shows clearly which units settled over the test, the relation between settlements and rocking and an overview of the rocking and settlement development along all tests.

The wave data and markers

The processing of the wave data was more complex. During the tests the waves are measured a meter in front of the toe of the breakwater. Measuring the waves at the toe of the breakwater would give irrelevant measurements since the waves there are already influenced by the breakwater and for a design, only non-disturbed waves are available. Moreover, the reflection analysis of the waves is less accurate with a breakwater in the flume than during calibration (section

6.1). Since the wave maker produces exactly the same waves with the same input file and absorbs the reflected waves almost perfectly, using the time series of the calibrated waves will give more accurate results than when the time series of the tests are used. The time series of the tests will only be used to check if the right input file is used and to extract the marker for rocking waves.

The marker for rocking waves should be combined with the time series of the calibration of the corresponding wave series of the test. To check whether the wave maker produces exactly synchronous time series, the produced force of the wave maker for the first 30 seconds (till the first reflected wave enters the wave maker) is compared. This is exactly synchronous for the time series of the tests and corresponding time series of the calibration.

Hereafter, the incoming waves are separated from the reflected waves with wavelab. For the resulting time series, it should be checked if it is still synchronous with the data of the tests (for combining the marker with the waves). This is done using the calculated wave series at the wave maker and at the toe of the breakwater. The force of the wave maker was 36 data points behind the calculated series and the time series from wave lab was also 36 data points behind the calculated wave series at the toe of the breakwater. This means that the wave series from wavelab can be combined with the marker from the test data.

Although the wave series and the markers are synchronous, the markers still do not mark the right wave in the time series. The following points should be accounted for:

1. The waves are measured at the location of the toe of the breakwater. Rocking is observed when the waves break at the slope of the breakwater, when the waves have travelled a meter further.

2. From the observations during the tests it followed that rocking consists of instability of the unit during run-up which tilts the unit up and a reverse velocity during run-down which enables the unit to fall back in its previous position. The falling back of the unit is better visible, because the water is less turbulent during run-down. Which means that rocking is always marked during run-down. Since a wave is defined between two downward-zero-crossings the markers are located near the boundary between two waves and therefore quite often in the wrong wave.

3. During the tests with wave series without wave trains, the unit lifts up during run-up of the large wave and falls back during the run-down of the subsequent small wave. Since the run-up is the cause of rocking, the wrong wave is marked.

4. Because a marker is a pulse of more than one datapoint, the marker overlaps sometimes two waves.

5. It happens that two markers are located in the same wave, while just one of these markers belongs to this wave. In this case the other marker belongs to the previous wave.

6. The data of the markers contains noise. If there is no pulse sent through the wave gauge, the value of the marker data is not always 0.

These points are accounted for by the following modifications of the marker data. The modifications are illustrated in figure 7.1.

The noise is removed by replacing the pulse by 1 and the other data points with 0 (to account for point 6).

The pulse is reduced to one data point to avoid a pulse overlaps multiple waves (to account for point 4).

The travel time from toe to location where the waves break is estimated with the mean propagation speed of the waves. Analysing the video's of the tests, this is approximately correct. For this shift of the marker no high degree of accuracy is needed, since the marker only has to mark the right wave, and not necessarily the right data point (to account for point 1).

The marker is shifted 1/4 wave period back to avoid the marker being near the boundary between 2 waves (to account for point 2).

The marker is replaced to the nearest top of the waves to avoid 2 markers within one wave (to account for point 5).

For wave series without wave trains and the Jonswap spectra, the marker is moved to the largest one of the wave with marker and the previous wave (if this previous wave is not marked itself). (to account for point 3)

The waves which caused rocking can now be distinguished correctly from the waves which did not cause rocking.

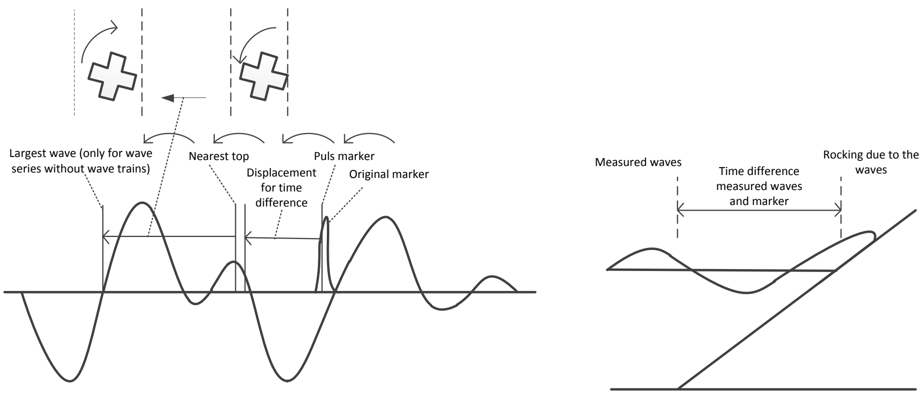

Figure 7.1: Illustration of the modification of the marker

The video's

To find the number of rocking units for every marker, the recorded video at the side of the flume is used. To make the counting of rocking units easier, more accurate and less time consuming for every marker a small part of the recorded video is extracted by Matlab. The extracted video is 8 seconds and the time when the observed rocking is marked is at the fourth second of the video. These small videos could be extracted this accurately by using the unprocessed marker data. First, the video of every test is synchronised with the marker data by the first marker. As described in section 6.2 this marker is visible in the video. Thereafter, for every marker the short video of 8 seconds is extracted at the corresponding point of time of the marker. In this case there is no need for processing the marker, since rocking is visible on the video at the same time it is visible for the observer.

7.2 First findings from the data analysis

For all tests, the waves which caused rocking and the waves which did not cause rocking are separated. To visualise the cause of rocking, the time series of the waves are plotted together with the processed marker. The wave heights, the wave heights with rocking and the wave heights without rocking are illustrated in histograms. An example is given in figure 7.2 and 7.3 for wave series 145203g3 of the third repetition of the tests.

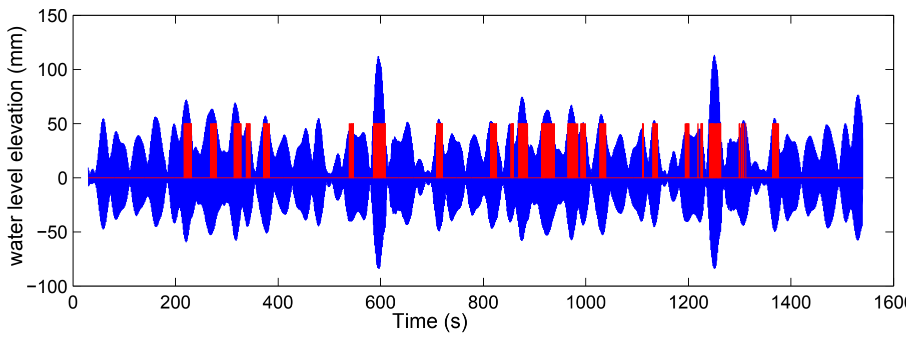

Figure 7.2: Time series of 145203g3-repetition3 in blue, with the markers in red

When the results of all tests are studied together with the information about the settlements and notes of the tests, the following is noticed:

1. For 88% of the waves, one or more units are rocking during more than 2% of the waves.

2. Whether the armour layer suffices the rocking requirement *'Not more than 2% of the units are allowed to rock during more than 2% of the waves'* for a test can not be directly concluded from this data. Since the marker indicates one or more units are rocking of the tested armour layer of 220 units.

3. In 32% of the tests is during more than 30% of the waves rocking observed of one or more units. This always appeared during tests after a test series with the highest $H_{2\%}/H_s$ ratio of 2.03. It never occurred in test series where none of the previous tests had a $H_{2\%}/H_s$ ratio of 2.03.

4. In 3 of the 4 repetitions, one of the test series with a $H_{2\%}/H_s$ ratio of 2.03 dislodged a unit, which moved during more than 30% of the waves of all subsequent test series.

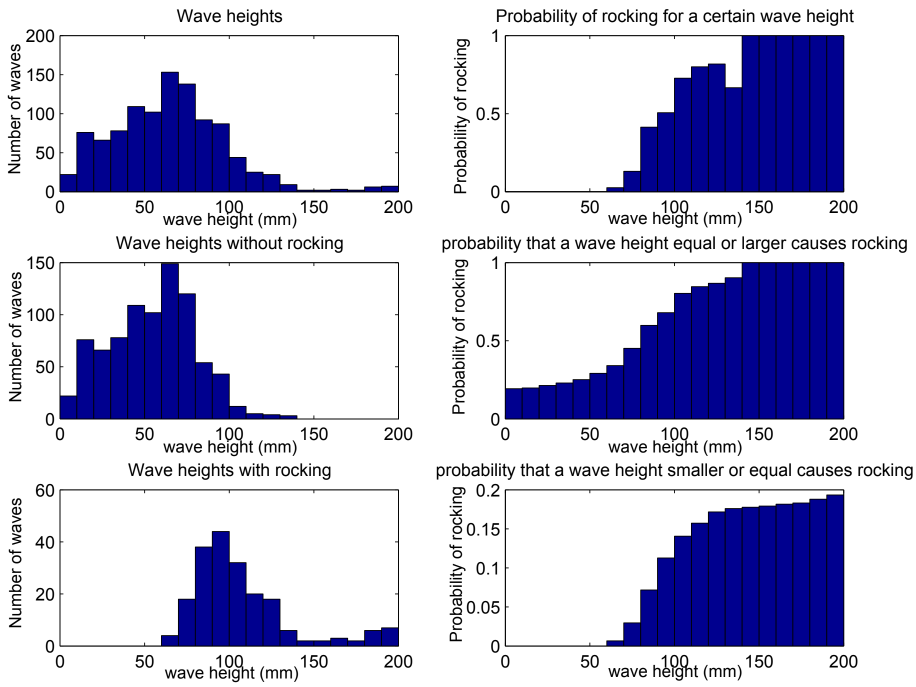

Figure 7.3: Waves with and without rocking for test series 145203g3-repetition3

5. The wave series with higher $H_{2\%}/H_s$ and $H_{0.1\%}/H_s$ ratios gave more rocking than the wave series with lower ratios, if none of the units was dislodged.

6. The pictures of the armour layers before and after a test showed that rocking is related to uneven settlements. When a unit started with rocking in a test, the unit itself had not visibly settled during the test while the neighbouring units did. Or the rocking unit had settled visibly and the neighbouring units did not.

7. The first wave which causes rocking is much higher than the last wave which causes rocking in a sequence of rocking inducing waves. This is illustrated in figure 7.4.

8. For an armour layer placed with a relative packing density (RPD) below 100%, the amount of rocking for the first tests is clearly larger than for an armour layer placed with the right RPD. When the units of the armour layer with a low RPD are settled to an RPD larger than 101% the rocking behaviour seems comparable to the tests of the repetitions with an RPD of 100% after placement.

9. A clear 'boundary wave' for rocking, as expected in the hypothesis of this research, is not found. The overlap of waves which cause rocking and which does not is large. For example for the test of figure 7.3, wave heights between $60mm$ and $140mm$ sometimes cause rocking (but not always).

10. The first wave heights of a group of rocking waves (the first wave in figure 7.4) also gives no clear ‘boundary wave’. The wave heights are within a range of a few cm, but there is a large amount of waves within the same range which cause no rocking.

11. The reason a wave sometimes causes rocking is sought in the steepness of these individual waves, the height of the top of the wave, the height of the trough and the previous wave. None of these give a clear explanation.

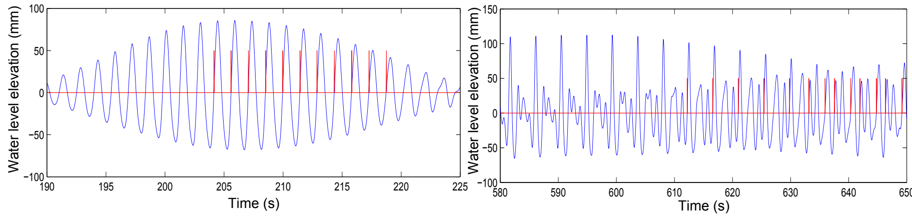

Figure 7.4: Sequent waves which cause rocking for a wave series with and without wave trains (red line is the rocking marker)

7.2.1 First results and expectations

The hypothesis that there is a better parameter for the design wave height to describe rocking than H_s and the hypothesis that there is a ‘boundary wave height’ for rocking will be evaluated regarding the first findings of the model tests.

All used wave series had the same design H_s, but the response of the armour layer on the wave load differed. Especially for the waves with the largest $H_{0.1\%}/H_s$ where another mechanism occurred than just rocking. The highest waves of these series dislodged units of the armour layer which thereafter almost continuously rocked. From this observation it can be concluded that H_s is indeed not a well fitting parameter. However the hypothesis of a ‘boundary wave’ for rocking needs to be more nuanced. There seem to be 3 categories of ‘boundary waves’ for rocking:

1. A ‘boundary wave height’ for rocking as described in the original hypothesis (the mean value is approximately $120mm$ during the model tests).

2. A ‘boundary wave height’ for dislodgement of units (the value is larger than $185mm$ during the model tests).

3. A ‘boundary wave height’ for rocking of dislodged units (the mean value is approximately $70mm$ during the model tests).

The concept ‘boundary wave’ itself needs to be nuanced too. Since the overlap between waves which cause rocking and which does not is quite wide, it seems more likely that every wave height has a certain probability of causing rocking of a unit. According to these first findings it can be concluded that the concept ‘boundary wave’ does not exist due to the following mechanism:

> Every wave loads the armour layer of the breakwater. This causes (very small) disturbances of the placement of the units. The larger the wave load, the larger the disturbance. Because the first under layer is not smooth and homogeneous, the settlements of the units due to the same load will differ. Uneven settlements influence the interlocking between the units. A unit will start rocking when the unloaded position of the unit differs from the position where it is kept in place by neighbouring units. In other words, when there is some space for rotation of the unit before it touches the neighbouring units. Uneven settlements of the armour layer will increase or decrease the space which allows rocking. Besides the rotational space between the units the settlements also influence the position of a unit on the under layer. Since the under layer is not smooth and homogeneous, the units can have a different stability on a different position. Whether a certain wave load causes rocking is dependent on the settlements caused by the previous waves.

This rocking stability mechanism holds until a large wave of category 2 dislodges a unit. Then the following mechanism occurs:

> This wave height causes very large disturbances, which distorts the placement of the armour layers in such a way that units are dislodged and do not interlock any more. When the position on the first under layer has changed in a negative way as well, these units are rocking for practically every wave afterwards.

The further analysis will be based on these two mechanisms of instability of Xbloc. Whether a wave causes rocking or not will have a certain probability, with a higher probability for higher waves. Combining the rocking probability with the criterion for rocking will result in a new design formula. The analysis based on this concept is described in the next section. The analysis of waves which can dislodge a unit is less accurate, since there are only 3 events where this happened to base the analysis on. A more detailed analysis on this phenomenon is therefore not possible with this data. Although it is advised to increase the Xbloc size when waves occur in the design wave conditions which can dislodge units, i.e. when waves larger than 1.85 times the design H_s occur in the time series.

7.3 Sorting of relevant tests

In the previous section it is mentioned that during 30% of the tests at least one of the units was dislodged. Because dislodgement of units is not desirable the Xbloc size should be increased when waves which can dislodge a unit occur. Since the rocking probability should be focussed on rocking of interlocking units and not on rotational movement of dislodged units, the tests with a dislodged unit should not be used for the analysis of rocking probability. It can separately be used to investigate the rocking probability of units with a lack of interlocking. In the previous section it is also mentioned that the armour layer with a too low relative packing density showed more rocking during the first tests. The relevance of these tests should be investigated first to determine whether these tests can be used for the analysis of rocking.

7.3.1 Influence of the relative packing density

The armour layer of the first repetition was placed with a too low relative packing density. The results of the first 9 tests gave a larger probability of rocking than the first tests of the other repetitions. This is shown in figure 7.5. The probability of rocking is calculated by dividing the number of waves which caused rocking by the total number of waves within a bin of wave heights with a band width of $10mm$. The tests of repetition 2, 3 and 4 are combined because those repetitions contain only one test with a RPD between 97% and 101%. It can be seen that the probability of one or more units rocking of the armour layer is much higher for repetition 1 compared to the other three.

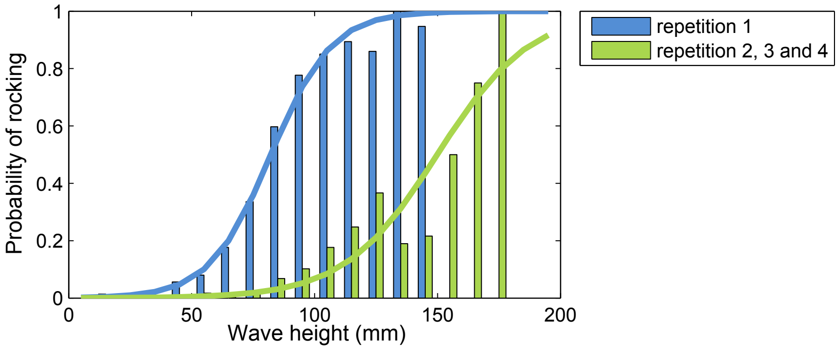

Figure 7.5: Comparison rocking probability of the different repetitions for all tests with an RPD between 97% and 101%

It is also noticed that the amount of waves which cause rocking decreases due to settlements, for the tests of the first repetition. When the armour layer is settled to an RPD over 101%, the amount of waves which cause rocking is stabilised. The repetitions which are placed with a RPD of 100% do not show a larger rocking probability for the first tests. The tests of the first repetition where the relative packing density is increased to 101% due to settlements gave more or less the same probability of rocking as for the tests of the other repetitions, this is shown in figure 7.6. Repetition 4 is not used because during the second test a unit was dislodged, so it is not relevant to compare the tests of repetition 4 in this case. It can be seen in figure 7.6 that the probability of rocking for the first repetition does not deviate much from the other repetitions any more. The tests of repetition 1 with an RPD larger than 101% are representative.

Conclusion

The first 9 tests of repetition 1 (which was placed with a too low RPD) are not representative for research on rocking of Xbloc armour units. The tests of repetition 1 where the armour layer is settled to an RPD larger than 101% show the same rocking behaviour as the tests with the right RPD and are therefore representative for the research. The 9 tests with a different rocking behaviour show the influence of placement with a low RPD. It can be concluded that placement with a lower RPD than the placement specifications describe, is not favourable, because it results in more rocking of more units. After 9 tests is the

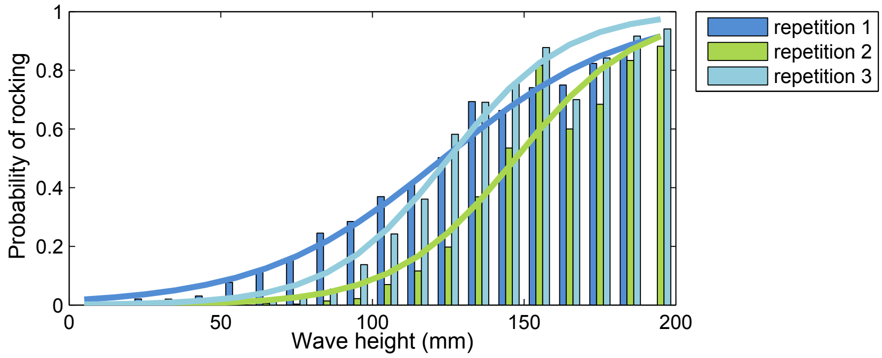

Figure 7.6: Comparison rocking probability for the tests with an RPD between 101% and 104%

armour layer settled, this is a wave series of approximately 9000 waves. Since a design storm is approximately 5,000-6,000 waves, an armour layer with a low packing density will show heavier rocking during the entire design storm than an armour layer placed according to the placement specifications.

7.3.2 Set of tests for analysis

For the analysis of rocking, the tests with a dislodged unit and with an other rocking behaviour due to a low RPD after placement can not be used. The test series which can be used for rocking analysis are shown in table 7.1. The utility of the remaining tests are shown in table 7.2.

Table 7.1: Relevant test series for rocking analysis

Wave series	repetition				Wave series	repetition				Wave series	repetition			
	1	2	3	4		1	2	3	4		1	2	3	4
115128g3			○		135146g3	○	○	○		145157g3	○	○	○	○
115128g5			○		135146g5	○	○	○		145157g5	○	○	○	
115128ug3			○		135146ug3		○	○		145157ug3	○	○	○	
115128ug5			○		135146ug5	○	○	○						
115138g3			○		135185g3	○	○	○		145203g3	○	○	○	◖
115138g5			○		135185g5	○		○		145203g5	◗	◖	○	
115138ug3			○		135185ug3	○	○	○		145203ug3	○	○	○	
115138ug5			○		JONSWAP3	○	○	○		JONSWAP5	○	○	○	

○ Test is used
◖ First half of the test is used
◗ Second half of the test is used

7.4 Probability of rocking

In this section the relation between the probability of rocking for an Xbloc and the height of the waves will be evaluated. The influence of the parameters: wave steepness breaker type of the waves on the breakwater (which is related

Table 7.2: Relevance of the other tests

Wave series	repetition				Wave series	repetition				Wave series	repetition			
	1	2	3	4		1	2	3	4		1	2	3	4
115128g3	∴	○		○	135146g3				○	145157g3				
115128g5	∴	○		○	135146g5				○	145157g5				○
115128ug3	∴	○		○	135146ug3	∴			○	145157ug3				○
115128ug5	∴	○		○	135146ug5				○					
115138g3	∴	○		○	135185g3				○	145203g3				◗
115138g5	∴	○		○	135185g5		†		○	145203g5	⊠	◗		○
115138ug3	∴	○		○	135185ug3				○	145203ug3				○
115138ug5	∴	○		○	JONSWAP3				○	JONSWAP5				○

○ Can be used for analysis of dislodged units
◗ Second half of the test can be used for analysis of dislodged units
∴ Low RPD, shows the influence of the RPD after placement of the armour layer
⊠ Unit dislodged and removed from slope, shows wave height for dislodgement and self healing effect of the armour layer, can not be used for the detailed analysis
† Corrupt datafile, can not be used

to the steepness) and the presence of wave trains will be investigated. Whether the wave height distribution influences the relation between wave height and rocking probability will be investigated too. First a global analysis will be made in section 7.4.1. This analysis is based on the fit of histogram data like in section 7.3.1 with the evaluation of the influence of the RPD. This visualises the influence of the parameters and gives insight in the rocking behaviour of the Xblocs in the model tests. But this only gives the probability for rocking of one or more units in the tested slope. To acquire a design formula from the rocking criterion and the test results the probability of rocking of an individual unit is required. This will be done by logistic regression based on the maximum likelihood and is described in detail in section 7.4.2.

7.4.1 Global analysis

The waves of the tests are plotted in a histogram according to their height. Also the waves which cause rocking are plotted in a histogram. The probability of rocking is calculated by dividing the number of waves causing rocking by the total number of waves in every bin of the histogram. Comparing parameters can be done by sorting the tests for a particular property of the wave series, combining the wave height and rocking histograms and calculating the rocking probability.

Influence of individual wave heights

When all tests are combined it is clearly visible that the rocking probability is highly dependent on the wave height. It is a nice S-curve which can be described with the logistic function of equation 7.1. The fit is weighted by the number of waves in the bin.

$$f(H) = \frac{1}{1 + e^{-a(H-b)}} \tag{7.1}$$

The histogram with the probability of rocking of one or more units of the data of all tests together is plotted with the logistic data fit in figure 7.7

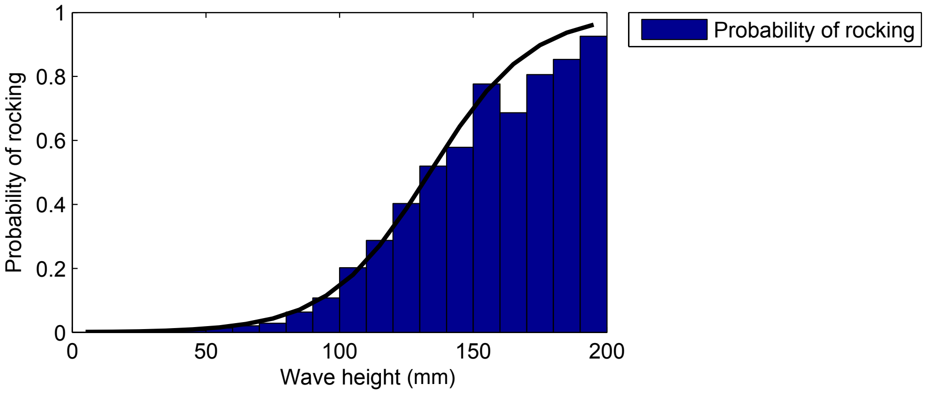

Figure 7.7: Probability of rocking of one or more units of the armour layer. The regression line is a weighted fit to the total number of waves in the bins of the histogram.

It can be seen that the bin 140-150 and the bins 160-200 show a smaller probability of rocking than the fitted line and for the rest of the data the line fits almost perfectly. This lower probability can be caused by the influence of, for instance, the type of breaking of the waves. This will be evaluated in the remainder of this section.

Influence of wave trains

First the influence of wave trains is evaluated. Besides the influence of the sequence of the wave height, this evaluation will also show the relevance of the wave series. It was assumed that the wave series made with a sum of 8 sinusoids will cause the same rocking behaviour of the units as for a (randomly generated) wave series from a Jonswap spectrum. It is very important to show whether this statement is true or not. When the wave series appear not to be causing the same rocking behaviour as a Jonswap spectrum, only the Jonswap spectra can be used to study the probability of rocking.

The groupiness of a Jonswap spectrum indicates longer wave trains than the wave series without wave trains and smaller wave trains than the wave series with wave trains. Because it is expected that wave trains have an unfavourable effect on rocking, it is expected that the wave series without wave trains has a smaller rocking probability than the Jonswap spectra and the wave series with wave trains have a larger rocking probability than the Jonswap spectra. The tests are divided in 3 groups: the Jonswap spectra, the wave series with wave trains and the wave series without wave trains. The resulting histograms and corresponding regression lines are given in figure 7.8.

From figure 7.8 it can be clearly seen that wave trains indeed influence the rocking probability. It can also be seen that the rocking probability for a Jonswap spectrum lies perfectly in between the results for the wave series with and without rocking, as expected. So it can be concluded that wave series made with 8 sinusoids are representative for waves from a spectrum. Therefore, all tests from table 7.1 can be used for further analysis of rocking.

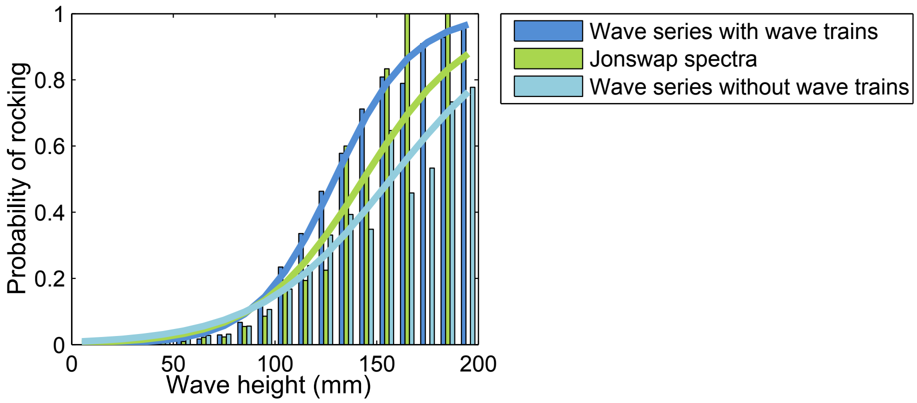

Figure 7.8: Probability of rocking of one or more units for the Jonswap spectra, the wave series with wave trains and the wave series without wave trains

Influence of wave steepness

The influence of wave steepness is evaluated by dividing the tests in groups with a wave steepness of 0.03 and 0.05. The resulting histogram and corresponding regression line are shown in figure 7.9.

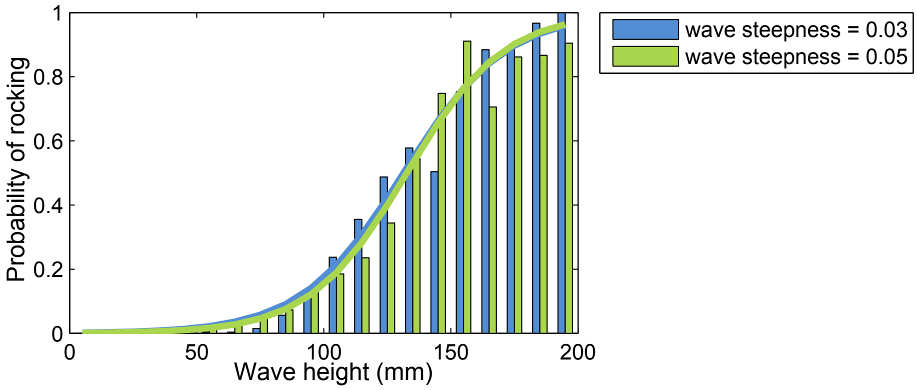

Figure 7.9: Probability of rocking of one or more units of the armour layer for different wave steepnesses

The lines of the wave series with a steepness of 0.03 and the wave series with a steepness of 0.05 are in close agreement such that it can be concluded that the wave steepness has no influence.

Influence of breaker type

As suggested in section 7.4.1, the lower rocking probability of the highest waves in relation to the regression line can be caused by another breaker type of the waves for the higher waves. The waves breaking on the breakwater are collapsing or surging breakers. Different breaker type can cause another wave height dependent maximum water velocity during run-up and run-down. To investigate the influence of the type of breaker, for all tests the individual waves are sorted by breaker type. The Iribarren parameters for all waves are calculated and the waves are divided in a group with collapsing breakers and a group with surging breakers. For the Iribarren number and its relation to the breaker type see section 3.1.2. The probability of rocking for both breaker types are shown in figure 7.10.

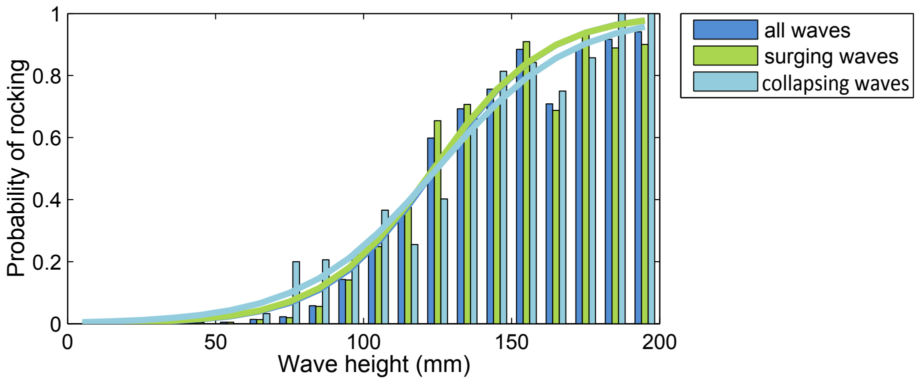

Figure 7.10: Probability of rocking of one or more units of the armour layer for different breaker types

It can be seen that the type of breaking of the waves has no influence on the rocking probability of the units. The explanation for the lower probability of rocking than the regression line for the highest waves should be found in another explanation. It can be that the waves higher than $140mm$ cause disturbances with a magnitude large enough to settle units to a somewhat more stable position, but not large enough to dislodge units. An other explanation can be that the waves higher than 140mm are overtopping waves and overtopping waves cause a smaller velocity in run-up and run-down or a more favourable direction of the velocity according to the wave load. The explanation of overtopping waves for the lower rocking probability seems most plausible, but can not be further investigated with the available data from this research.

Influence wave height distribution

Whether the height distribution of the waves influences the rocking probability is also investigated. The absence or presence of high waves can stabilise or destabilise the units by different magnitudes of disturbances of the armour layer of the previous waves. Figure 7.11 shows the probability curves for rocking for the tests with different wave height distributions.

Studying figure 7.11 it should be kept in mind that for the used tests for the wave height distributions with $H_{2\%}/H_s$=1.15, $H_{0.1\%}/H_s$=1.28 and $H_{2\%}/H_s$=1.15, $H_{0.1\%}/H_s$=1.38 only tests of repetition 3 are included (see table 7.1). Comparing the probability curves of these wave height distributions with the other (where multiple repetitions are used) is not quite accurate. When the curves of these wave height distributions are ignored, the wave height distribution seems to have a small influence. Although the relation between wave height distribution and rocking probability does not become clear. This figure does not show a relation between, for example, a higher $H_{2\%}$ or $H_{0.1\%}$ and a larger or smaller

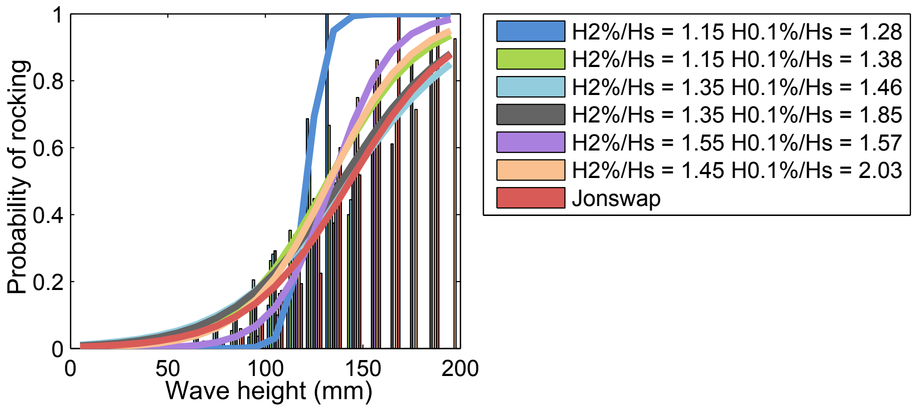

Figure 7.11: Probability of rocking of one or more units of the armour layer for different wave height distributions

probability of rocking. Based on this analysis, a conclusion for the influence of the wave height distribution can not be made.

Conclusion

From this global analysis on the probability of rocking it follows that the main parameter of the waves which determines the stability of Xbloc is the height of the waves. An other very important result of this analysis is the conclusion that the hand-made wave series induce the same rocking behaviour as a Jonswap spectrum. This analysis shows also that wave trains influence the stability of Xbloc. The steepness of the waves and the breaker type of the waves do not influence the relation between the rocking probability and the wave height. The influence of the wave height distribution did not become clear from this analysis. Additionally the results suggest that overtopping waves cause a smaller wave load than expected according to their wave height.

7.4.2 Detailed analysis

The rocking probability curves found with the histogram method give a clear view of the influence of several parameters. But deriving a design formula according to the rocking criterion is not possible from these curves. Since this curves represent the probability that one or more units are rocking of the tested slope for a certain wave height. To derive a design formula according to *'not more than 2% of the units are allowed to move during more than 2% of the waves'* the rocking probability of an individual unit is needed. To derive the rocking probability of an individual unit, the number of rocking units for every marked wave are counted, using the short video for every marker. Hereafter the probability function for rocking of an individual unit can be found with logistic regression based on the maximum likelihood fit of the dataset. The likelihood of the probability function is described in equation 7.2. For the probability function, a binomial logistic function is used.

$$\mathcal{L}(\beta_1, \beta_2, \ldots \mid x_1, \ldots, x_n) = \prod_{i=1}^{n} \binom{100}{N_{x_i}} \left(\frac{1}{1+e^{\beta_1+\beta_2 H_{x_i}+\ldots}}\right)^{N_{x_i}} \left(\frac{1}{1+e^{\beta_1+\beta_2 H_{x_i}+\ldots}}\right)^{1-N_{x_i}} \tag{7.2}$$

In this equation $\mathcal{L}(\beta_1, \beta_2, \ldots \mid x_1, \ldots, x_n)$ indicates the likelihood that the dataset $x_1 \ldots x_n$ occurs for the logistic probability function with coefficients β_1 and β_2. Every wave of all tests is an individual data point of the dataset. The parameter $N(x_i)$ indicates the number of rocking units for the wave of data point x_i. The total number of units on the slope is set on 100, because in the rows above row 10 from below it was not possible to observe rocking, see section 6.3. The number of units in a row was 11, of which the unit at the wall was held in place by a chain. The number of units which can move and of which movement is observable are 100 for the tested slope. The parameter $H(x_i)$ indicates the wave height of the wave of data point x_i. This function includes only the influence of the wave height. By including more coefficients $(\beta_3, \ldots)$ in the probability function, the influence of more parameters can be investigated. Since the wave height is the main parameter of influence, the wave height is always included in the calculation of maximum likelihood. The other parameters are alternately included to evaluate the influence of the parameter and the influence of the parameter in relation to the influence of the wave height. The coefficients $\beta_1, \beta_2, \ldots$ of the function which give the maximum likelihood for the dataset are calculated with Matlab. The results for different parameter combinations are given in table 7.3.

The steepness of the waves is included in the maximum likelihood calculation as the individual steepness of the waves.

The wave trains are included by the mean group length $(\bar{j})$. For every wave series, the mean number of subsequent waves equal or larger than H_s is calculated. This parameter is included as 1/(number of waves) to give realistic results for an extrapolation to regular waves. Other asymptotic functions for numbers between 1 and infinity gave less accurate results.

The breaker type is included binomially using a 1 for a surging breaker and a 0 for a collapsing breaker. The breaker type is calculated with the Iribarren number according to section 3.1.2.

The wave height distribution is included by a parameter for the ratio between the highest waves of the wave series: $H_{2\%}/H_s$, $H_{0.1\%}/H_s$ and $H_{0.1\%}/H_{2\%}$.

The standard deviation in this table indicates the accuracy of the coefficient. When the value of the coefficient divided by its standard deviation is very large, this indicates a very accurate value of the coefficient. From this, also the influence of the parameter can be evaluated. When the coefficient divided by the standard deviation is smaller than one, it is likely that the parameter is zero. It can then be concluded that this particular parameter has no influence on the rocking probability curve. Looking at the values of the coefficients relative to the standard deviation in table 7.3, it can be concluded that the parameter $H_{0.1\%}/H_{2\%}$ of the wave height distribution has no influence on the rocking probability curve. The other parameters seems to influence the rocking probability,

Table 7.3: Coefficients of the logistic probability function for maximum likelihood fits with different parameters

Parameters	coefficients			standard deviation					
	β_1	β_2	β_3	σ_1	σ_2	σ_3	$\lvert\frac{\beta_1}{\sigma_1}\rvert$	$\lvert\frac{\beta_2}{\sigma_2}\rvert$	$\lvert\frac{\beta_3}{\sigma_3}\rvert$
wave height	10.2	-0.0385		0.0415	$3.35 * 10^{-4}$		247	115	
wave height & steepness	10.3	-0.0382	-1.03	0.0415	$4.76 * 10^{-4}$	0.969	246	80	1.07
wave height & 1/wave trains	10.1	-0.0382	0.259	0.0452	$3.36 * 10^{-4}$	0.0349	224	114	7.40
wave height & breaker type	10.1	-0.0382	0.0982	0.0650	$3.63 * 10^{-4}$	0.0404	156	105	2.43
wave height $H_{2\%}/H_s$	9.23	-0.0390	0.774	0.186	$3.51 * 10^{-4}$	0.140	50	112	5.54
wave height & $H_{0.1\%}/H_s$	9.97	-0.0389	0.188	0.0938	$3.61 * 10^{-4}$	0.0579	106	108	3.24
wave height & $H_{0.1\%}/H_{2\%}$	10.2	-0.0385	0.0184	0.125	$3.52 * 10^{-4}$	0.105	82	109	0.176

since all other coefficients relative to the standard deviation are larger than one. To evaluate the influence of parameters further, the range of the parameters in this research and the corresponding range of the coefficient times the parameter are given in table 7.4. By comparing the variation in rocking probability according to the parameter with the variation in rocking probability according to the wave height, the influence of the parameters becomes clear.

Table 7.4: Range of parameters of the logistic probability functions

Parameters	range parameters		range coefficients	
	min	max	min	max
wave height	0	200	0	7.7
wave height steepness	0 0.005	200 0.08	0 0.00515	7.7 0.0824
wave height 1/wave trains	0 1	200 0.0625	0 -0.259	7.7 -0.0162
wave height breaker type	0 0	200 1	0 0	7.7 -0.0982
wave height $H_{2\%}/H_s$	0 1.15	200 1.45	0 0.0224	7.7 0.0283
wave height $H_{0.1\%}/H_s$	0 1.28	200 2.03	0 0.00422	7.7 0.00670
wave height $H_{0.1\%}/H_{2\%}$	0 1.08	200 1.40	0 0.0119	7.7 0.0154

From this evaluation it follows that only the groupiness of the waves has a significant influence besides the influence of the wave height.

7.4.3 Rocking relation

The probability of rocking for the armour layer of the model tests can be described with equation 7.3 with $\bar{j}$ for the mean group length, or equation 7.4 when the influence of groupiness is omitted.

$$f_{rocking}(H, \bar{j}) = \frac{1}{1 + e^{10.1 - 0.0382*H + 0.259*1/\bar{j}}} \tag{7.3}$$

$$f_{rocking}(H) = \frac{1}{1 + e^{10.2 - 0.0385*H}} \tag{7.4}$$

To expand this rocking relation for other Xbloc sizes it is assumed that the scale factor found in previous research also holds for the rocking relation (section 3.3). In other words, the rocking probability is proportional to $H/\Delta D_n$. Including the nominal diameter of $39.55mm$ and the relative density of 1.38 of the used Xblocs , it results in the following rocking relations:

$$f_{rocking}(H, \bar{j}) = \frac{1}{1 + e^{10.1 - 1.45*H/(\Delta D_n) + 0.259*1/\bar{j}}} \tag{7.5}$$

$$f_{rocking}(H) = \frac{1}{1 + e^{10.2 - 1.46*H/(\Delta D_n)}} \tag{7.6}$$

The standard deviations of the three parameters indicate the accuracy of the fitted probability curve. Using these standard deviations a 90% confidence interval of the fit can be derived. The plot of the rocking probability with 90% confidence interval for normalised waves with respect to the Xbloc size is given in figure 7.12.

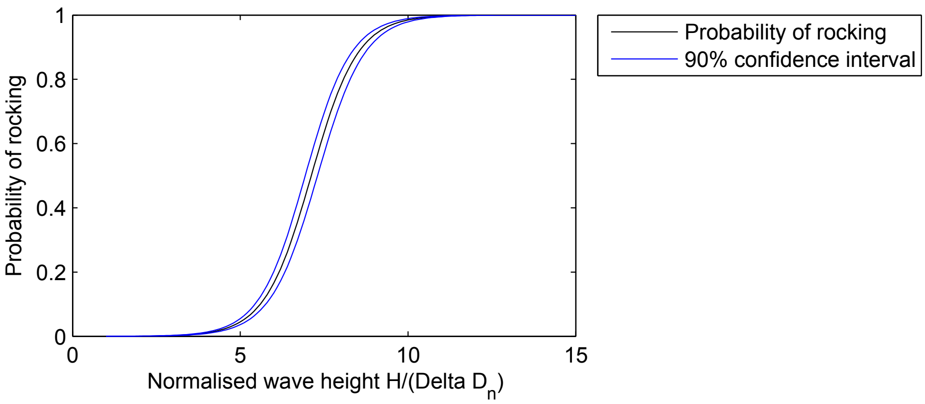

Figure 7.12: Probability of rocking of a single unit for the normalised wave height and mean group length of the Jonswap spectrum (1.4)

The formulas of the confident intervals are given in equations 7.7 and 7.8.

$$f_{rocking}(H, \bar{j}) = \frac{1}{1 + e^{10.2 - 1.43*H/(\Delta D_n) + 0.316*1/\bar{j}}} \tag{7.7}$$

$$f_{rocking}(H, \bar{j}) = \frac{1}{1 + e^{10.0 - 1.47*H/(\Delta D_n) + 0.201*1/\bar{j}}} \tag{7.8}$$

The confidence interval for the rocking probability curve without influence of wave trains is given in equations 7.9 and 7.10.

$$f_{rocking}(H) = \frac{1}{1 + e^{10.3-1.44*H/(\Delta D_n)}} \tag{7.9}$$

$$f_{rocking}(H) = \frac{1}{1 + e^{10.2-1.48*H/(\Delta D_n)}} \tag{7.10}$$

Conclusion

From the detailed analysis a quantitative description of the probability of rocking is made. This probability is only dependent on the wave height and the mean length of wave trains. The parameters related to the steepness of the waves, the breaker type of the waves and the wave height distribution have no significant influence on the probability of rocking.

7.5 Design method for Xbloc

The rocking criterion prescribes that *"not more than 2% of the units are allowed to move during more than 2% of the waves"*. Translating this in terms of the rocking probability it can be concluded that the probability of rocking for $H_{2\%}$ should not be larger than 0.02. This means that for waves smaller than $H_{2\%}$ it is expected that less than 2% of the units are rocking (since the probability is smaller than 0.02). It is expected than for waves higher than $H_{2\%}$ more than 2% of the units will rock. This is exactly the largest amount of movement accepted by the rocking criterion. The size of the Xbloc should be chosen such that the rocking probability for $H_{2\%}$ is smaller than or equal to 0.02 (see equation 7.11 and equation 7.14 for the criterion without influence of wave trains). To derive a conservative design formula the upper bound of the confidence interval is used.

$$f_{rocking}(H_{2\%}, \bar{j}) = 0.02 \geq \frac{1}{1 + e^{10.0-1.47*H_{2\%}/(\Delta D_n)+0.201*1/\bar{j}}} \tag{7.11}$$

$$f_{rocking}(H_{2\%}) = 0.02 \geq \frac{1}{1 + e^{10.2-1.48*H_{2\%}/(\Delta D_n)}} \tag{7.12}$$

From these equations the design formula can be derived, equation 7.13 and 7.14.

$$\frac{ln(\frac{1}{0.02}-1)-10.0-\frac{0.201}{\bar{j}}}{-1.47} \geq \frac{H_{2\%}}{\Delta D_n} \quad \Rightarrow \quad \frac{H_{2\%}}{\Delta D_n} \leq 4.16 + \frac{0.137}{k} \tag{7.13}$$

$$\frac{ln(\frac{1}{0.02}-1)-10.2}{-1.48} \geq \frac{H_{2\%}}{\Delta D_n} \quad \Rightarrow \quad \frac{H_{2\%}}{\Delta D_n} \leq 4.26 \tag{7.14}$$

From the model tests it was also found that waves larger than 1.85 times the current design wave height are likely to dislodge units. Wave series with a $H_{0.1\%}/H_s$ ratio of 2.03 caused a dislodged unit in 3 of the 4 repetitions; wave series with a smaller $H_{0.1\%}/H_s$ ratio (of which the highest ratio is 1.85) did not dislodge a unit in one of the repetitions. It is therefore advised to also take the highest waves of the design storm into account (equation 7.15).

$$\frac{H_{0.1\%}}{\Delta D_n} \leq 1.85 * 2.77 = 5.12 \tag{7.15}$$

New design formula in relation with the current design formula

The design formula of equation 7.13, 7.14 and 7.15 allow smaller Xbloc sizes in most design storms, especially for shallow water. The current design formula is for most cases conservative, only very wide wave height distributions with a large $H_{2\%}/H_s$ ratio and a large $H_{0.1\%}/H_s$ ratio needs larger Xblocs than the current design formula prescribes. Since this research is focused on the influence of wave load on rocking and the influence of the shape of the waves is omitted, all correction factors except the one for deep water should still be used.

7.6 Analysis of dislodged units

Since investigation of the behaviour of dislodged units are out of the scope of this research and counting the number of moving units for every marked wave height is very time consuming, rocking of dislodged units is analysed globally. The figures of this analysis and corresponding conclusions can be found in appendix G. In general, the same parameters are influencing the rocking probability. The probability of rocking is much larger than for interlocking units.

7.7 Other interlocking armour units

For other interlocking armour units it is expected that a comparable rocking probability holds. It is also expected that for other interlocking armour units a risk of dislodgement occurs from a certain wave height. Because the interlocking between different armour units differs, it is expected that the coefficients will differ. To find the design formula according to the rocking criterion for the other interlocking units, new research is required. The research method used here is applicable for other units.

7.8 Conclusions

The analysis of the model test data confirms the hypothesis that *"there is a better fitting parameter for the wave height than H_s for the design of Xbloc"*. Although the hypothesis that *"there is a 'boundary wave height' for rocking"* does not hold the (from this hypothesis expected) better fitting wave height $H_{2\%}$ is confirmed. This parameter for the wave height in the design formula resulted from the rocking criterion in combination with the probability of rocking for a certain wave height. Besides the advise to use $H_{2\%}$, it is also advised to check the highest waves in the design storm for the risk of dislodgement of units, since a dislodged unit does not adheres to the placement specifications any more.

For most cases the current design formula prescribes a larger Xbloc than the new design formula, for wide spectra with very high maximum waves in relation to H_s, the new formula prescribes larger Xblocs. It should be kept in mind that during this research it is chosen to omit the influence of skewness of the waves by testing in deep water without a slope of the foreshore to be able to look purely at the influence of the wave height. Since it is expected that the shape of the waves influences the stability of armour units, new research should be done to investigate whether the slope of the foreshore should be included in the design formula or not. Since the shape of the waves changes especially in very shallow water with a steep foreshore, and the current design formula fits very well in this situation, it is advised to not replace the current design formula by the new ones, but extend the current design formula with the new ones. The largest calculated Xbloc size of the 3 formula (7.14, 7.15 and 3.19) will give a good and conservative estimate of the required size of the armour units.

Chapter 8

Conclusions and recommendations

8.1 Conclusions

8.1.1 Xbloc stability

The expectations from literature and existing model tests performed by DMC were confirmed by the results from the model tests. The wave height is the most important parameter for designing an armour layer for rocking and $H_{2\%}$ is mathematically a better fitting parameter for the wave height according to the rocking criterion than H_s. In addition to the design formula with $H_{2\%}$ (based on the rocking criterion), also a design formula with $H_{0.1\%}$ should be used (based on the dislodgement of units). It was found in the model tests that the highest waves caused a risk to distorting the armour layer such that armour units are dislodged and do not adhere to the placement specifications any more (do not interlock any more).

For shallow water however, the current design formula prescribes larger Xblocs than the new formulas. In shallow water, especially with a steep foreshore, waves become asymmetric. Asymmetry of waves has an adverse influence on the stability of armour units. Since the influence of the shape of the waves is omitted during this research by using only sinusoidal waves, the new design formula will underestimate the required Xbloc size in this case.

Therefore, it is advised to use the largest calculated Xbloc size from equations 8.1 (current design formula), 8.2 (rocking based design formula) and 8.3 (dislodgement based design formula).

$$\frac{H_s}{\Delta D_n} \leq 2.77 \tag{8.1}$$

$$\frac{H_{2\%}}{\Delta D_n} \leq 4.26 \tag{8.2}$$

$$\frac{H_{0.1\%}}{\Delta D_n} \leq 5.12 \tag{8.3}$$

For Jonswap spectra it suffices to use equation 8.2, because this formula gives comparable results to the formula where the mean group length is included for Jonswap. The wave trains of swell have an unfavourable influence on the stability of Xbloc. When swell occurs it is advised to take the mean group length ($\bar{j}$) into account according to equation 8.4.

$$\frac{H_{2\%}}{\Delta D_n} \leq 4.16 + \frac{0.137}{\bar{j}} \tag{8.4}$$

The results for the different parameters found in this research are briefly summarised below.

The wave height is the main influence on the probability of rocking. The design of the size of Xbloc should be mainly wave height based. With respect to rocking, $H_{2\%}$ is a suitable parameter. With respect to dislodgement of units, $H_{0.1\%}$ is a suitable parameter.

Influence of the wave height distribution on the probability distribution function of rocking is not found in this research (influence of ratio $H_{2\%}/H_s$ and the ratio $H_{0.1\%}/H_s$ on the rocking probability function). Although it was expected that a larger wave load due to some of the previous waves cause a larger probability of rocking due to all subsequent waves, this was not found in the results. Only for the waves which dislodge units it is found that all subsequent waves have a larger probability of rocking. Dislodgement of units is not desirable and is treated separately.

Influence of the steepness of the waves on rocking is not found in this research. The weak relation found in section 7.4.2 is so small relative to the influence of the wave height, that it can be concluded that the steepness is of no influence.

The influence of wave trains on rocking can not be neglected. Although the influence is small compared to the influence of the wave height, it is not small enough to be neglected. For swell it is advised to include the mean group length ($\bar{j}$). This parameter is related to the spectral narrowness parameter of the spectrum.

The influence of the shape of the waves on rocking is not studied during the model tests. However, it is expected to be of influence according to the literature. Therefore more research is needed on the influence of the shape of the waves on rocking.

Influence of the breaker type of the waves on rocking is not found. The weak relation is negligible in comparison to the influence of the other parameters.

The influence of the relative packing density on rocking is significant. When an armour layer is placed with a lower packing density than follows from the placement specifications, the probability of rocking is significantly higher. It is advised not to place the armour layer with a relative packing density smaller than the packing density of the placement specifications.

The influence of overtopping waves on the wave load is expected to explain the decrease in rocking probability for the waves larger than $140mm$ in figure 7.7. The correctness of this hypothesis should be studied.

The present research method is quite innovative. Making wave series with a chosen wave height distribution to be able to omit the influence of the shape of the waves worked very well. The rocking behaviour of the armour units loaded by the hand-made wave series is comparable with the rocking behaviour of the armour layer due to waves of a Jonswap spectrum. The method of marking the waves which caused rocking also worked very well. Rocking could be analysed in much detail. The only disadvantage is that counting the number of rocking units afterwards is quite time consuming.

8.1.2 Single layer concrete armour unit in general

For other interlocking armour units it is expected that a comparable rocking probability holds. It is also expected that for other interlocking armour units a risk of dislodgement occurs from a certain wave height. Because the interlocking between different armour units differs, it is expected that the coefficients will differ. To find the design formula according to the rocking criterion for the other interlocking units, new research is required. The research method used here is applicable for other units.

8.2 Recommendations for further research

Every research has its limitations, and this one is no exception. As mentioned before, it is assumed that the description of rocking can be made more accurate when the influence of the shape of the waves on rocking will be investigated. But also the assumption that scaling the probability curve of rocking with $H/(\Delta D)$ and the geometry of the breakwater needs some more attention. During the tests some remarkable observations were made, which are also interesting for more research. From the above some recommendations for further research are:

The scaling of the rocking probability curve should be checked by a repetition of the tests with a larger armour unit size.

The influence of the shape of the waves should be investigated by repeating the tests with wave series of a Jonswap spectrum with different wave height distributions modified by a foreshore.

The geometry of the breakwater should be varied to investigate the influence of several parameters on the rocking probability. Similarly, a smaller and larger freeboard will show what the influence of the number of rows is on rocking and show whether the hypothesis of a lower wave load by overtopping waves is correct. Also the influence of the permeability of the core and a toe are interesting to investigate.

The wave height which dislodges units is not analysed in detail. The design formula related to dislodgement of units needs some more research.

Bibliography

[Verhagen et al.(2009)Verhagen, d'Angremond, and van Roode] H.J. Verhagen, K. d'Angremond, and F. van Roode. *Breakwaters and Closure dams.* VSSD, 2nd edition edition, 2009. ISBN 978-90-6562-173-3.

[Sin(1982)] *Failure of Sines breakwater.* Port Sines Investigating Panel. American Society of Civil Engineers, 1982. ISBN 0-87262-298-3.

[RM(2007)] *The Rock Manual, The unse of rock in hydraulic engineering*, 2007. ISBN 978-0-86017-683-1.

[CEM(2004)] *Coastal Engineering Manual*, 2004. U.S. Army Corps of Engineers.

[BS(2000)] *British Standard 6439.* BSI, 389 Chiswick High Road, London, W4 4AL, 2000.

[SPM(1984)] *Shore Protection Manual*, 1984. Waterways Experiment Station, Corps of Engineers, Coastal Engineering Research Ceter. U.S. Government Printing Office Washington D.C.

[Holthuijsen(2008)] L.H. Holthuijsen. *Waves in oceanic and coastal waters.* Cambridge University Press, 2008.

[Schiereck(2001)] G.J. Schiereck. *Introduction to Bed, Bank and Shore protection.* VSSD, 2001. ISBN 90-407-1683-8.

[Groenendijk(1998)] H.W. Groenendijk. Shallow foreshore wave height statistics. Master's thesis, TU Delft, 1998. URL `repository.tudelft.nl`.

[van Vledder(1983)] G. Ph. van Vledder. Preliminary investigation into the occurrence of wave groups in seas and swell. Master's thesis, TU Delft, 1983. URL `repository.tudelft.nl`.

[van Vledder(1992)] G. Ph. van Vledder. Statistics of wave group parameters. In *International Conference on Coastal Engineering, Venice*, 1992. Delft Hydraulics.

[Stam(1988)] C.J.M. Stam. De korrelatieparameter in de twee-dimensionale rayleigh kansdichtheidsfunktie voor opeenvolgende golfhoogten. Master's thesis, TU Delft, 1988. URL `repository.tudelft.nl`.

[TAW(2002)] *Technisch Rapport Golfoploop en Golfoverslag bij Dijken*, 2002. Technische Adviescommissie voor de Waterkeringen.

[van der Meer(1988)] J.W. van der Meer. *Rock slopes and gravel beaches under wave attack*. PhD thesis, TU Delft, 1988. URL `repository.tudelft.nl`.

[Hovestad(2005)] M. Hovestad. Breakwaters on steep foreshores. the influence of the foreshore steepness on armour stability. Master's thesis, TU Delft, 2005. URL `repository.tudelft.nl`.

[Tromp(2004)] M. Tromp. Influences of fluid accelerations on the threshold of motion. Master's thesis, TU Delft, 2004. URL `repository.tudelft.nl`.

[Dessens(2004)] M. Dessens. The influence of flow acceleration on stone stability. Master's thesis, TU Delft, 2004. URL `repository.tudelft.nl`.

[Mertens(2007)] M. Mertens. Stability of rock on slopes under wave attack. Master's thesis, TU Delft, 2007. URL `repository.tudelft.nl`.

[Verhagen et al.(2006)Verhagen, Reedijk, and Muttray] H.J. Verhagen, B. Reedijk, and M. Muttray. The effect of foreshore slope on breakwater stability. In *International conference on Coastal Engineering ICCE'06, San Diego, Sept.* World Scientific, 2006.

[SWA(2006)] *SWAN User Manual*, 2006. URL `swanmodel.sourceforge.net`. The SWAN team. Delft University of Technology, Faculty of Civil Engineering and Geosciences, Environmental Fluid Mechanics Section.

[Rattanapitikon(2010)] W. Rattanapitikon. Verification of conversion formulas for computing representative wave heights. *Elsevier Ocean Engineering*, 37: 1554–1563, 2010. Thammasat University Thailand.

[Battjes and Groenendijk(2000)] J.A. Battjes and H.W. Groenendijk. Wave height distributions on shallow foreshores. In *Coastal Engineering 40, 161-182*, 2000.

[xbl(2003a)] *Xbloc armour unit development. Hydraulic performance of Xbloc armour units - 2-D model tests at WL Delft*, 2003a. Delta Marine Consultants.

[xbl(2003b)] *Xbloc armour unit development. Results structural tests.*, 2003b. Delta Marine Consultants.

[xbl(2011)] *Guidelines for Xbloc Concept Designs*, 2011. Delta Marine Consultants.

[wav(2010)] *Wave flume manual*, 2010. Delta Marine Consultant.

[xbl(2008)] *Specification for application of Xbloc*, 2008. Delta Marine Consultants.

[ede(1999)] *Wave generation using Ocean and Wave*, 1999. Edinburgh Designs.

List of Figures

List of Tables

Appendix A

Wave height distribution of Battjes and Groenendijk

A.1 Derivation method shallow water wave height distribution

The shallow water wave height distribution of *Battjes and Groenendijk(2000)* is a composed Weibull distribution as described in section 3.1.2. The cumulative shallow water wave height distribution and the probability density function are resumed in equation A.1 and A.2.

$$F(H) = \begin{cases} 1 - exp[-(\frac{H}{H_1})^{k_1}] & \text{for } H \leq H_{tr} \\ 1 - exp[-(\frac{H}{H_2})^{k_2}] & \text{for } H \geq H_{tr} \end{cases} \tag{A.1}$$

$$f(H) = \begin{cases} \frac{k_1 H^{k_1 - 1}}{H_1^{k_1}} exp[-(\frac{H}{H_1})^{k_1}] & \text{for } H \leq H_{tr} \\ \frac{k_2 H^{k_2 - 1}}{H_1^{k_2}} exp[-(\frac{H}{H_2})^{k_2}] & \text{for } H \geq H_{tr} \end{cases} \tag{A.2}$$

The coefficients k_1 and k_2 are empirically found and are 2.0 respectively 3.6. The transitional wave height H_{tr} is dependent on the fore shore and can be calculated by equation A.3.

$$H_{tr} = 0.36d \tag{A.3}$$

Both scale parameters H_1 and H_2 can be found by solving equation A.4 and A.5 based on continuity of the cumulative probability function and the root-mean-square wave height of the shallow water wave height distribution.

$$H_2 = H_{tr}\left(\frac{H_{tr}}{H_1}\right)^{-\frac{k_1}{k_2}} \tag{A.4}$$

$$H_{rms} = \sqrt{H_1^2 \gamma\left[\frac{2}{k_1} + 1, \left(\frac{H_{tr}}{H_1}\right)^{k_1}\right] + H_2^2 \Gamma\left[\frac{2}{k_2} + 1, \left(\frac{H_{tr}}{H_2}\right)^{k_2}\right]} \tag{A.5}$$

Battjes and Groenendijk (2000) provided table A.1 with the values of the normalised $\tilde{H_1}$ and $\tilde{H_2}$ according to the normalised $\tilde{H_{tr}}$. (Normalised to the root-mean-square wave height.)

$$H_{rms} = \sqrt{8m_0} \tag{A.6}$$

$$\tilde{H_{tr}} = 0.36\frac{d}{H_{rms}} = 0.12\frac{d}{\sqrt{m_0}} \tag{A.7}$$

From this table the values can be interpolated. The recipe for finding the shallow water wave height distribution with the compesed Weibull distribution is as follows:

1. Given $\sqrt{m_0}$ and d, calculate $\tilde{H_{tr}} = 0.12\frac{d}{\sqrt{m_0}}$
2. Read the coresponding $\tilde{H_1}$ and $\tilde{H_2}$ from table A.1
3. Calculate the corresponding wave height distribution and the desired $H_{x\%}$

[Groenendijk(1998)]

A.2 Adjustments of Rattanapitikon

Rattanapitikon (2010) evaluated a number of conversion formulas with a large amount of shallow water wave data. With this data he calibrated the constants also for the composed Weibull of *Battjes and Groenendijk (2000)*. He also evaluated other calculation methods for the transitional wave height. This resulted in the

Original calculation of H_{tr}:

$$\tilde{H_{tr}} = 0.49\frac{d}{H_{rms}} \quad k_1 = 2.2 \;\; k_2 = 3.4 \tag{A.8}$$

Calculation of H_{tr} with the slope of the foreshore (m):

$$\tilde{H_{tr}} = \frac{(0.35+5.8a)d}{H_{rms}} \quad k_1 = 2.2 \;\; k_2 = 3.3 \tag{A.9}$$

Calculation of H_{tr} with the wave breaking criterion of *Goda (1970)* (L_0 is the deep water wave length related to T_p):

$$\tilde{H_{tr}} = \frac{1.1}{H_{rms}}0.1L_0\left(1 - exp\left(-1.5\frac{\pi d}{L_0}(1 + 15m^{\frac{4}{3}})\right)\right) \quad k_1 = 2.2 \;\; k_2 = 3.4 \tag{A.10}$$

The transitional wave height calculated with the breaker criterion of *Goda (1970)* appeared to be most accurate according to the wave data of *Rattanapitikon (2000)*.

Table A.1: Normalised shallow water wave height parameters for wave height distribution of Groenendijk and Battjes

$\tilde{H}_{tr}$	$\tilde{H}_1$	$\tilde{H}_2$	$\tilde{H}_s$
0.050	12.193	1.060	1.279
0.100	7.003	1.060	1.279
0.150	5.063	1.060	1.279
0.200	4.022	1.060	1.279
0.250	3.365	1.060	1.279
0.300	2.908	1.060	1.279
0.350	2.571	1.060	1.279
0.400	2.311	1.060	1.279
0.450	2.104	1.060	1.279
0.500	1.936	1.061	1.280
0.550	1.796	1.061	1.281
0.600	1.678	1.062	1.282
0.650	1.578	1.064	1.284
0.700	1.492	1.066	1.286
0.750	1.419	1.069	1.290
0.800	1.356	1.073	1.294
0.850	1.302	1.077	1.300
0.900	1.256	1.083	1.307
0.950	1.216	1.090	1.315
1.000	1.182	1.097	1.324
1.050	1.153	1.106	1.335
1.100	1.128	1.116	1.346
1.150	1.108	1.126	1.359
1.200	1.090	1.138	1.372
1.250	1.075	1.150	1.381
1.300	1.063	1.162	1.389
1.350	1.052	1.175	1.399
1.400	1.043	1.189	1.403
1.500	1.030	1.217	1.406
1.550	1.024	1.231	1.408

$\tilde{H}_{tr}$	$\tilde{H}_1$	$\tilde{H}_2$	$\tilde{H}_s$
1.600	1.020	1.246	1.410
1.650	1.016	1.261	1.411
1.700	1.013	1.275	1.412
1.750	1.011	1.290	1.413
1.800	1.009	1.305	1.413
1.850	1.007	1.320	1.414
1.900	1.006	1.334	1.414
1.950	1.004	1.349	1.415
2.000	1.004	1.363	1.415
2.050	1.003	1.378	1.415
2.100	1.002	1.392	1.415
2.150	1.002	1.407	1.415
2.200	1.001	1.421	1.415
2.250	1.001	1.435	1.415
2.300	1.001	1.449	1.415
2.350	1.001	1.462	1.415
2.400	1.000	1.476	1.416
2.450	1.000	1.490	1.416
2.500	1.000	1.503	1.416
2.550	1.000	1.516	1.416
2.600	1.000	1.529	1.416
2.650	1.000	1.542	1.416
2.700	1.000	1.555	1.416
2.750	1.000	1.568	1.416
2.800	1.000	1.580	1.416
2.850	1.000	1.593	1.416
2.900	1.000	1.605	1.416
2.950	1.000	1.617	1.416
3.000	1.000	1.630	1.416

Appendix B

Data existing model tests

Table B.1 gives the data of the existing model tests used for the analysis in chapter 4. In the first column can be seen that some tests belong to the same project, but have a different relative water depth. This is because the projects are tested with different water depths and different wave loads. The D_n is calculated using equation 3.20, where D_n is the cubic root of the volume of the Xbloc. The correction factor (C) is calculated using table 3.3. In accordance with the relation between D_n and the volume, the correction factor for D_n is the cubic root of the correction factor found in table 3.3. The columns with D_n-$H_{2\%}$ indicate that the D_n is calculated with equation 3.20 where H_s is replaced by $H_2\%$. For the calculation of D_n-$H_{2\%}$ not all correction factors are used to show that the correction factors for the foreshore are dependent on a not good fitting parameter for the wave height. When there is no correction for the relative water depth and the slope of the foreshore is used, this is indicated by 'no C_d, no C_a'. When only the correction of the relative water depth is not used, this is indicated by 'no C_d'. The Δ depends on the density of the used model Xbloc, as can be seen in this column the Δ (and the density) differs slightly for the different model Xblocs (see column 'sufficient D_n').

Table B.1: Data of existing model tests

Model test	relative water depth $[m]$	slope foreshore $[-]$	H_s $[m]$	$H_{2\%}$ $[m]$	steepness $[-]$	Δ $[-]$	C $[-]$	D_n $[m]$	C no C_d, no C_a $[-]$	D_n $H_{2\%}$ $[m]$	C no C_d $[-]$	D_n $H_{2\%}$ $[m]$	sufficient D_n $[m]$
Project 1	2.5	1:41.25	0.074	0.097	0.030	1.32	1.260	0.0268	1	0.027	1.260	0.033	0.039
Project 2.1	3.3	1:30	0.067	0.093	0.044	1.32	1.301	0.0239	1.301	0.033	1.301	0.033	0.030
Project 2.2	2.6	1:30	0.071	0.094	0.049	1.33	1.182	0.023	1.145	0.029	1.182	0.030	0.032
Project 2.3	2.3	1:30	0.069	0.094	0.048	1.33	1.301	0.024	1.260	0.032	1.301	0.033	0.032
Project 2.4	2.0	1:30	0.093	0.121	0.058	1.32	1.182	0.030	1.145	0.038	1.182	0.039	0.037
Project 2.5	3.8	1:30	0.066	0.091	0.045	1.32	1.301	0.024	1.260	0.031	1.301	0.032	0.037
Project 3.1	2.4	1:50	0.1	0.137	0.047	1.32	1.145	0.031	1.145	0.043	1.145	0.043	0.030
Project 3.2	1.9	1:50	0.095	0.119	0.046	1.32	1	0.026	1	0.033	1	0.033	0.030
Project 4.1	4.1	flat	0.094	0.133	0.052	1.40	1.145	0.028	1	0.034	1	0.034	0.033
Project 4.2	4.1	flat	0.09	0.12	0.049	1.32	1.145	0.028	1	0.033	1	0.033	0.037
Project 4.3	4.1	flat	0.09	0.119	0.049	1.32	1.145	0.028	1	0.033	1	0.033	0.037

Appendix C

Calibration of the waves in the flume

The first tests of the calibration in the wave flume gave wave series which mismatched both the theoretical time series and the theoretical wave height distribution. To find the cause of this mismatch a number of conceivable causes were considered and tested, related to both the input of the wave maker and the physical processes in the flume. The first section gives a description of the programming of the wave maker. The second section describes the possible causes of the mismatch, the method of testing and the results. After all these tests and the needed adjustments in programming the wave flume, the wave series deviates less than 2% of the theoretical wave series as described in section 6.1 and table 6.1.

C.1 The input file for the wave maker

The input for the wave maker is a time series described in a sea-file. This sea-file is generated from a wav-file by the ocean compiler. This wave file should contain amongst others: a description of the water level elevation, the length of the time series and a command for which water depth dependent force matrix should be used. The description of the water level elevation can be in terms of several wave spectra, single harmonic waves and functions of single harmonic waves. Two examples of a function for the water level elevation are described in equations C.1 and C.2.

$$single\,harmonic\,wave \Leftrightarrow single(frequency, amplitude, angle, phase) \quad \text{(C.1)}$$

$$jonswap\,spectrum \Leftrightarrow jonswap(peakfrequency, \alpha, \gamma, \sigma_a, \sigma_b) \quad \text{(C.2)}$$

The length of the generated data set in the sea-file is defined in the r-number. The r-number represents the number of generated data points by the input-file-generator as a power of 2. So an r-number of 6 generates an input file with 64 data points. The frequency of the wave maker is 32 Hz, which means that an input file with r-number 6 has a repeat time of 2 seconds (64 data point divided by 32 data point per second). The wave maker does not stop automatically after elapsing of the repeat time, it starts over with the same signal till the wave maker is stopped manually. For a time series of 1000 waves with a period of 1.46 seconds (a significant wave height of $99.5mm$ in combination with a wave steepness of 0.03 gives a period of 1.46) an r-number of 16 satisfies. The required repeat time for a wave series of at least 1000 waves is at least 1460 seconds; the r-number of 16 gives a repeat time of 2048 seconds. [ede(1999)]

C.2 Testing of the possible causes for the mismatch in theoretical waves and measured waves in the flume

C.2.1 Type of harmonic and units of parameters

The water level elevation in the wave-file is described with a summation of 8 'single' waves, see equation C.1. Not all properties of this input 'single' are explained in the manual. The units of the frequency and amplitude are given: Hertz and meter. But the unit for the phase not. In general a phase is given in radians, but time or degrees is also possible. The use of the right phase is very important, so it is useful to first be certain about the right unit. To test the unit of the phase a wave with a period of 2 seconds is generated in the flume. First with $\varphi = 0$. Thereafter with a phase of 2π, a phase of 2 and a phase of 360. If the time series with a phase of 2π are exactly the same as the time series with a phase of 0, the unit of the phase is radians. When the time series with a phase of 2 is exactly the same, the unit is seconds. And when the time series with a phase of 360 is the same, the unit is degrees. In figure C.1 the time series for a phase of 0, 2π and 2 are shown. It becomes clear that the unit of the phase is radians.

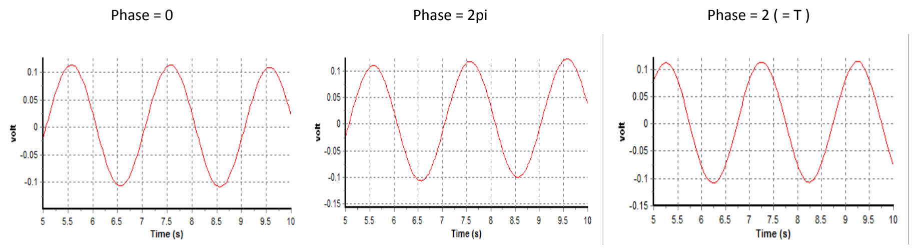

Figure C.1: Time series for a wave with a period of 2 seconds, and different phases

It is also not known if this 'single' represents a sine or cosine. Usually one 'single' wave is used. Whether the generated harmonic is a sine or cosine makes no fundamental differences in this generated time series. But in case of a summation of several harmonics the time series is completely different for a sine than for a cosine. In the Matlab calculations it was assumed that the harmonic was a sine. Finding this assumption not correct will explain the large deviations in the results of the first tests. To test the 'single' wave represents, a summation a single waves with a frequency of $0.5Hz$ and a single wave of $1Hz$ is generated in the flume. Because it is not known if the wave maker has some time delay, one single wave does not show whether it is a sine or cosine. The time series of the waves at the wave gauges can be calculated using a sine and a cosine. The time series which match with the measured time series at the wave gauges shows which harmonic the 'single' wave represents. Figure C.2 shows the measured and calculated time series. It can be concluded that the 'single' wave represents a cosine.

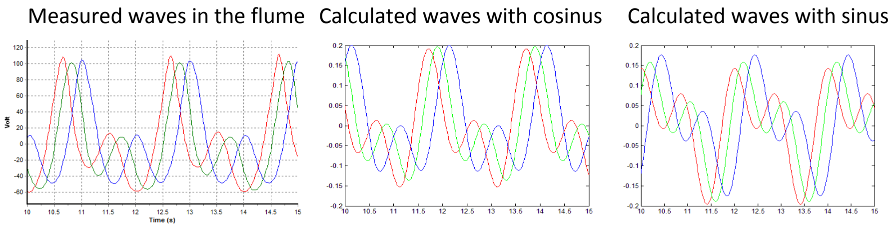

Figure C.2: Time series for a wave with a period of 2 seconds, and different phases

The equivalent harmonic function to the 'single' wave input is given in equation C.3.

$$single(f, a, \theta, \phi) \;\Leftrightarrow\; a[m] * cos(2\pi * f[Hz] * t + \phi[rad]) \tag{C.3}$$

After the input of the wave groups was modified to harmonics of a cosine, the time series and wave height distributions still deviated enormously from the calculated time series and wave height distributions. The wave series without wave trains and the wave series with the largest ratio's between $H_(0.1\%)$ and H_s were least alike the results from Matlab.

C.2.2 Error in Matlab calculations

An other explanation for the deviation in the tests is an error in the calculation of the phase at the wave board. If, for example, the wave number is not correctly calculated in the Matlab file the phase at the wave board is not correct and the waves in the flume deviates from the calculated waves. But from the tests of the previous section, the tests with a sum of two harmonics, the time series at the wave gauges in front of the wave maker and the time series at the location of the breakwater fitted both with the calculated time series in Matlab. An error in the wave number would have given a deviation at, at least, one of these locations. So it can be concluded that the wave number is calculated correctly.

C.2.3 Non linear effects

An other error in the Matlab calculation can be the assumption that linear wave theory can be applied. For shallow water the non-linear effects are not negligible and, for example, Stokes wave theory should be used. Studying the time series measured in the wave flume, it is striking that the waves are quite asymmetric. Especially the wave series without wave trains. The amplitude of the crests is much larger than the amplitude of the trough. This can indicate that the waves are too steep for this water depth, become unstable and second (or even third) order Stokes waves originates in the waves. A second order Stokes wave has a phase speed of twice the phase speed of the linear wave and an amplitude depending on the water depth, the phase speed and the amplitude of the linear wave. The second order (or third order) Stokes waves are bounded to the linear waves and travels with the same propagation speed. The water level elevation of a linear wave with a second order Stokes correction can be described with equation C.4.

$$\eta(x,t) = a\,cos(\omega t+kx)+k\,a^2\,\frac{cosh(kd)}{4sinh^3(kd)}\,(2+cosh(2kd))\,cos(2(\omega t+kx)) \quad \text{(C.4)}$$

Because the Stokes wave correction is not included in the input of the wave maker and originates short after the wave board, it can occur that a part of the Stokes correction starts to propagate as a free wave. This can be an explanation for the deviation of the waves in the flume compared to the theoretical waves. To prevent the free waves of the Stokes correction, the Stokes correction can be included in the input of the wave generator. In this way the generated waves are not unstable and the time series should be in accordance with a Matlab calculation where the second order Stokes wave is included. After some new tests with a second order Stokes wave correction, the deviation of theoretical and occurring waves did not decrease. The amplitude of the second order Stokes wave correction is very small, negligible small, and has as can be expected no effect. The reason for the asymmetry of the waves should be found somewhere else than a too small water depth with non-linear effects. Because it especially occurred with the wave series without wave trains, it is plausible to conclude that this asymmetry originates from the combination of waves in the wave group. The wave series without wave trains include phase speeds which are approximately twice the phase speeds of other waves in this group (see section 5.5.1). Due to a combination of the amplitudes of these waves and the phases at the location of the wave gauges, this waves can coincidentally look like stokes waves. However the explanation for the deviation of theoretical and occurring waves can not be found in non-linearity.

C.2.4 Rounding of frequencies

The difficulty with a summation of several sinusoids in comparison with a single harmonic is the sensitivity to errors due to rounding off, during the input file generation, of in particular the frequencies. A series with ill rounded frequencies cancel the advantageous properties of the fractions with prime numbers, which are essential to generate the right wave height distributions. So a rounding of error seems to be a plausible explanation for the large deviations in the wave records. The r-number not only determine the repeat time, it also influences level of the rounding off of the frequencies. The frequencies are rounded to frequencies which 'fits' in the data set. So for a data set of 64 data points and a duration of 2 seconds the largest frequency is a wave of 2 data points, a wave of 16 Hz. The smallest frequency is a wave of twice the data points, a wave of 0.25 Hz. Only frequencies between 0.25 Hz and 16 Hz rounded to a multiple of 0.25 Hz 'fits' in the data points, so the frequencies will be rounded to a multiple of 0.25. To decrease the rounding off error, a larger r-number should be chosen. At some point increasing the r-number is not useful any more, because the wave reflection analysis program, Wavelab, does not support frequency bins smaller than $1/2^16$. The use of more exact frequencies will give difficulties in the reflection analysis. The Matlab file is used again to investigate te influence of rounding off to a fraction of 2 to the power something. The rounding off appeared to be of major influence in case of the used r-number of 16 (rounding to a fraction of 2^12). An r-number of 20 appeared to give minor rounding off errors and should be used for the wave groups. After testing the wave series with an r-number of 20, the time series and wave height distributions from the flume were practically the same as the theoretically and desired time series and wave height distributions. The too small r-number appeared to be the main cause of deviation from the theoretical values. Nineteen of the 24 wave series has now a deviation smaller than 3% in the H_s, and the rations between $H_{2\%}$, $H_{0.1\%}$ and H_s. The other five wave groups deviates from the theory due to wave breaking or a large location dependency of a part of the waves. How these wave groups should be treated is described in the next sections.

C.2.5 Location dependency

Two wave groups have a practically identical time series compared to the theoretical time series, the H_s and $H_{0.1\%}/H_s$ has a deviation less than 3%, but the $H_{2\%}/H_s$ deviates with about 10%. For these two groups the location dependency of the waves with a wave height between $H_{3\%}$ and $H_{1\%}$ is very large. The value of $H_{2\%}/H_s$ differs from 1.3 to 1.45, while 1.35 is desired, in a span of 1 meter distance from the location of the toe of the breakwater for one of the groups. For the other group $H_{2\%}/H_s$ differs from 1.12 to 1.25 while 1.15 is desired. Since the wave gauges for one reflection analysis are spread over 0.7 meter, the reason for the deviation of these groups can be that the location of the calculation of the reflection analysis slightly differs from the location of the Matlab calculation. It happens that exactly at $H_{2\%}$ a jump occurs in the wave height distribution when the location slightly differs. Because of this jump only $H_{2\%}$ differs from the calculated value, $H_{2.1\%}$ does not deviate. This wave series can therefore be used for the model tests.

C.2.6 Wave breaking

In the case of the three other not matching wave groups, the waves start to break directly after the wave board. The breaking of the waves looks more like white capping than shallow water related wave breaking. It only occurs during the highest waves in the time series of wave series without wave trains, with the highest $H_{0.1\%}/H_s$ and the wave steepness of 0.05. None of the waves with a steepness of 0.03 are breaking. The cause of this white capping seems to be the large difference in propagation speed of the mutual harmonics. The waves seems to become too steep very locally by overtaking waves. Especially because the wave series with wave trains with the same wave height distribution does not show white capping. The white capping of the waves can be prevented by choosing an other steepness or other frequencies. A steepness of 0.04 gives better results, but still some waves are breaking. Choosing an even smaller steepness will be not possible, because these wave series with a steepness of 0.03 already exist. Making groups with other frequencies in such a way that the propagation speed does not differ that much any more will also be not very helpful, because that wave series will have wave trains and that wave series also already exist. These three wave series should not be used in the test programme, since the wave breaking makes them irrelevant.

Appendix D

Specifications of the wave series

This appendix gives the specifications of the used wave series during model testing. See table D.1. The basis formula is a summation of 8 harmonics (equation D.1). The wave series will be described in terms of the amplitude vector (A), the phase speed vector (ω) and the phase vector (φ). The phase vector differs at the location of the breakwater (φ_{bw}) and the location of the wave maker (φ_{wm}). The name of the wave series is as described in table 5.2.

$$wave\,group = \sum_{i=1}^{8}(A_i\,cos(\omega_i\,t + \phi_i)) \tag{D.1}$$

Table D.1: Specifications of the wave groups

Wave series	A [mm]	ω [rad/s]	φ_{bw} [rad]	φ_{wm} [rad]
115128g3	[0 1 3 15 34 4 1 3]	[4.19 4.25 4.28 4.30 4.40 4.42 4.46 4.51]	[625 635 639 642 657 660 665 673]	[658 668 673 676 692 695 701 709]
115138g3	[9 0 0 27 4 14 4 9]	[4.22 4.29 4.32 4.34 4.44 4.46 4.50 4.55]	[433 440 443 445 455 457 461 466]	[466 474 477 480 491 493 498 503]
135146g3	[23 16 16 13 2 0 0 0]	[4.36 4.43 4.46 4.48 4.59 4.61 4.65 4.70]	[541 550 553 556 568 571 576 582]	[576 585 590 592 606 609 614 621]
135185g3	[17 14 7 12 14 14 10 1]	[4.26 4.33 4.35 4.37 4.47 4.49 4.53 4.58]	[541 550 553 556 568 571 576 582]	[574 584 588 591 605 607 613 620]
145157g3	[21 15 0 15 12 12 0 0]	[4.30 4.37 4.40 4.42 4.52 4.54 4.58 4.63]	[1835 1865 1878 1886 1929 1937 1954 1976]	[1870 1900 1913 1922 1966 1975 1992 2014]
145203g3	[10 10 19 10 10 14 14 11]	[4.23 4.30 4.32 4.34 4.44 4.46 4.50 4.55]	[237 241 242 243 249 250 252 255]	[270 275 277 278 285 286 289 292]
115128ug3	[3 16 1 4 1 3 35 3]	[2.19 2.20 2.22 3.27 3.28 4.38 4.40 4.41]	[304 306 308 454 455 608 610 612]	[318 321 323 477 478 643 645 648]
115138ug3	[0 21 0 5 26 7 12 0]	[2.95 2.97 2.99 4.41 4.42 5.92 5.94 5.95]	[304 306 308 454 455 608 610 612]	[324 327 329 490 491 667 669 672]
135146ug3	[0 10 21 12 0 15 21 0]	[2.58 2.60 2.62 3.86 3.87 5.18 5.20 5.21]	[304 306 308 454 455 608 610 612]	[321 324 326 483 484 654 656 659]
135185ug3	[5 11 14 18 18 7 9 14]	[2.91 2.93 2.95 4.35 4.36 5.83 5.85 5.87]	[191 192 193 284 285 381 382 383]	[211 212 214 319 320 438 439 441]
145157ug3	[21 14 5 7 9 9 9 9]	[3.32 3.34 3.36 4.96 4.97 6.65 6.67 6.69]	[1212 1220 1228 1812 1816 2428 2436 2444]	[1235 1243 1252 1854 1859 2501 2510 2518]
145203ug3	[13 12 12 13 12 13 13 16]	[2.72 2.75 2.78 4.10 4.11 5.50 5.52 5.54]	[295 298 301 443 444 594 596 598]	[314 317 320 475 476 645 647 650]
115128g5	[0 1 3 15 34 4 1 3]	[5.40 5.49 5.53 5.55 5.68 5.70 5.75 5.82]	[625 635 639 642 657 660 665 673]	[675 686 691 694 711 714 721 729]
115138g5	[9 0 0 27 4 14 4 9]	[5.45 5.54 5.58 5.61 5.73 5.76 5.81 5.87]	[433 440 443 445 455 457 461 466]	[484 492 496 498 510 513 518 524]
135146g5	[23 16 16 13 2 0 0 0]	[5.63 5.72 5.76 5.79 5.92 5.95 6.00 6.06]	[541 550 553 556 568 571 576 582]	[595 605 609 612 627 630 636 644]
135185g5	[17 14 7 12 14 14 10 1]	[5.49 5.58 5.62 5.65 5.77 5.80 5.85 5.92]	[541 550 553 556 568 571 576 582]	[592 602 607 610 625 628 633 641]
145157g5	[21 15 0 15 12 12 0 0]	[5.55 5.64 5.68 5.71 5.84 5.86 5.91 5.98]	[1835 1865 1878 1886 1929 1937 1954 1976]	[1888 1919 1932 1941 1986 1995 2013 2036]
145203g5	[10 10 19 10 10 14 14 11]	[5.46 5.54 5.58 5.61 5.73 5.76 5.81 5.87]	[237 241 242 243 249 250 252 255]	[288 293 295 297 304 306 309 313]
115128ug5	[3 16 1 4 1 3 35 3]	[2.82 2.84 2.86 4.22 4.23 5.66 5.68 5.70]	[304 306 308 454 455 608 610 612]	[323 326 328 487 488 662 664 667]
115138ug5	[0 21 0 5 26 7 12 0]	[3.81 3.83 3.86 5.70 5.71 7.64 7.66 7.69]	[304 306 308 454 455 608 610 612]	[333 335 337 509 510 705 707 710]
135146ug5	[0 10 21 12 0 15 21 0]	[3.34 3.36 3.38 4.99 5.00 6.69 6.71 6.73]	[304 306 308 454 455 608 610 612]	[328 330 332 497 498 682 685 687]
135185ug5	[5 11 14 18 18 7 9 14]	[3.75 3.78 3.80 5.61 5.63 7.52 7.55 7.57]	[191 192 193 284 285 381 382 383]	[219 220 222 338 339 474 476 478]
145157ug5	[21 14 5 7 9 9 9 9]	[4.28 4.31 4.34 6.40 6.42 8.58 8.61 8.64]	[1212 1220 1228 1812 1816 2428 2436 2444]	[1245 1254 1262 1880 1884 2550 2558 2567]
145203ug5	[13 12 12 13 12 13 13 16]	[3.52 3.55 3.59 5.30 5.31 7.10 7.12 7.15]	[295 298 301 443 444 594 596 598]	[321 324 327 491 493 677 680 682]

Appendix E

Graphics of the wave series

This appendix shows for every wave series the target wave height distribution, which follows from the representative existing model test. This wave height distribution is associated with the waves of an offshore Jonswap spectrum influenced by a foreshore. The wave height distributions of the hand-made wave series are given as calculated with Matlab and for the calibrated wave series in the wave flume. These wave series are made in such a way that the wave height distribution in deep water is comparable with the wave height distribution of a Jonswap spectrum influenced by the foreshore. It can be clearly seen by comparing the graphics of the wave height distributions that the target wave height distribution is nicely simulated by both the calculated and measured wave height distribution in the flume. Only the 3 wave series where breaking of the waves by a white capping like phenomenon occurs, deviate from the target wave height distribution (series 135185ug5, 145157ug5 and 145203ug5). Comparing the calculated time series of the wave series with the measured ones, it can be clearly seen that the waves in the flume are practically the same as the calculated waves. Only the three wave series with breaking waves show large differences between both time series. A detail of the highest waves in the time series is included to show whether wave trains are present or not in the time series of the waves.

H2%/Hs = 1.15 ; H0.1%/Hs = 1.28 ; Grouped ; steepness = 0.03

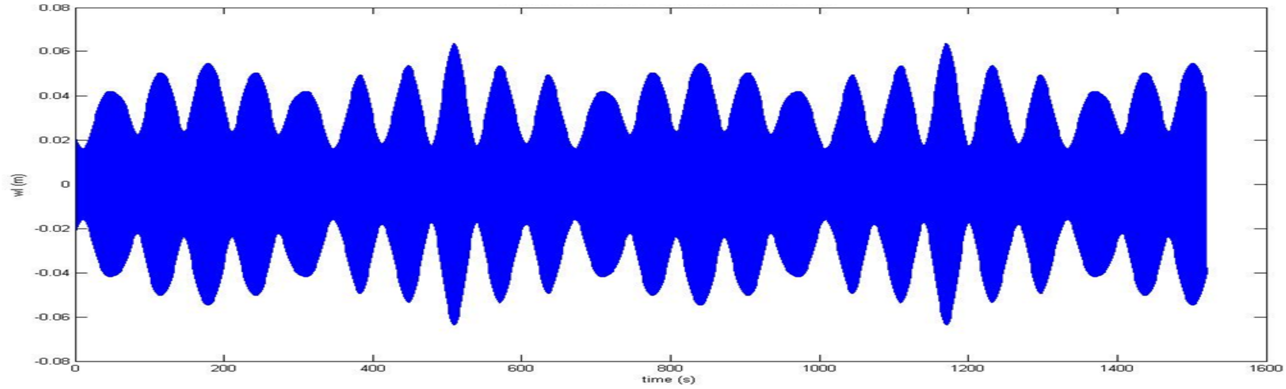

Calculated time series (Matlab)

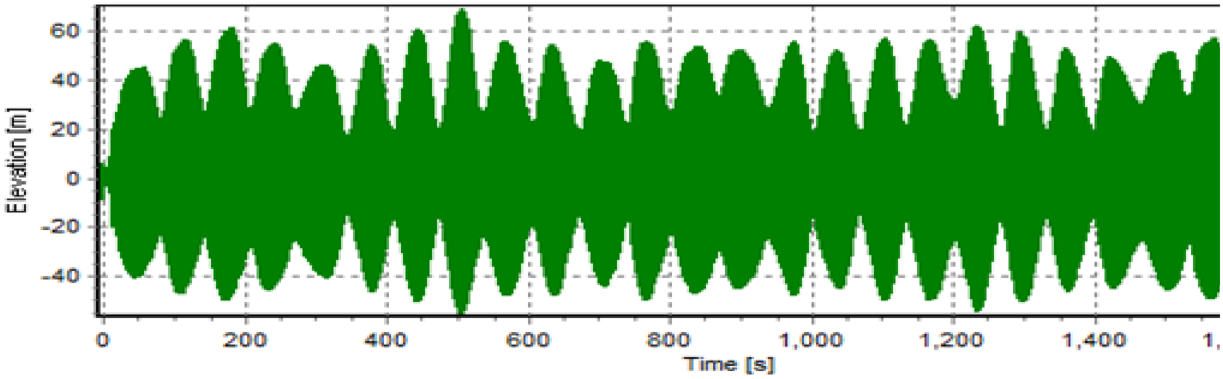

Occurred time series in the flume (Wavelab)

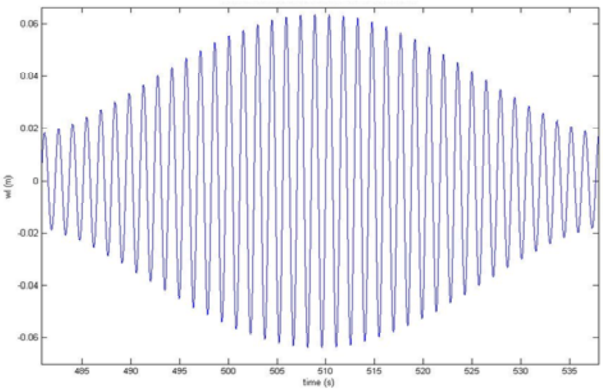

Detail of calculated time series (Matlab)

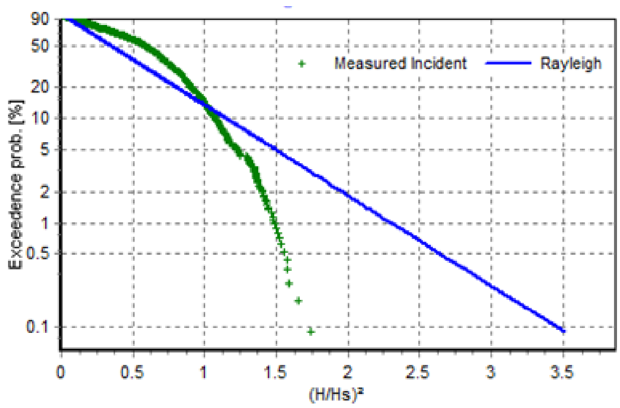

Target wave height distribution (existing model test)

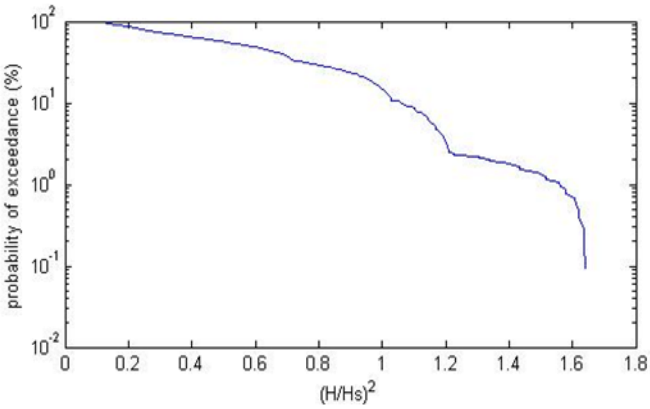

Calculated wave height ditribution (Matlab)

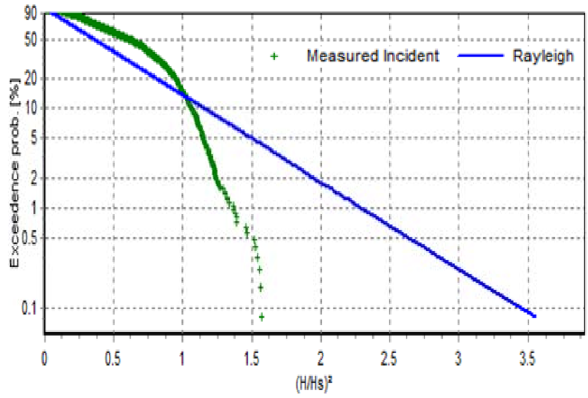

Occurred wave height distribution in the flume (Wavelab)

H2%/Hs = 1.15 ; H0.1%/Hs = 1.28 ; Grouped ; steepness = 0.05

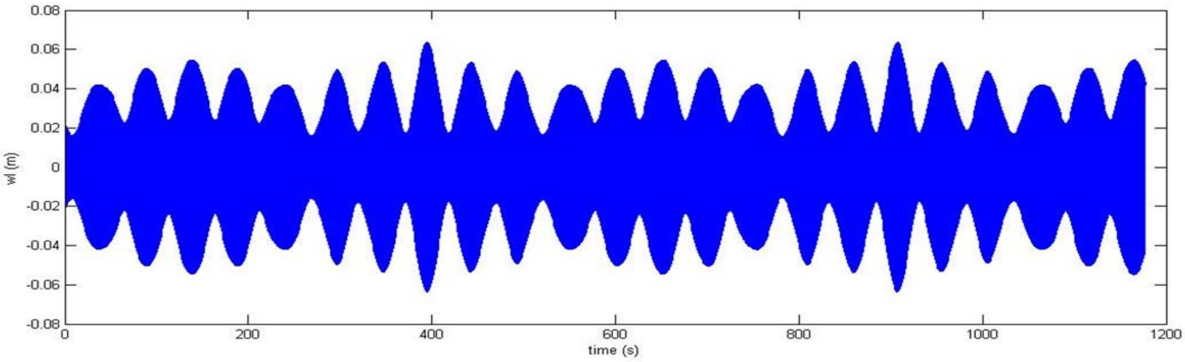

Calculated time series (Matlab)

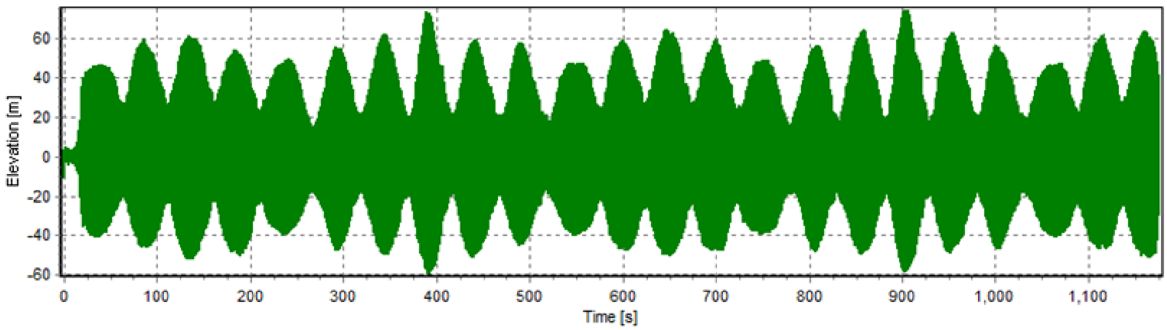

Occurred time series in the flume (Wavelab)

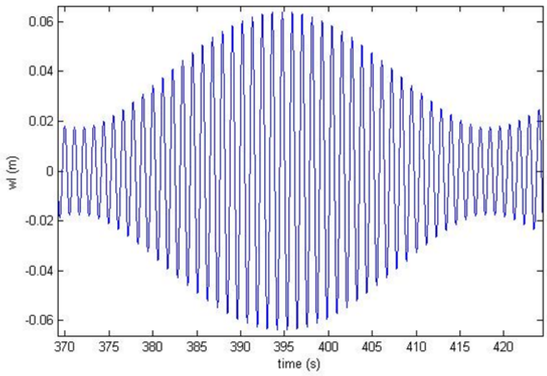

Detail of calculated time series (Matlab)

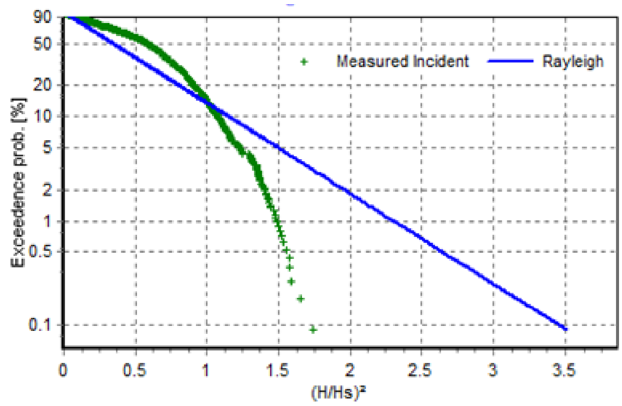

Target wave height distribution (existing model test)

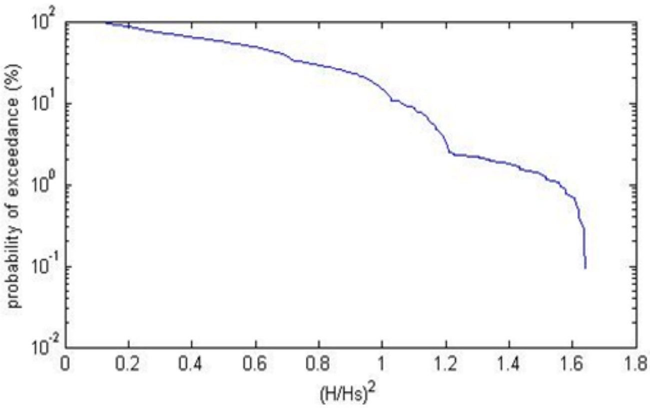

Calculated wave height ditribution (Matlab)

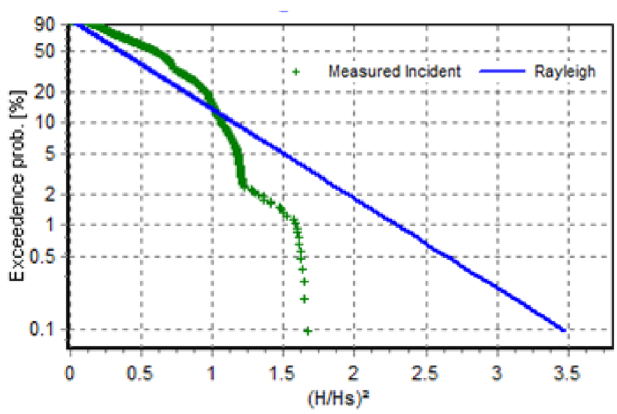

Occurred wave height distribution in the flume (Wavelab)

H2%/Hs = 1.15 ; H0.1%/Hs = 1.28 ; Ungrouped ; steepness = 0.03

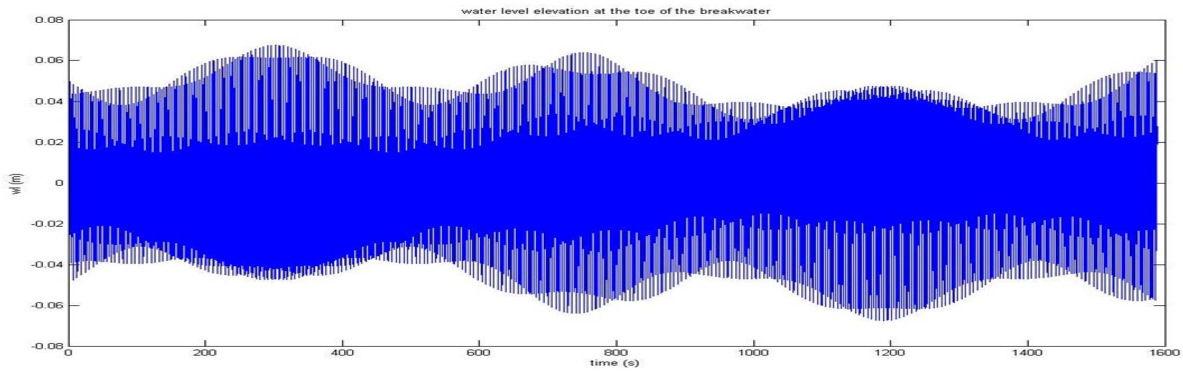

Calculated time series (Matlab)

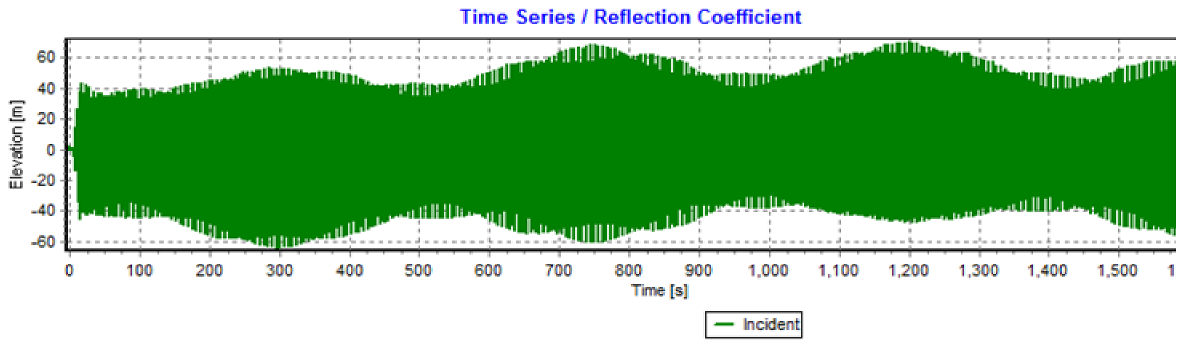

Occurred time series in the flume (Wavelab)

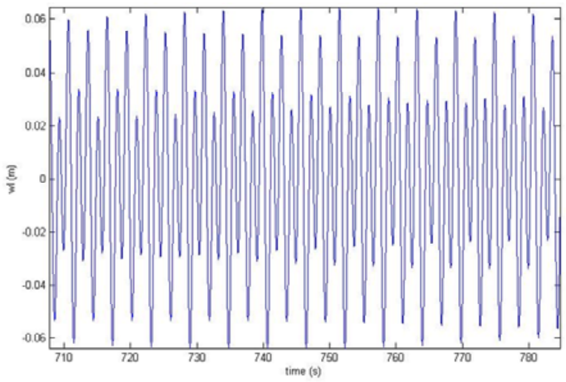

Detail of calculated time series (Matlab)

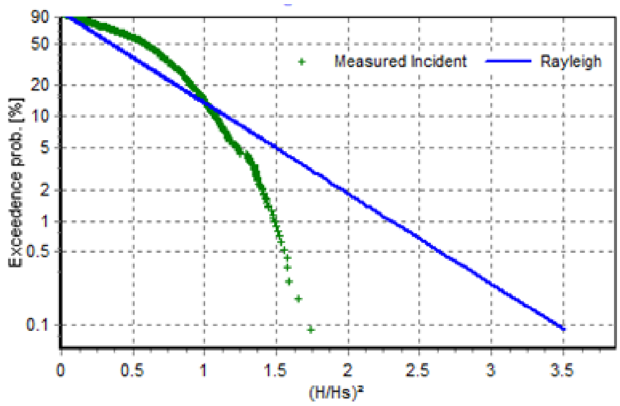

Target wave height distribution (existing model test)

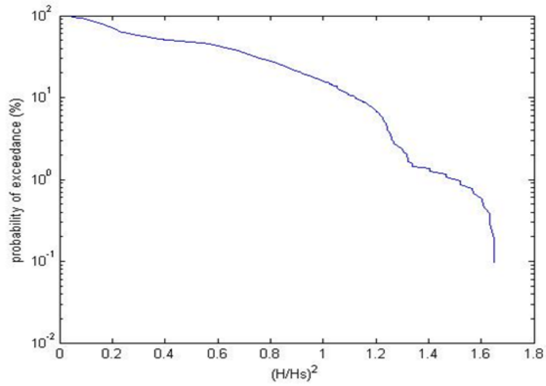

Calculated wave height ditribution (Matlab)

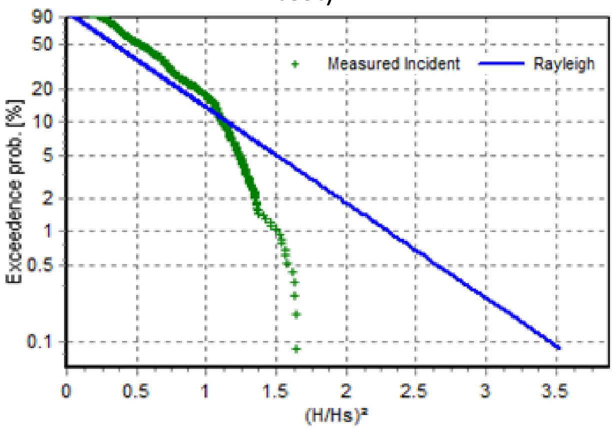

Occurred wave height distribution in the flume (Wavelab)

H2%/Hs = 1.15 ; H0.1%/Hs = 1.28 ; Ungrouped ; steepness = 0.05

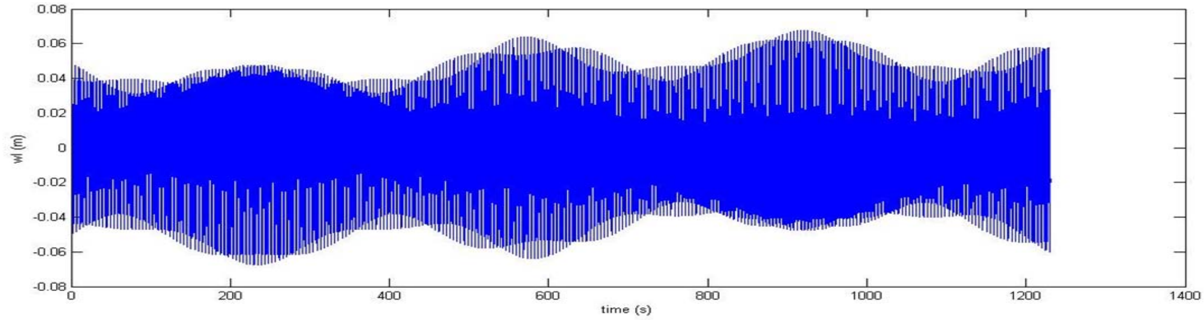

Calculated time series (Matlab)

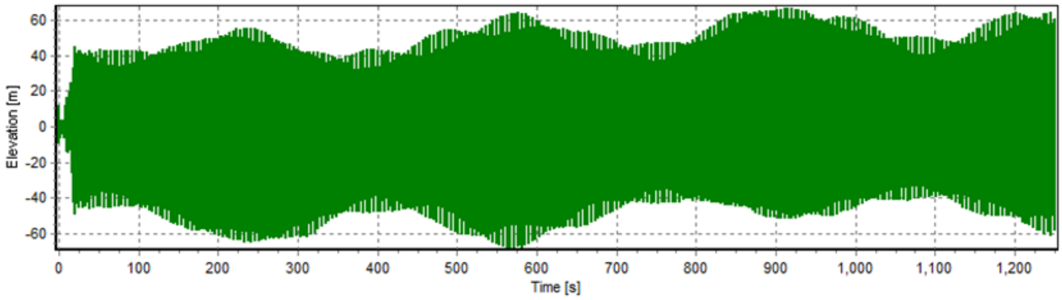

Occurred time series in the flume (Wavelab)

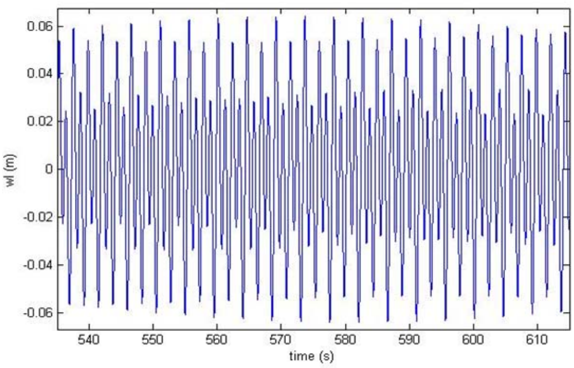

Detail of calculated time series (Matlab)

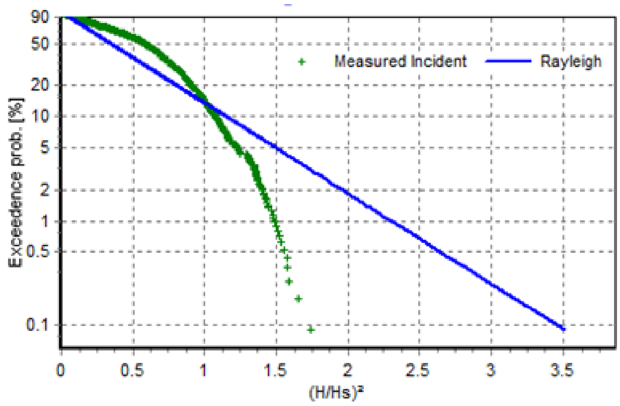

Target wave height distribution (existing model test)

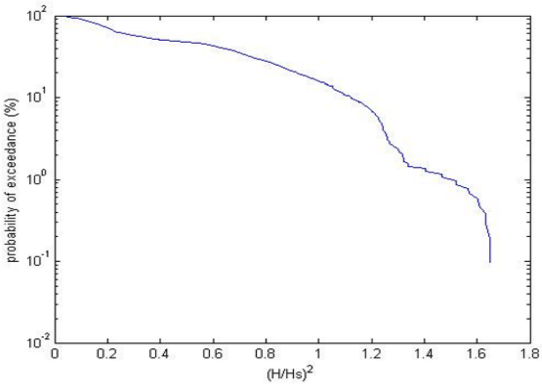

Calculated wave height ditribution (Matlab)

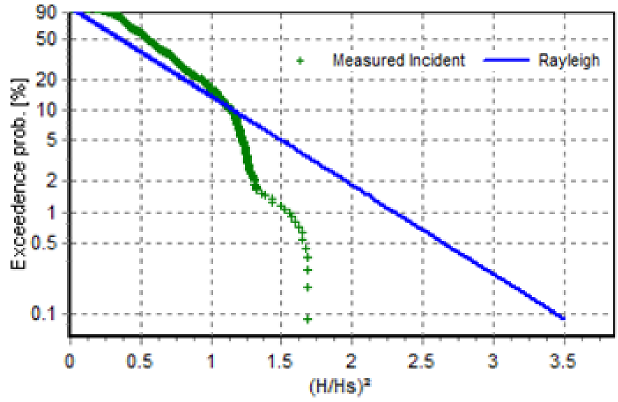

Occurred wave height distribution in the flume (Wavelab)

H2%/Hs = 1.15 ; H0.1%/Hs = 1.38 ; Grouped ; steepness = 0.03

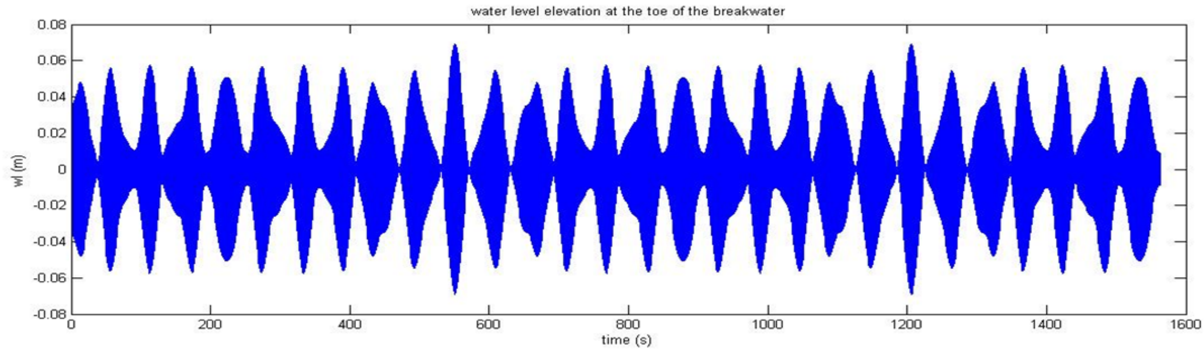

Calculated time series (Matlab)

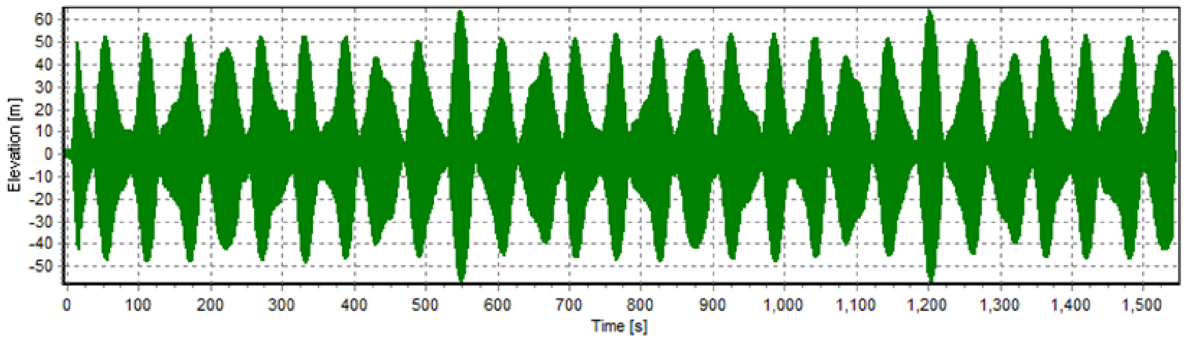

Occurred time series in the flume (Wavelab)

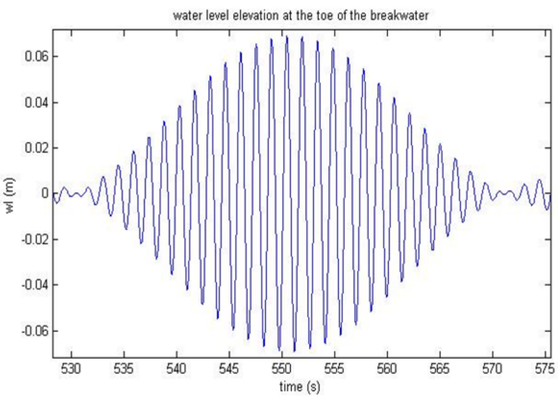

Detail of calculated time series (Matlab)

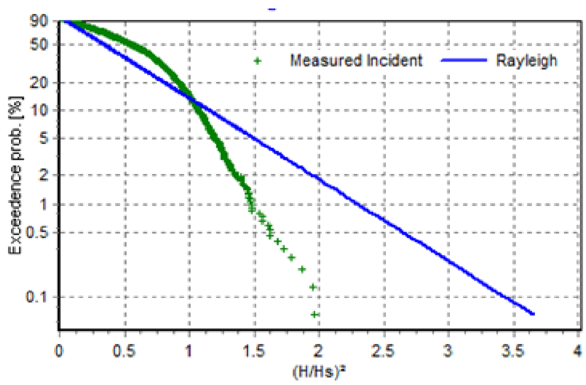

Target wave height distribution (existing model test)

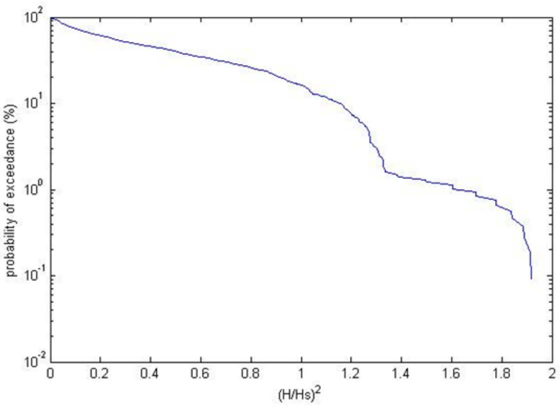

Calculated wave height ditribution (Matlab)

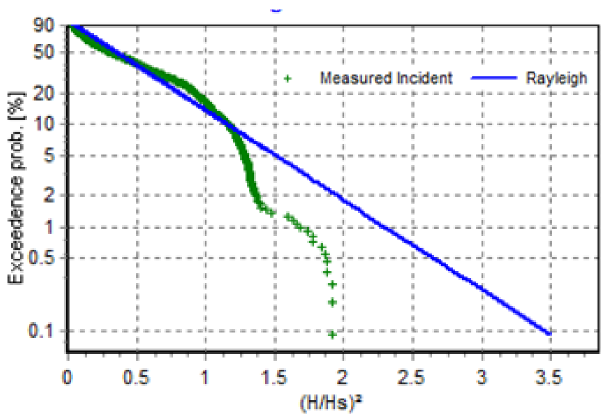

Occurred wave height distribution in the flume (Wavelab)

H2%/Hs = 1.15 ; H0.1%/Hs = 1.38 ; Grouped ; steepness = 0.05

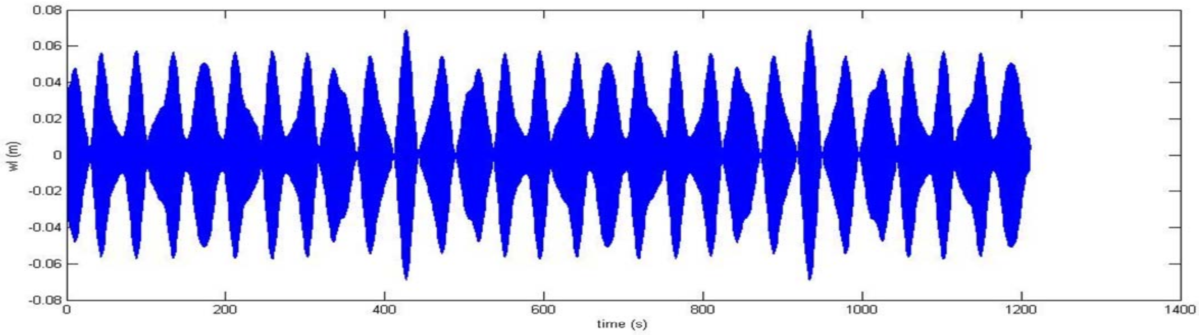

Calculated time series (Matlab)

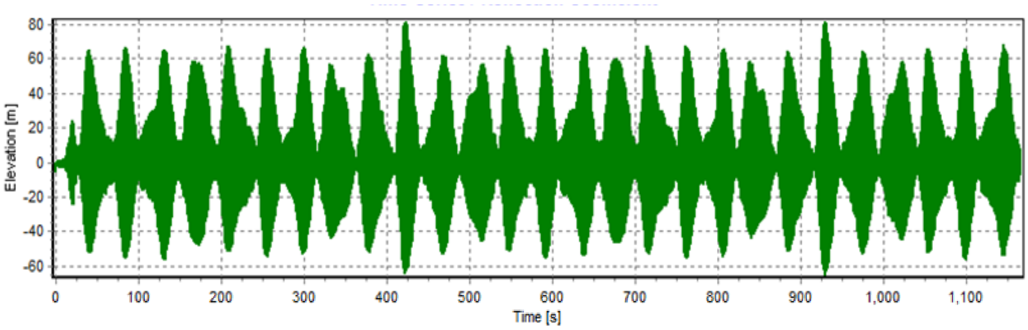

Occurred time series in the flume (Wavelab)

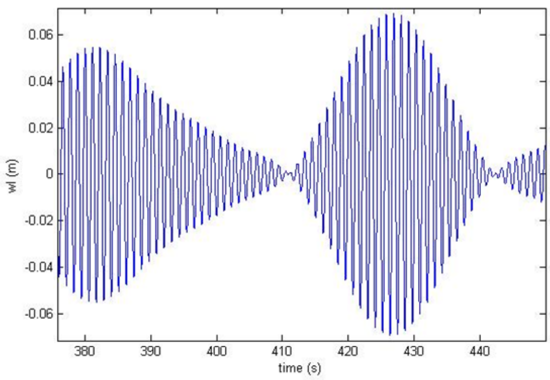

Detail of calculated time series (Matlab)

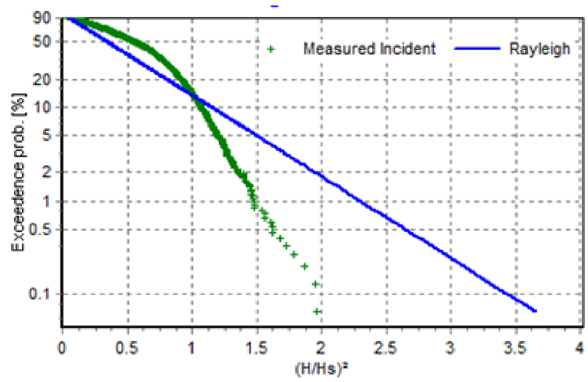

Target wave height distribution (existing model test)

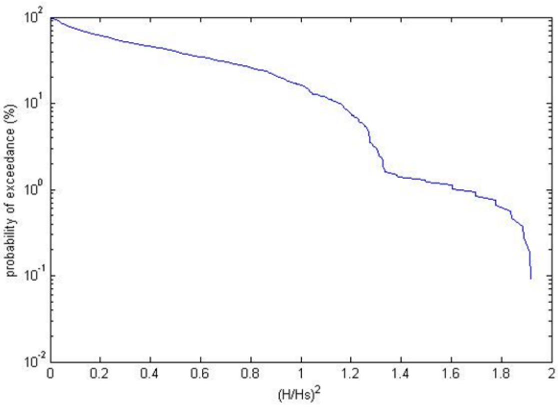

Calculated wave height ditribution (Matlab)

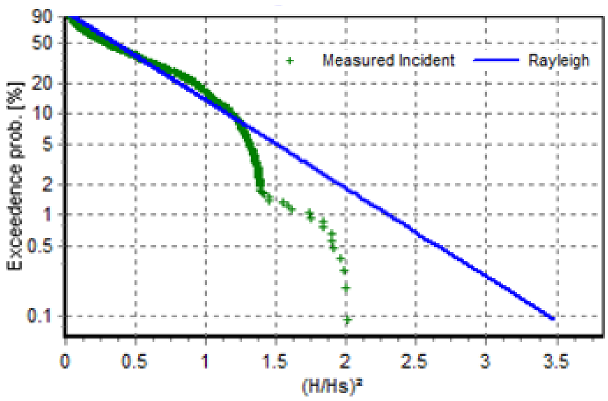

Occurred wave height distribution in the flume (Wavelab)

H2%/Hs = 1.15 ; H0.1%/Hs = 1.38 ; Ungrouped ; steepness = 0.03

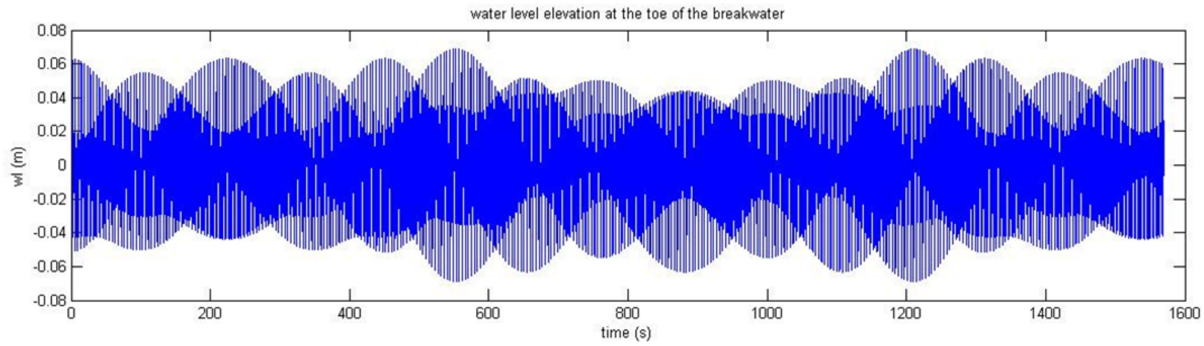

Calculated time series (Matlab)

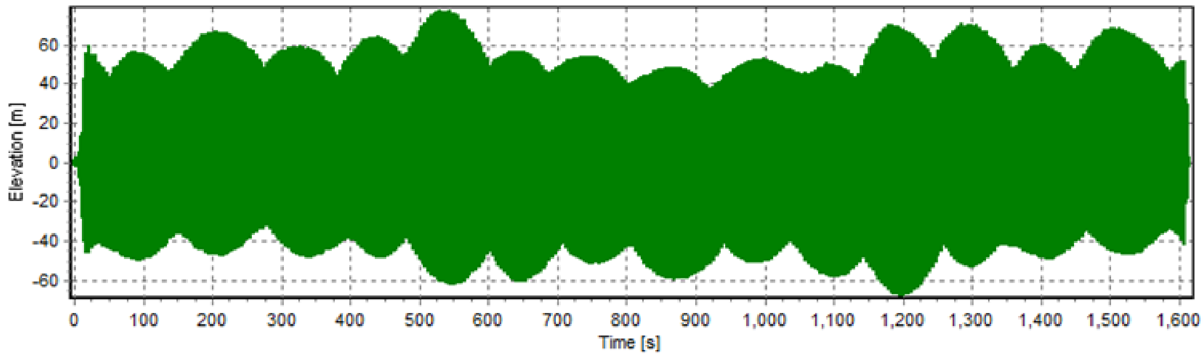

Occurred time series in the flume (Wavelab)

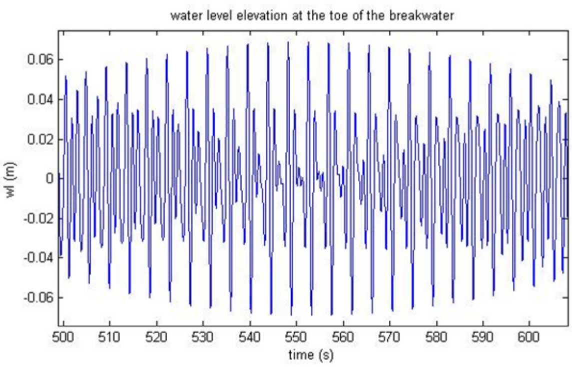

Detail of calculated time series (Matlab)

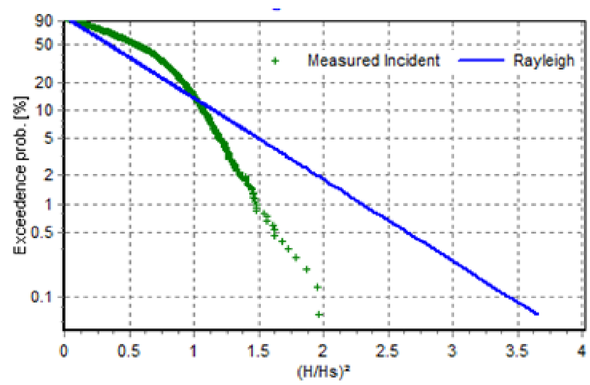

Desired wave height distribution (existing model test)

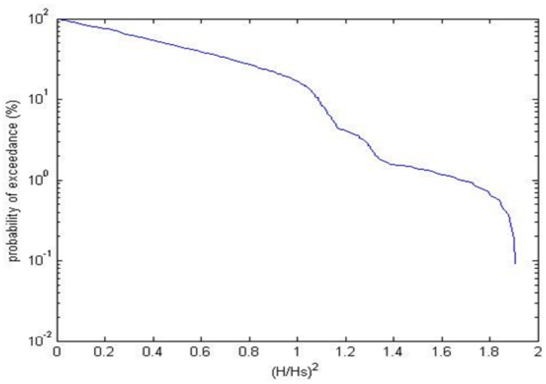

Calculated wave height ditribution (Matlab)

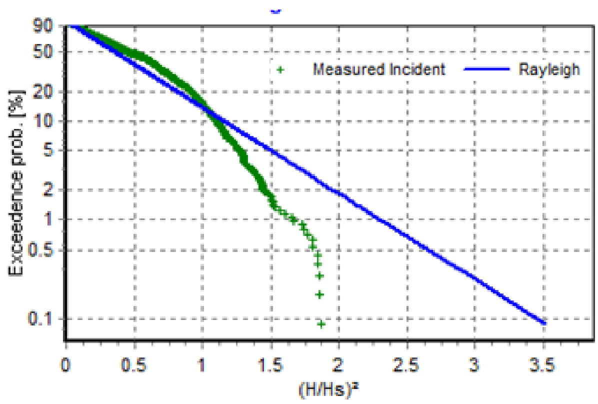

Occurred wave height distribution in the flume (Wavelab)

H2%/Hs = 1.15 ; H0.1%/Hs = 1.38 ; Ungrouped ; steepness = 0.05

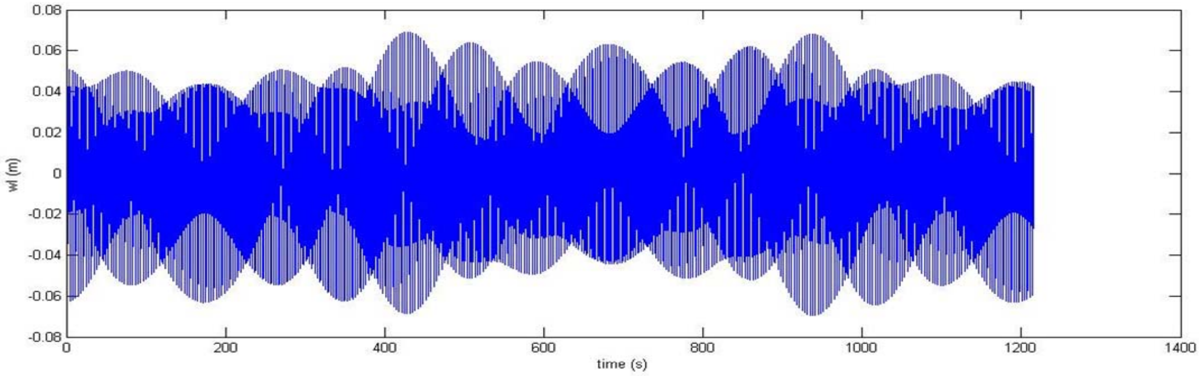

Calculated time series (Matlab)

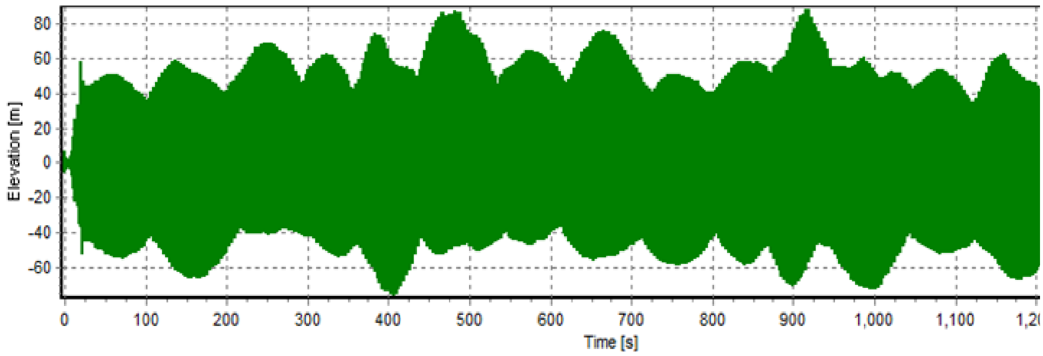

Occurred time series in the flume (Wavelab)

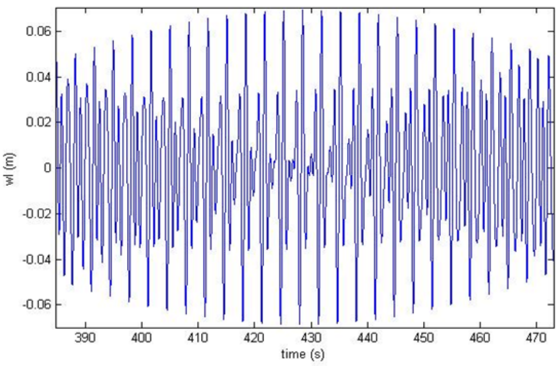

Detail of calculated time series (Matlab)

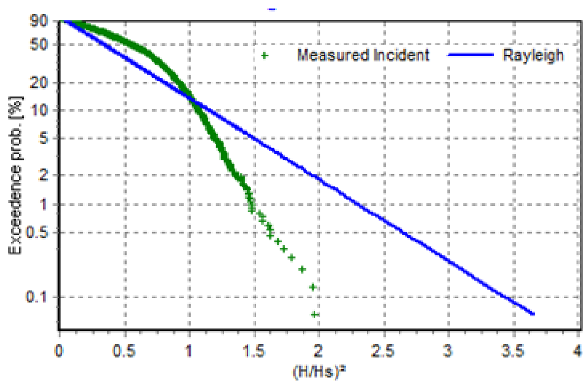

Target wave height distribution (existing model test)

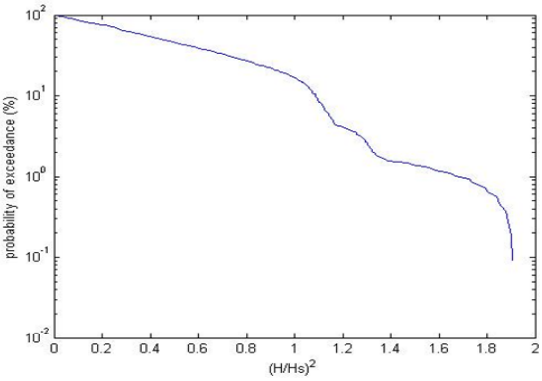

Calculated wave height ditribution (Matlab)

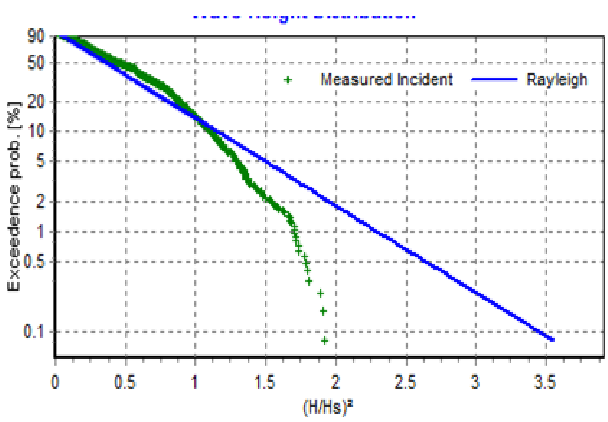

Occurred wave height distribution in the flume (Wavelab)

H2%/Hs = 1.35 ; H0.1%/Hs = 1.46 ; Grouped ; steepness = 0.03

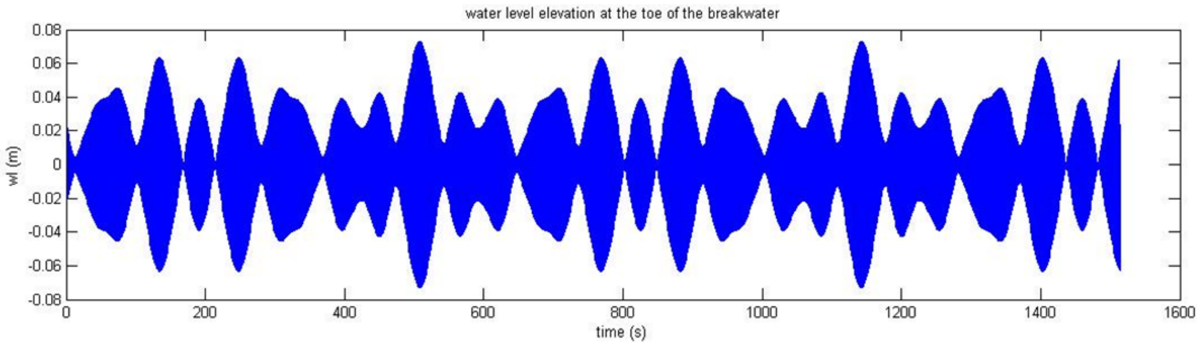

Calculated time series (Matlab)

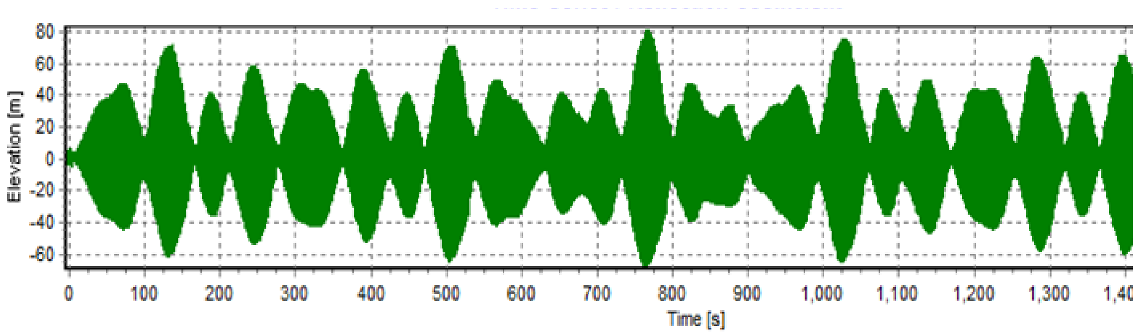

Occurred time series in the flume (Wavelab)

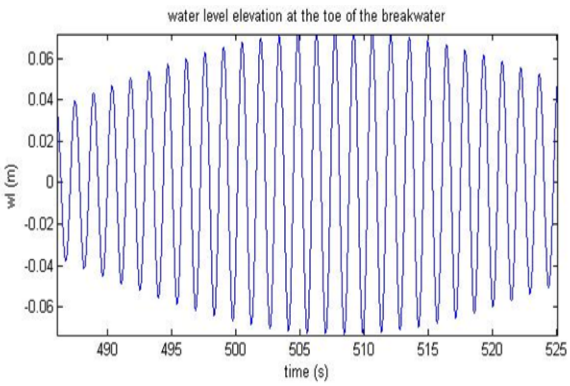

Detail of calculated time series (Matlab)

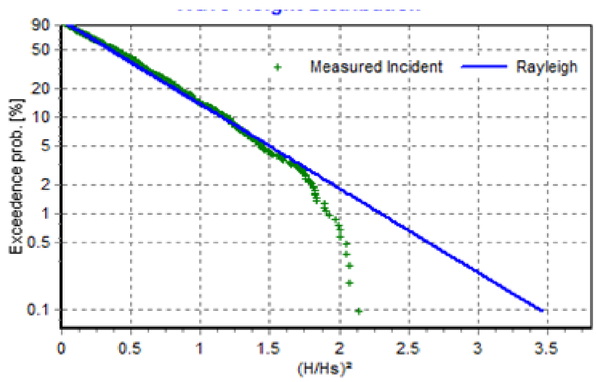

Target wave height distribution (existing model test)

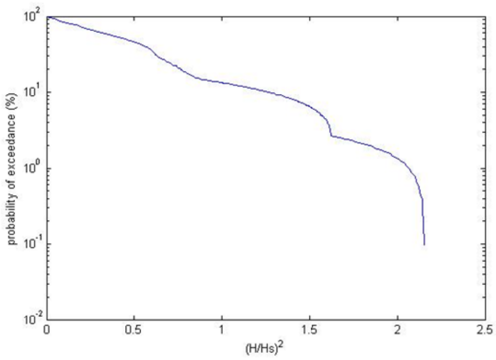

Calculated wave height ditribution (Matlab)

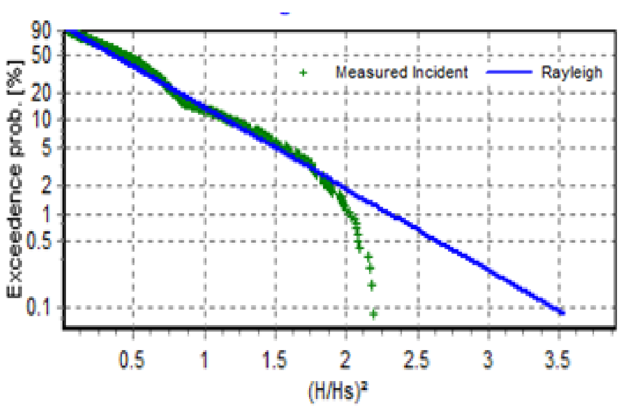

Occurred wave height distribution in the flume (Wavelab)

H2%/Hs = 1.35 ; H0.1%/Hs = 1.46 ; Grouped ; steepness = 0.05

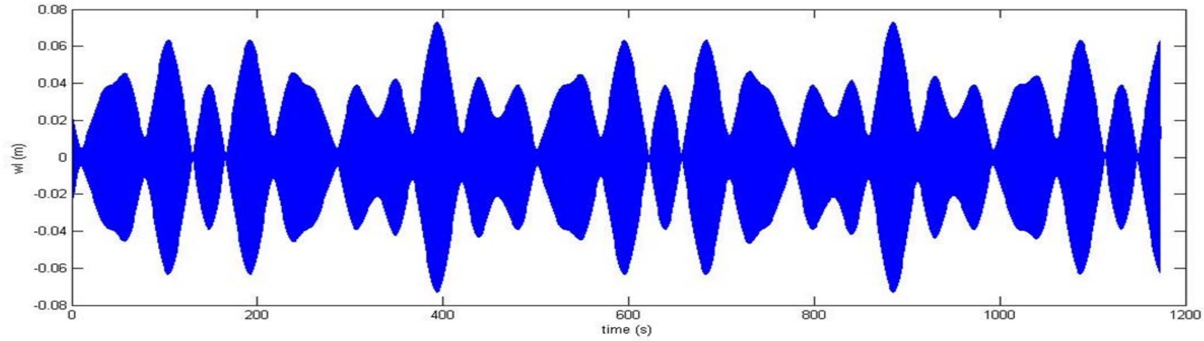

Calculated time series (Matlab)

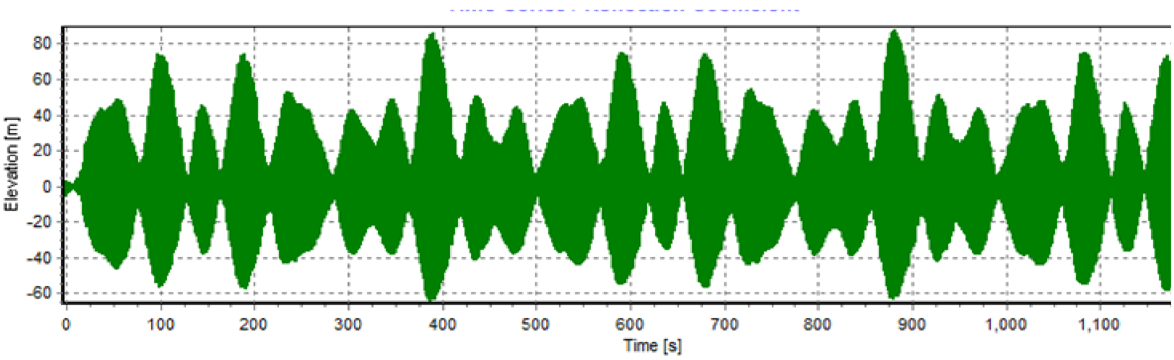

Occurred time series in the flume (Wavelab)

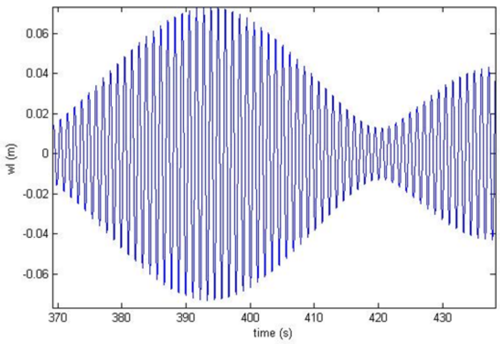

Detail of calculated time series (Matlab)

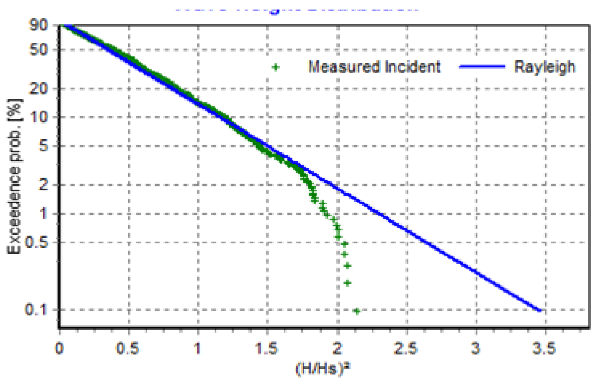

Target wave height distribution (existing model test)

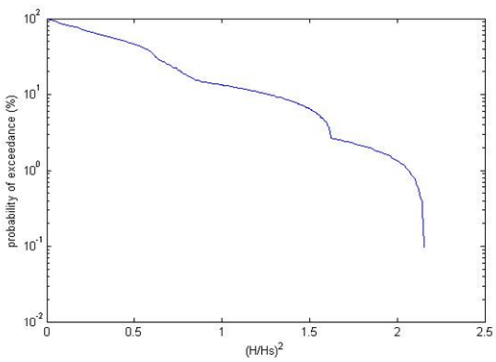

Calculated wave height ditribution (Matlab)

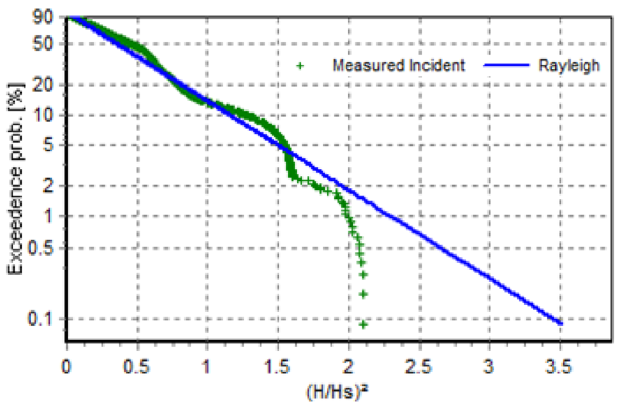

Occurred wave height distribution in the flume (Wavelab)

H2%/Hs = 1.35 ; H0.1%/Hs = 1.46 ; ungrouped ; steepness = 0.03

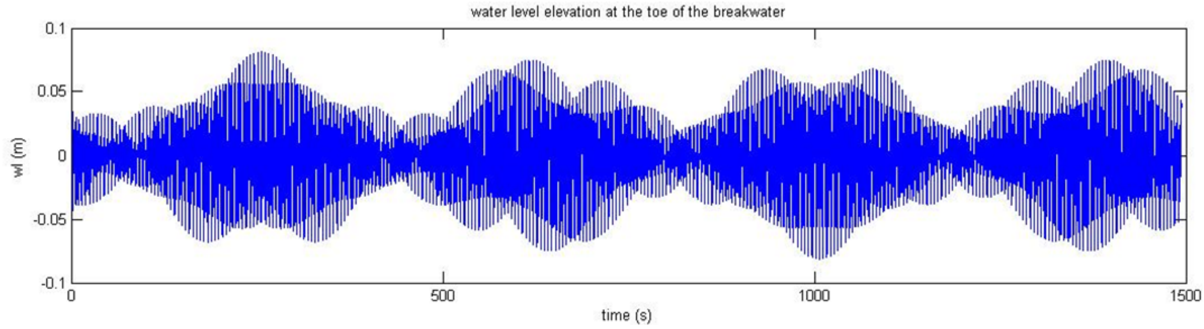

Calculated time series (Matlab)

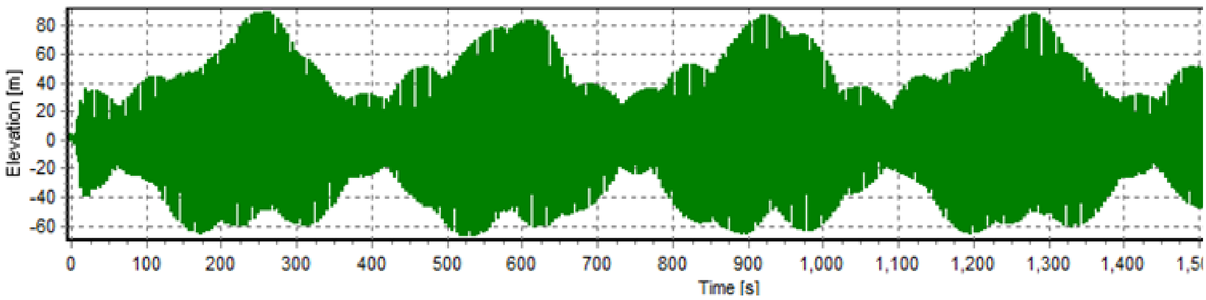

Occurred time series in the flume (Wavelab)

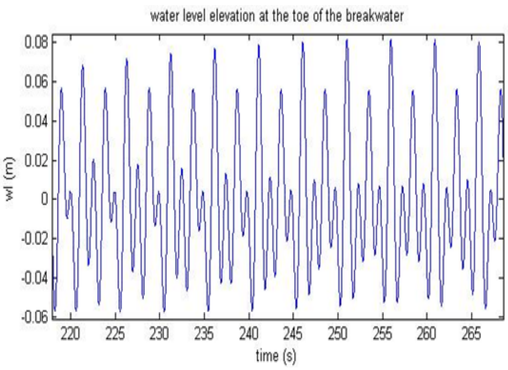

Detail of calculated time series (Matlab)

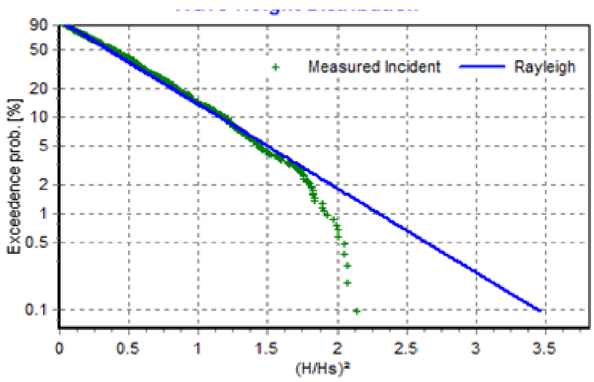

Target wave height distribution (existing model test)

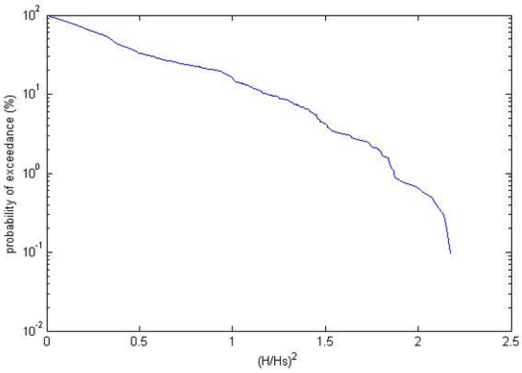

Calculated wave height ditribution (Matlab)

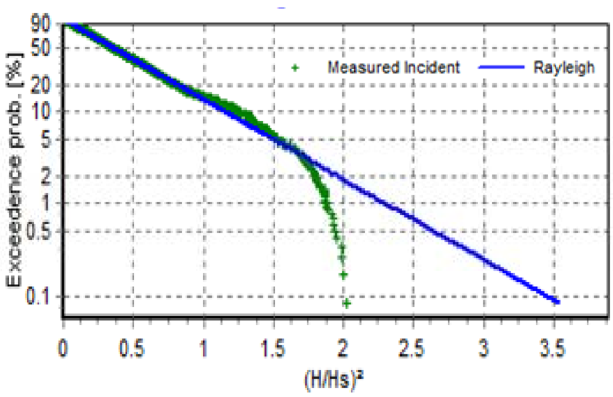

Occurred wave height distribution in the flume (Wavelab)

H2%/Hs = 1.35 ; H0.1%/Hs = 1.46 ; ungrouped ; steepness = 0.05

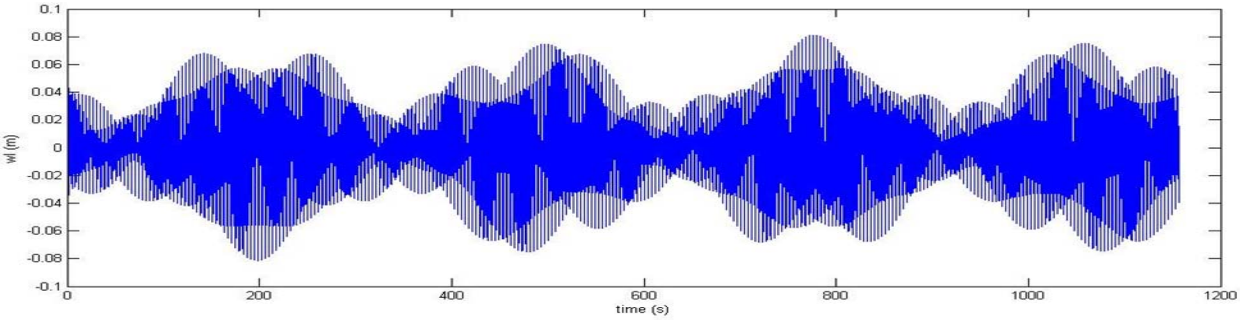

Calculated time series (Matlab)

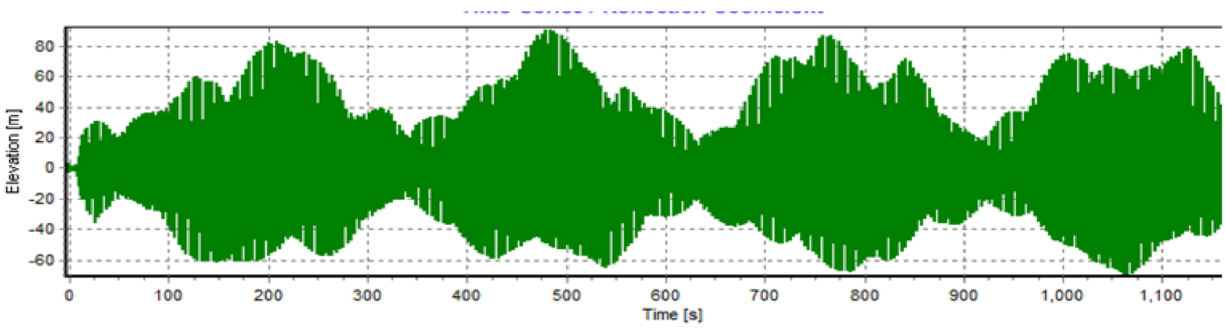

Occurred time series in the flume (Wavelab)

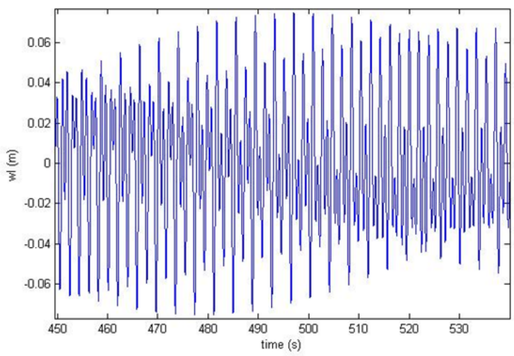

Detail of calculated time series (Matlab)

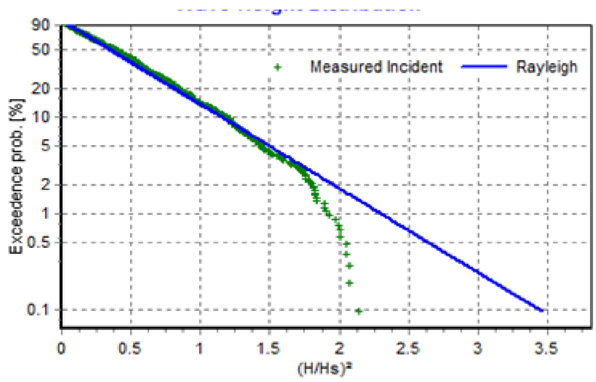

Target wave height distribution (existing model test)

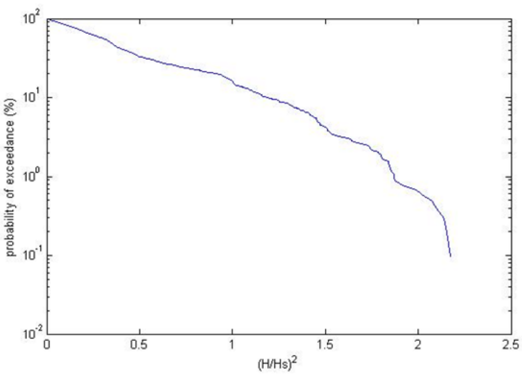

Calculated wave height ditribution (Matlab)

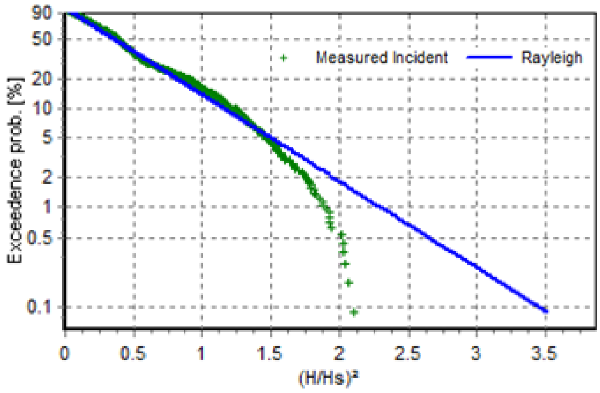

Occurred wave height distribution in the flume (Wavelab)

H2%/Hs = 1.35 ; H0.1%/Hs = 1.85 ; grouped ; steepness = 0.03

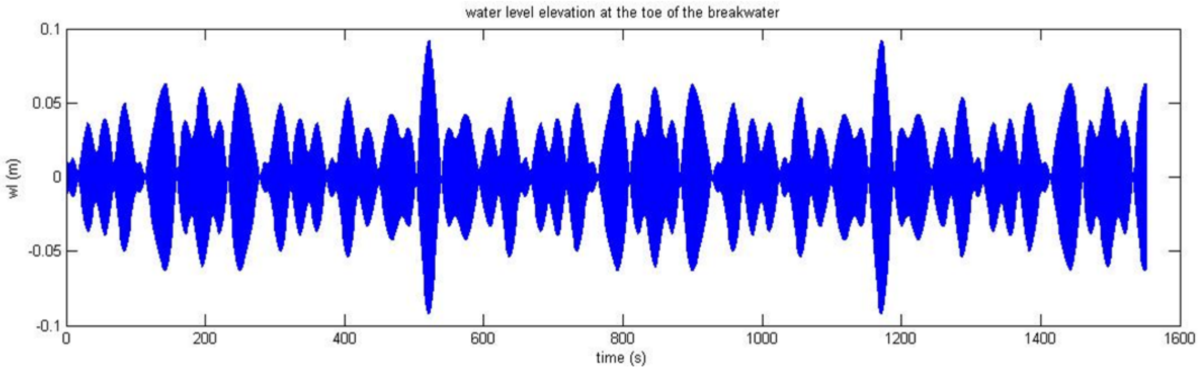

Calculated time series (Matlab)

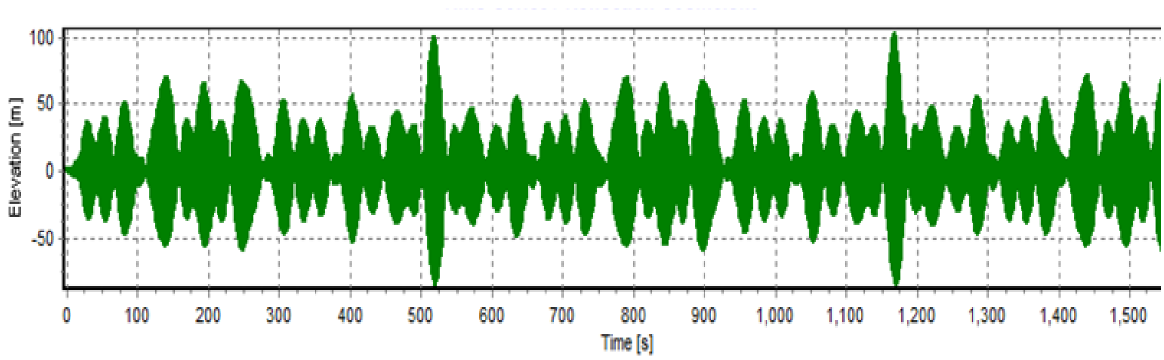

Occurred time series in the flume (Wavelab)

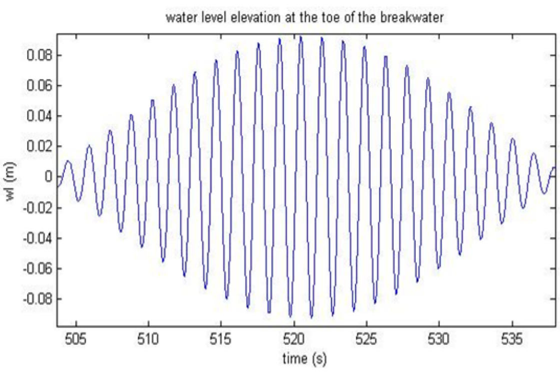

Detail of calculated time series (Matlab)

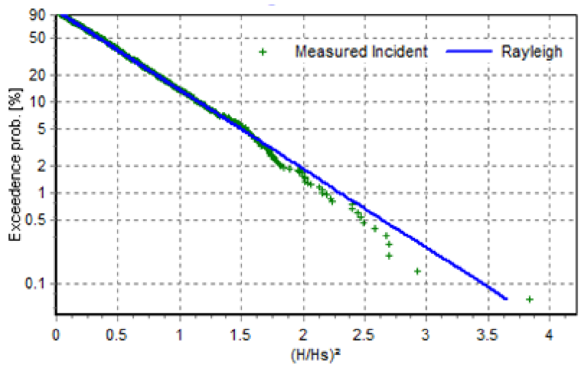

Target wave height distribution (existing model test)

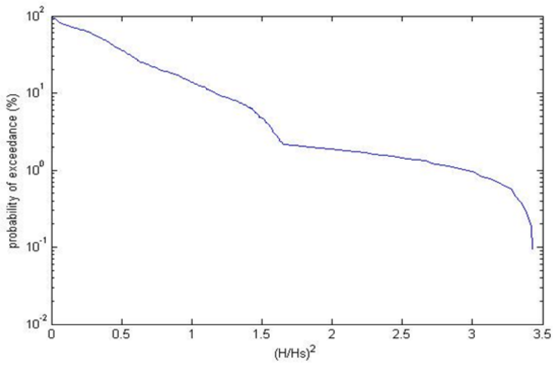

Calculated wave height ditribution (Matlab)

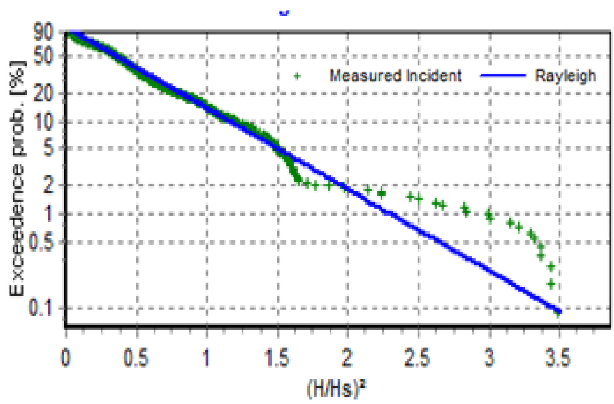

Occurred wave height distribution in the flume (Wavelab)

H2%/Hs = 1.35 ; H0.1%/Hs = 1.85 ; grouped ; steepness = 0.05

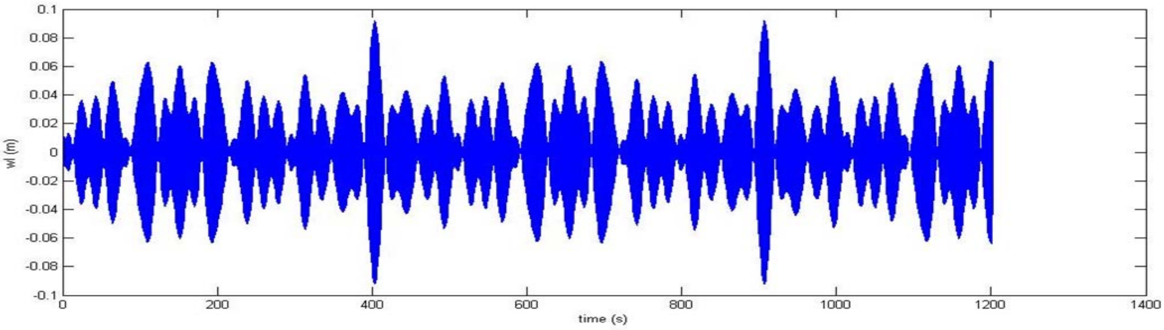

Calculated time series (Matlab)

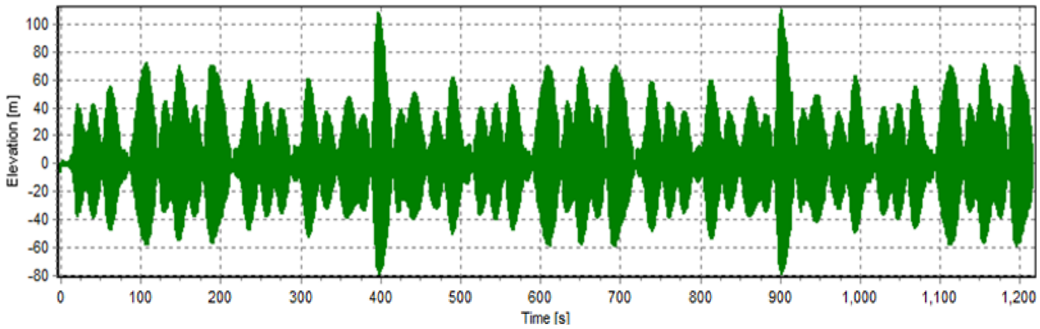

Occurred time series in the flume (Wavelab)

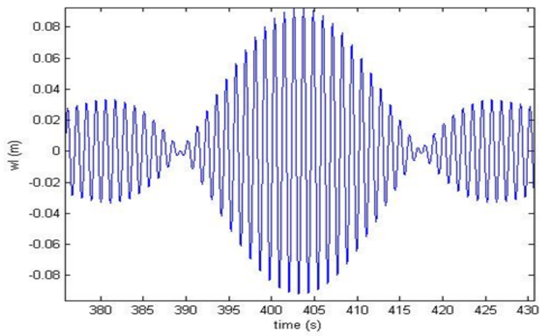

Detail of calculated time series (Matlab)

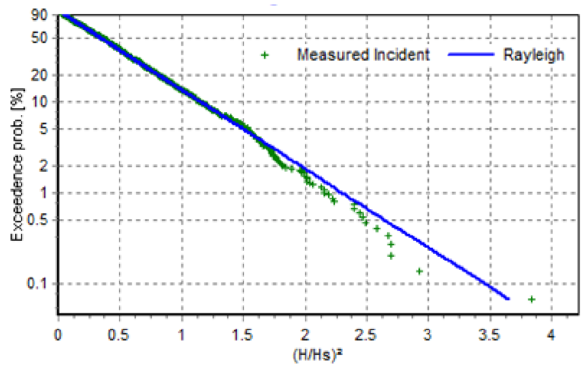

Target wave height distribution (existing model test)

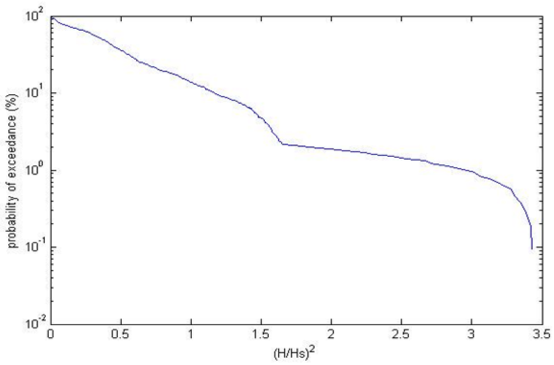

Calculated wave height ditribution (Matlab)

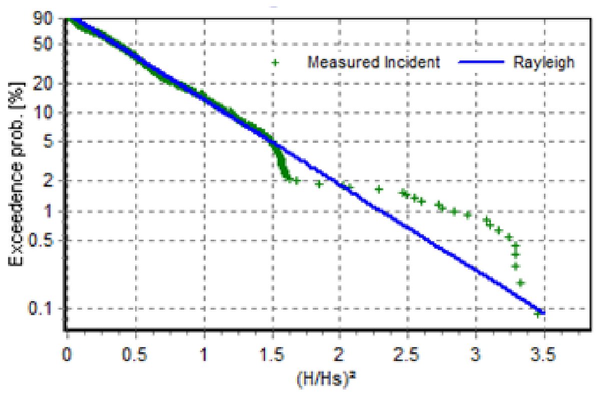

Occurred wave height distribution in the flume (Wavelab)

H2%/Hs = 1.35 ; H0.1%/Hs = 1.85 ; ungrouped ; steepness = 0.03

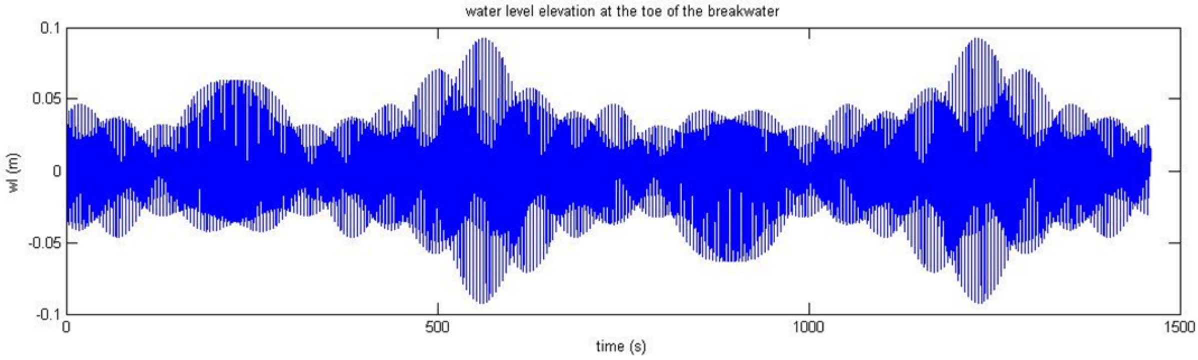

Calculated time series (Matlab)

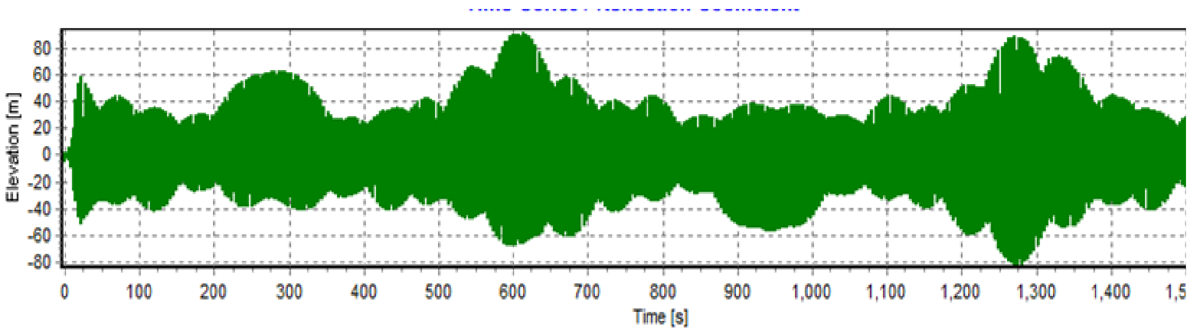

Occurred time series in the flume (Wavelab)

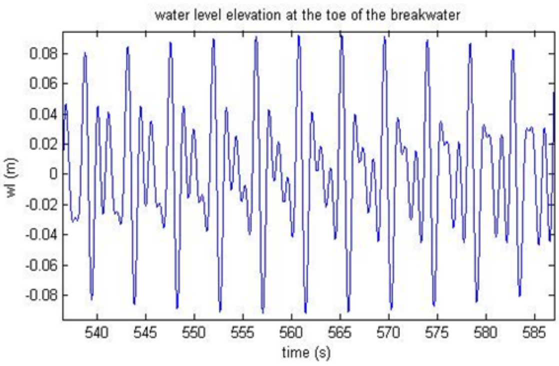

Detail of calculated time series (Matlab)

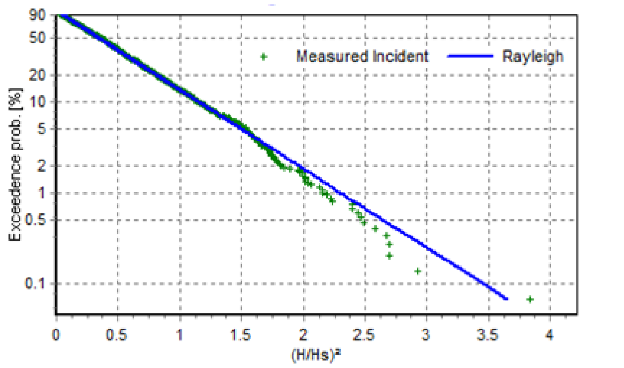

Target wave height distribution (existing model test)

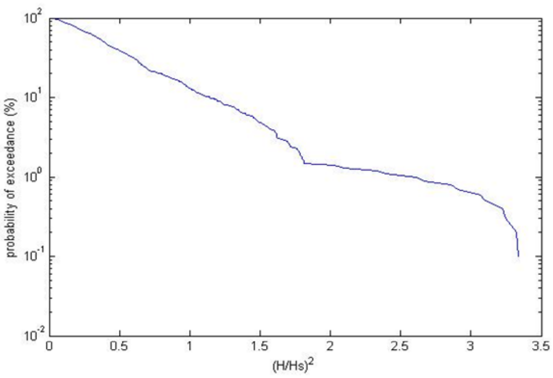

Calculated wave height ditribution (Matlab)

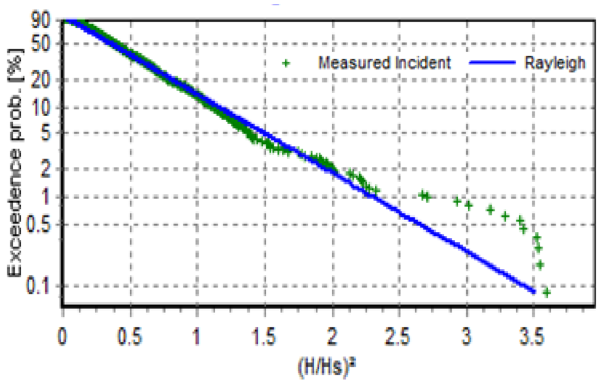

Occurred wave height distribution in the flume (Wavelab)

H2%/Hs = 1.35 ; H0.1%/Hs = 1.85 ; ungrouped ; steepness = 0.05

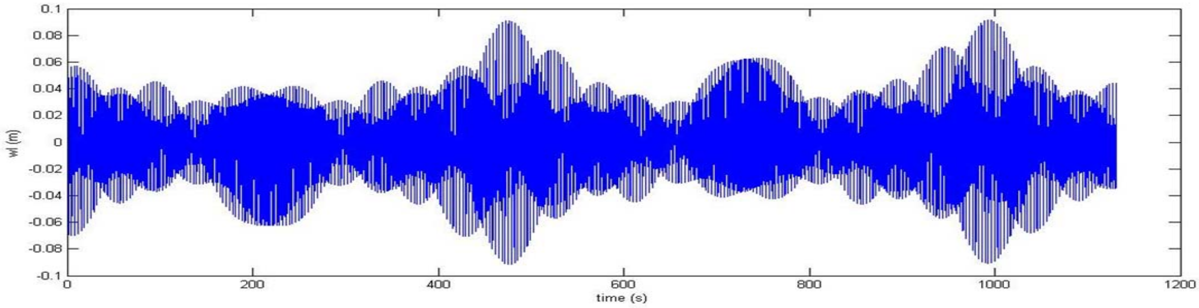

Calculated time series (Matlab)

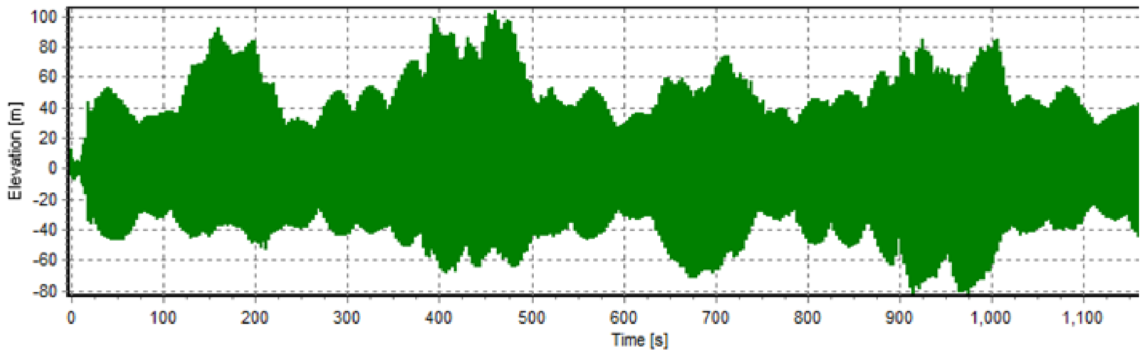

Occurred time series in the flume (Wavelab)

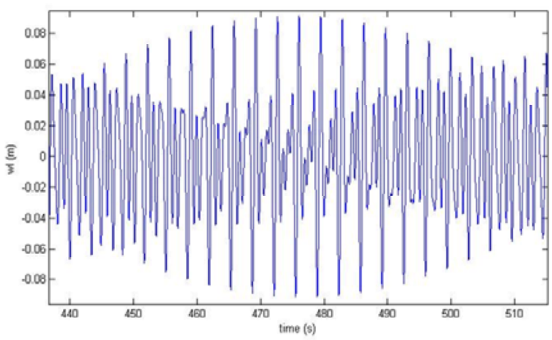

Detail of calculated time series (Matlab)

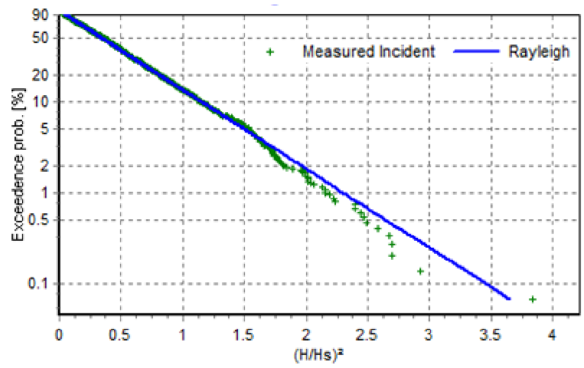

Target wave height distribution (existing model test)

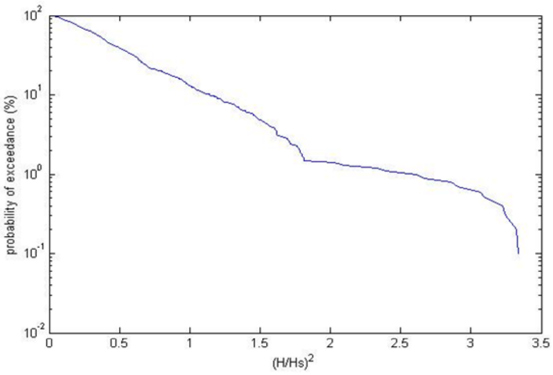

Calculated wave height ditribution (Matlab)

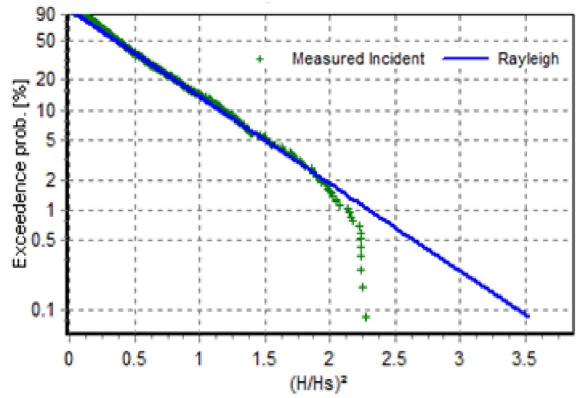

Occurred wave height distribution in the flume (Wavelab)

H2%/Hs = 1.45 ; H0.1%/Hs = 1.57 ; grouped ; steepness = 0.03

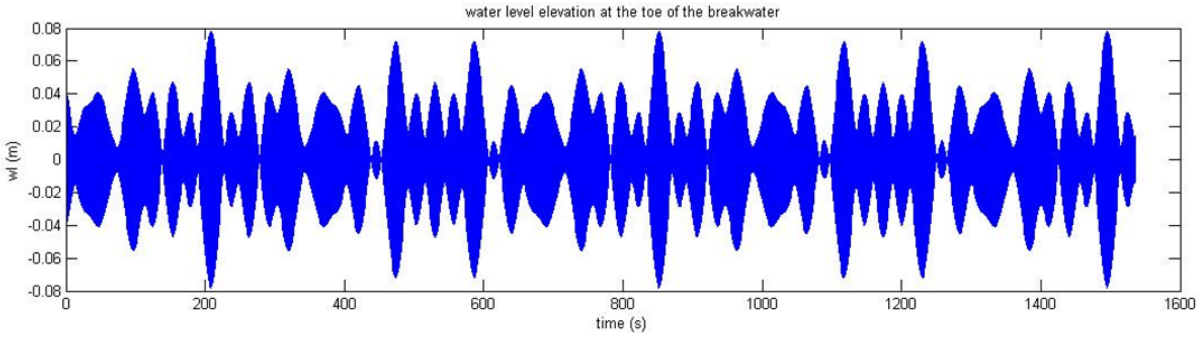

Calculated time series (Matlab)

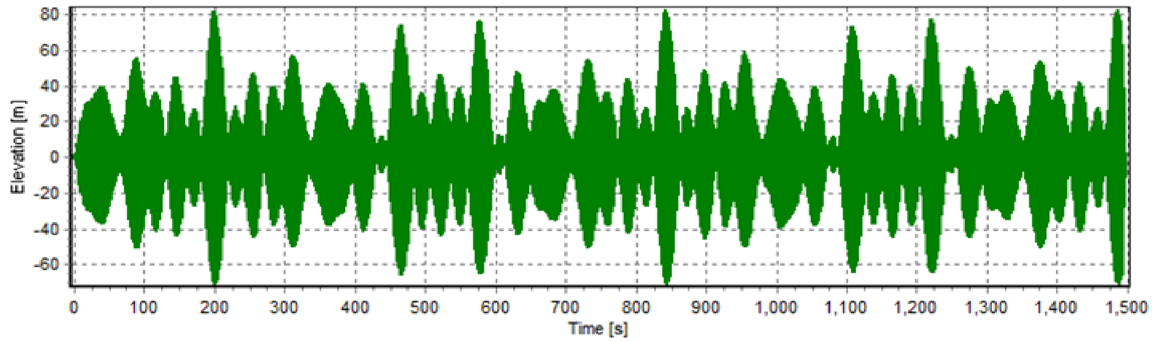

Occurred time series in the flume (Wavelab)

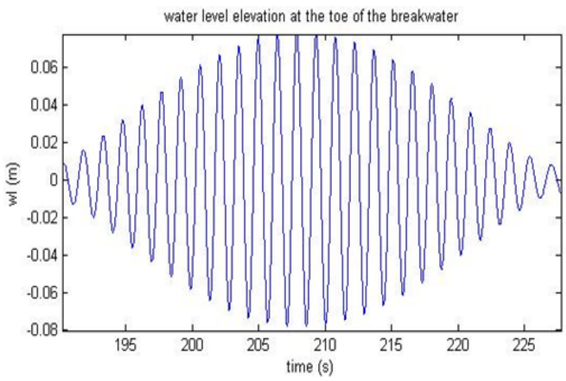

Detail of calculated time series (Matlab)

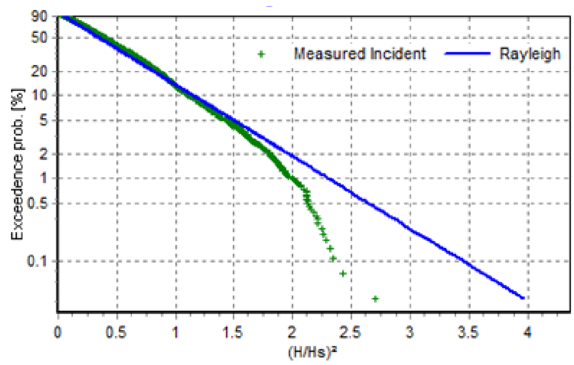

Target wave height distribution (existing model test)

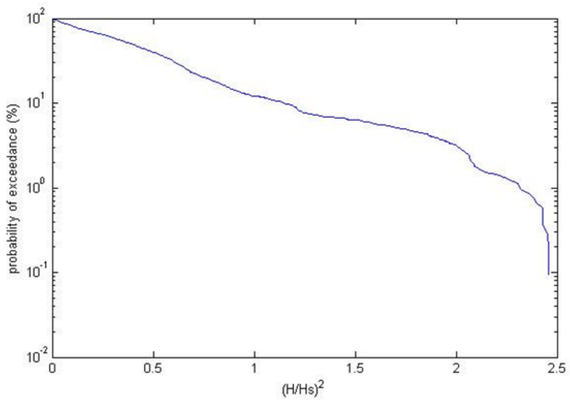

Calculated wave height ditribution (Matlab)

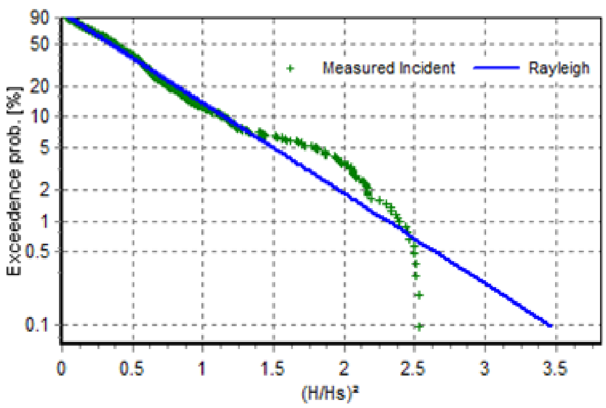

Occurred wave height distribution in the flume (Wavelab)

H2%/Hs = 1.45 ; H0.1%/Hs = 1.57 ; grouped ; steepness = 0.05

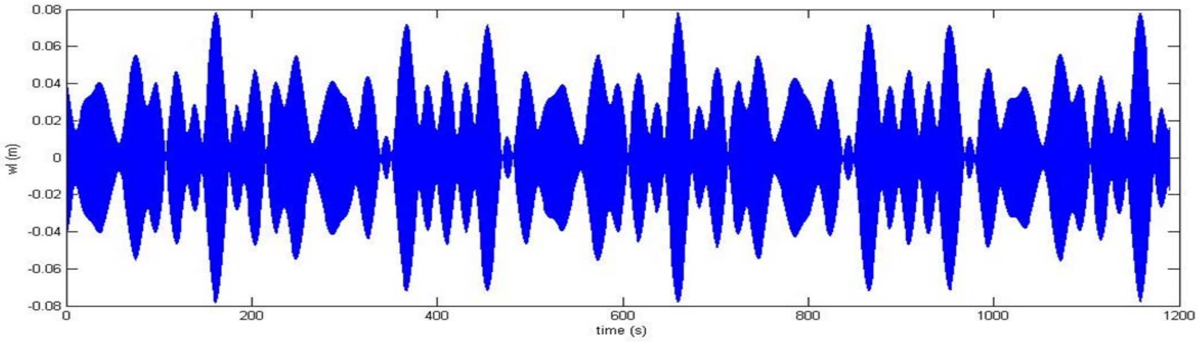

Calculated time series (Matlab)

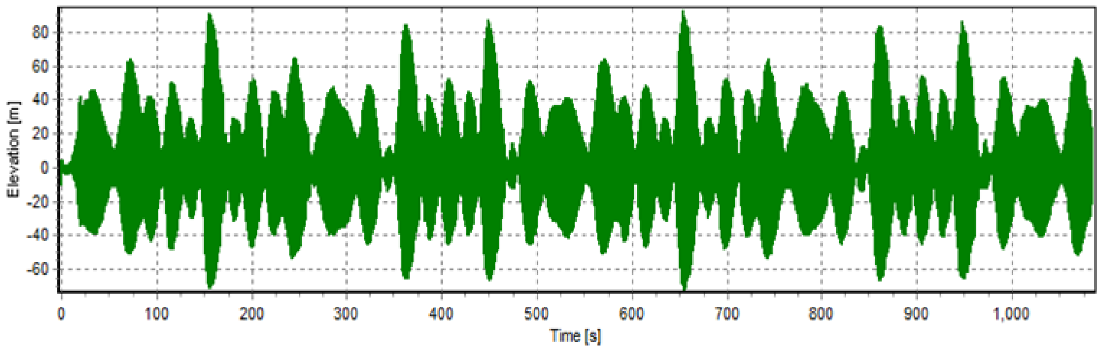

Occurred time series in the flume (Wavelab)

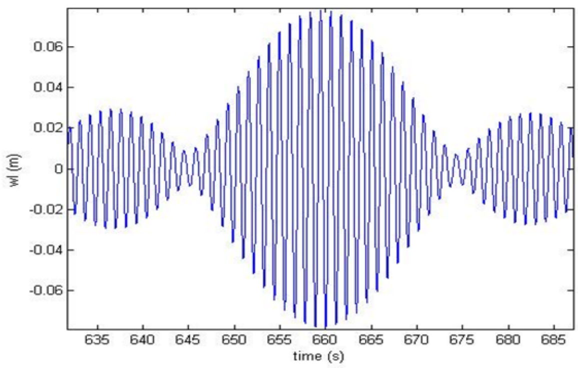

Detail of calculated time series (Matlab)

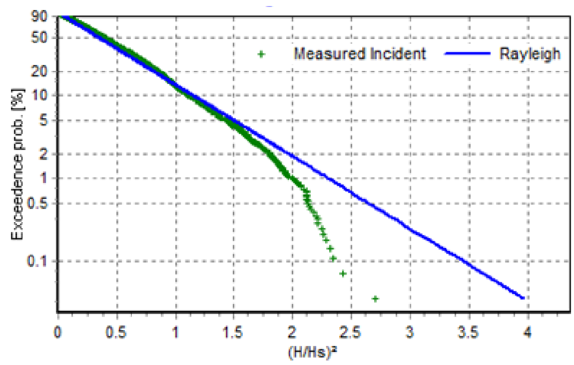

Target wave height distribution (existing model test)

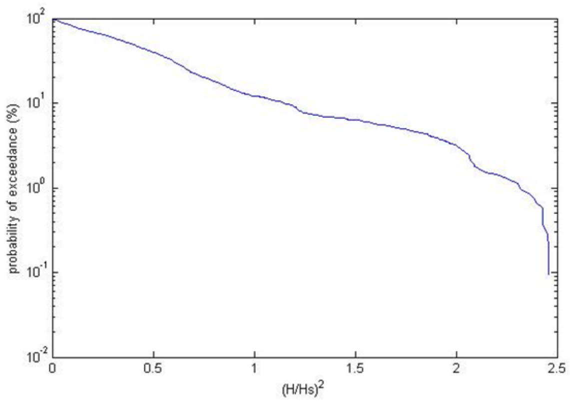

Calculated wave height ditribution (Matlab)

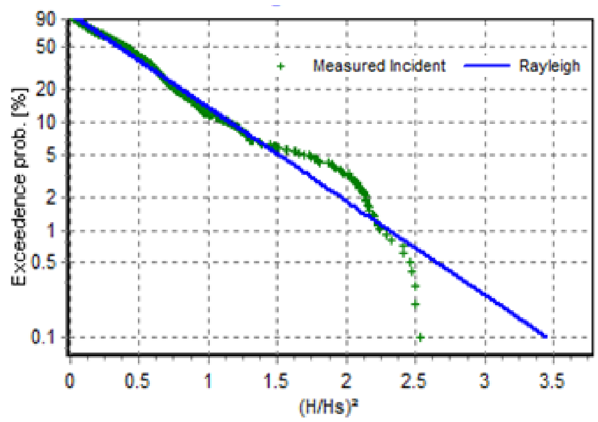

Occurred wave height distribution in the flume (Wavelab)

H2%/Hs = 1.45 ; H0.1%/Hs = 1.57 ; ungrouped ; steepness = 0.03

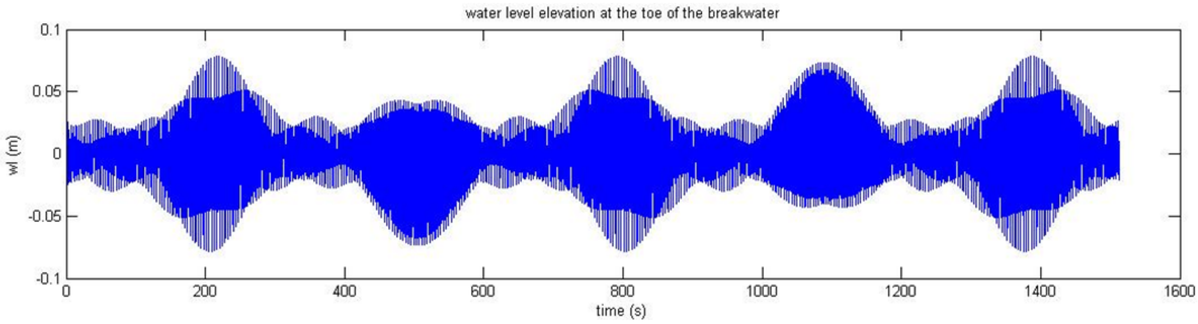

Calculated time series (Matlab)

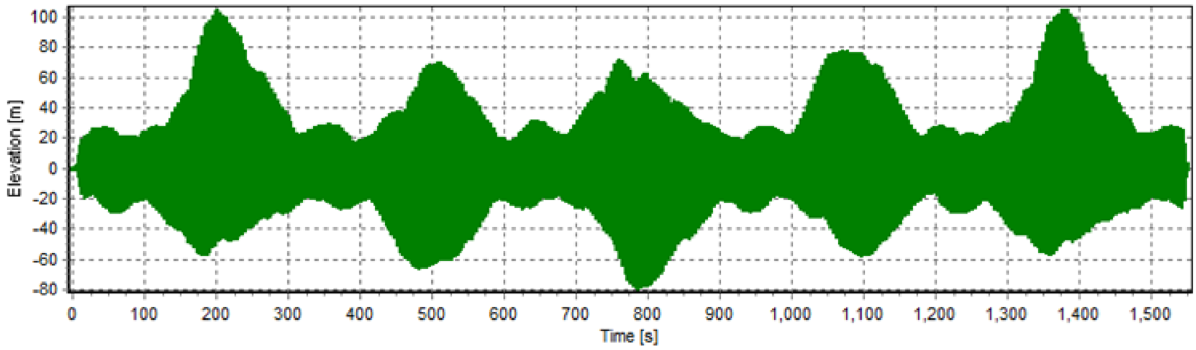

Occurred time series in the flume (Wavelab)

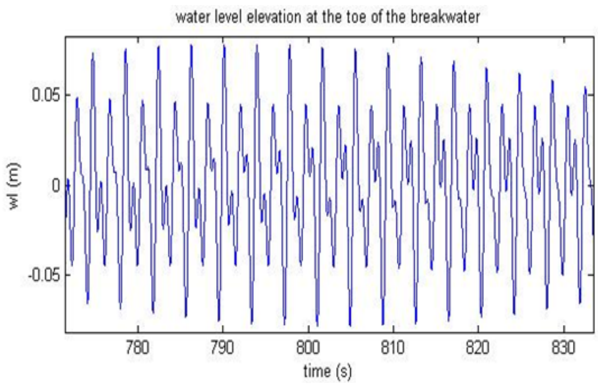

Detail of calculated time series (Matlab)

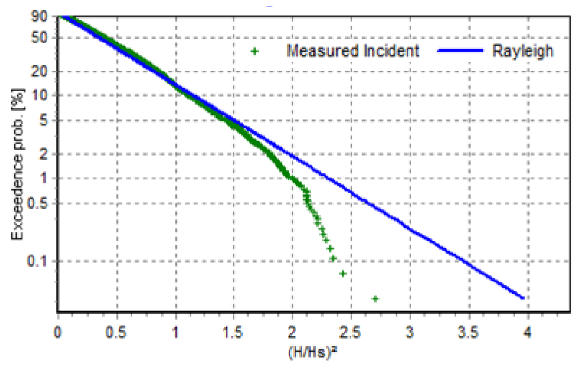

Target wave height distribution (existing model test)

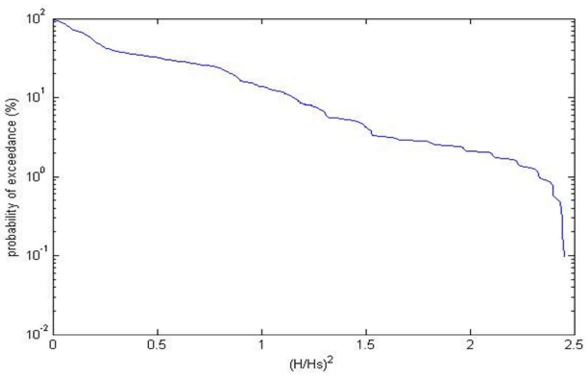

Calculated wave height ditribution (Matlab)

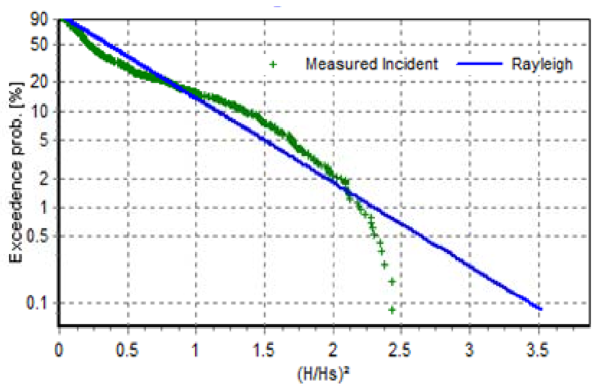

Occurred wave height distribution in the flume (Wavelab)

H2%/Hs = 1.45 ; H0.1%/Hs = 1.57 ; ungrouped ; steepness = 0.05

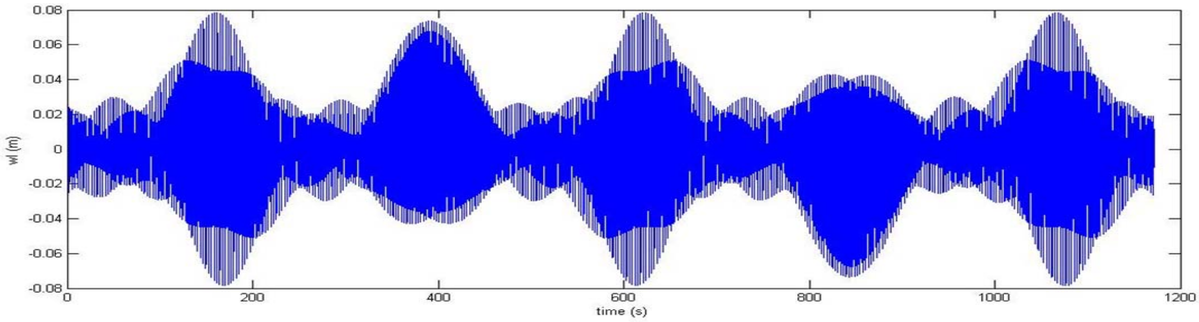

Calculated time series (Matlab)

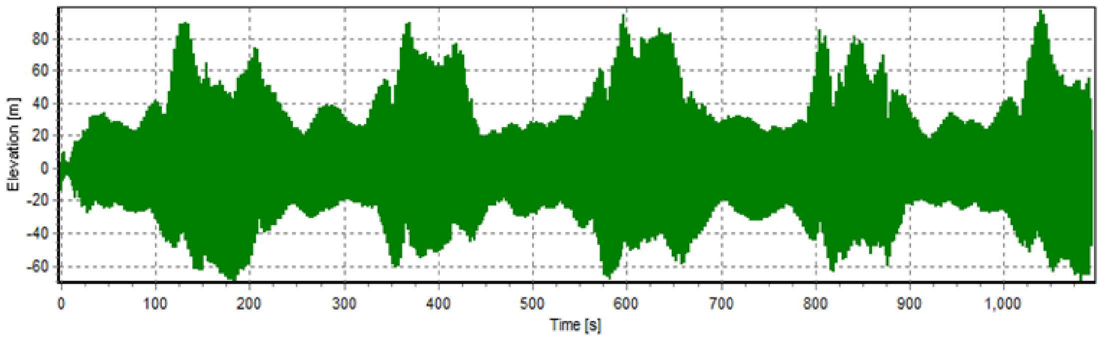

Occurred time series in the flume (Wavelab)

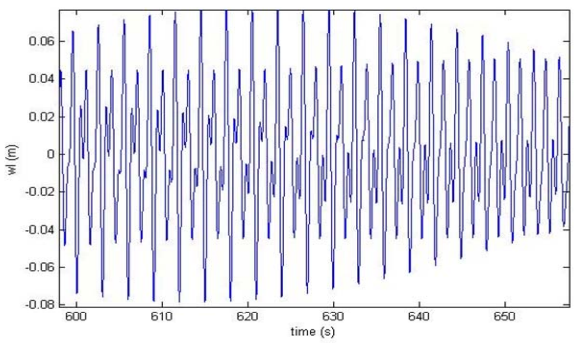

Detail of calculated time series (Matlab)

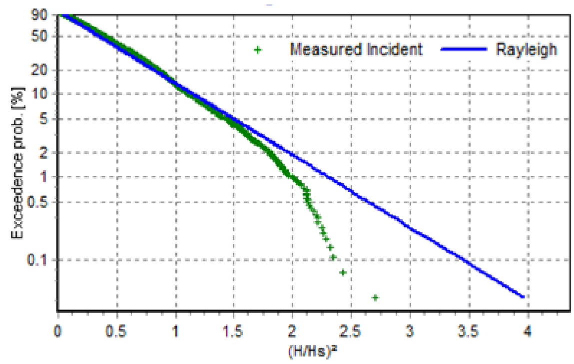

Target wave height distribution (existing model test)

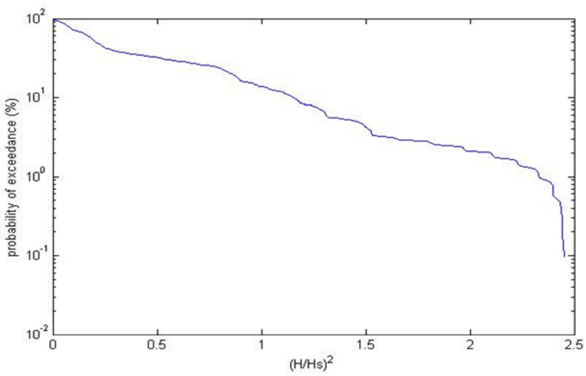

Calculated wave height ditribution (Matlab)

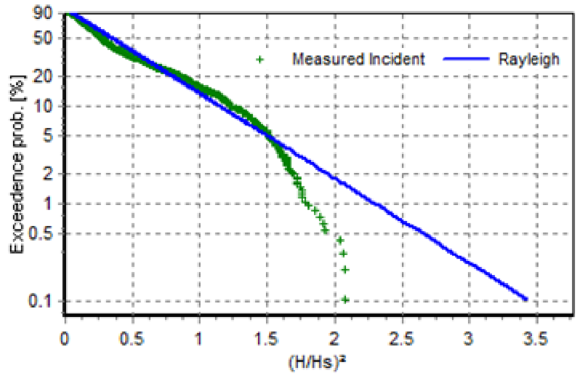

Occurred wave height distribution in the flume (Wavelab)

H2%/Hs = 1.45 ; H0.1%/Hs = 2.03 ; grouped ; steepness = 0.03

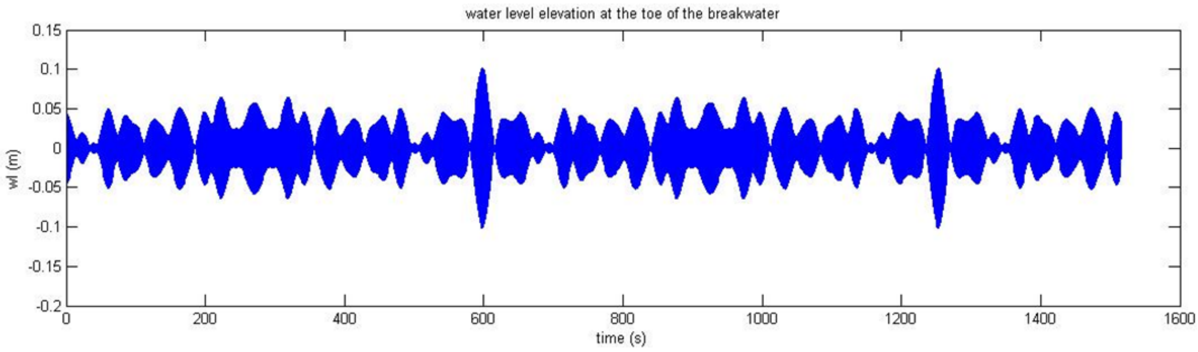

Calculated time series (Matlab)

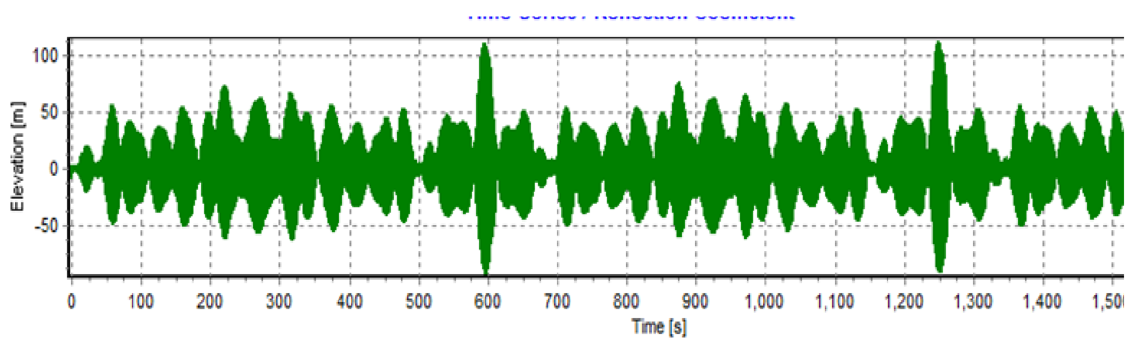

Occurred time series in the flume (Wavelab)

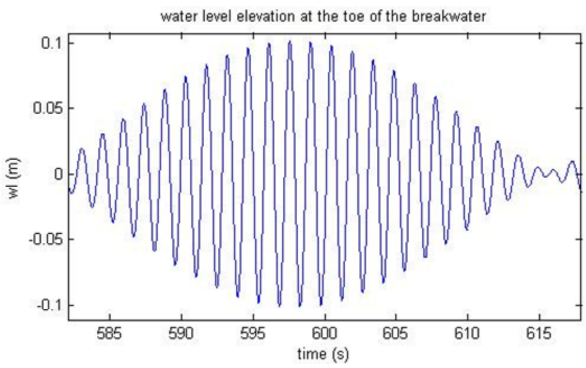

Detail of calculated time series (Matlab)

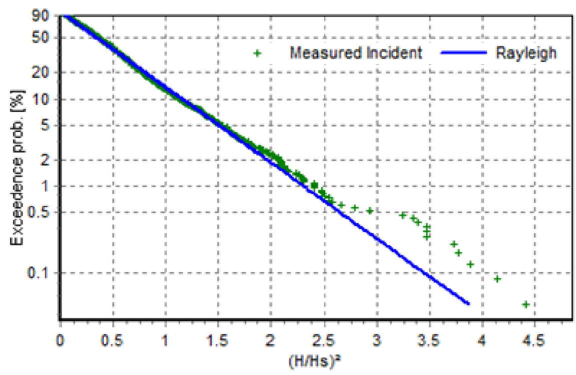

Target wave height distribution (existing model test)

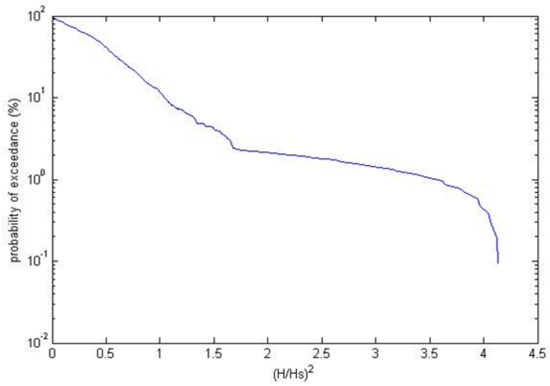

Calculated wave height ditribution (Matlab)

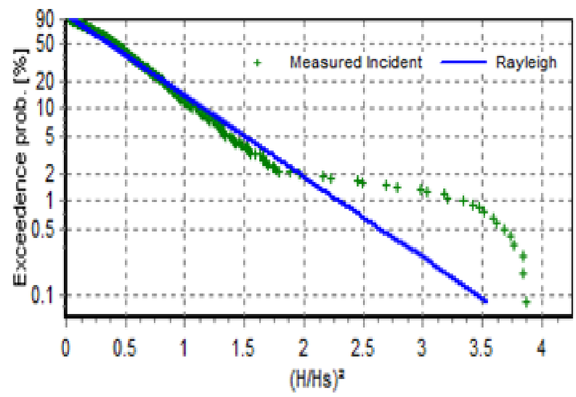

Occurred wave height distribution in the flume (Wavelab)

H2%/Hs = 1.45 ; H0.1%/Hs = 2.03 ; grouped ; steepness = 0.05

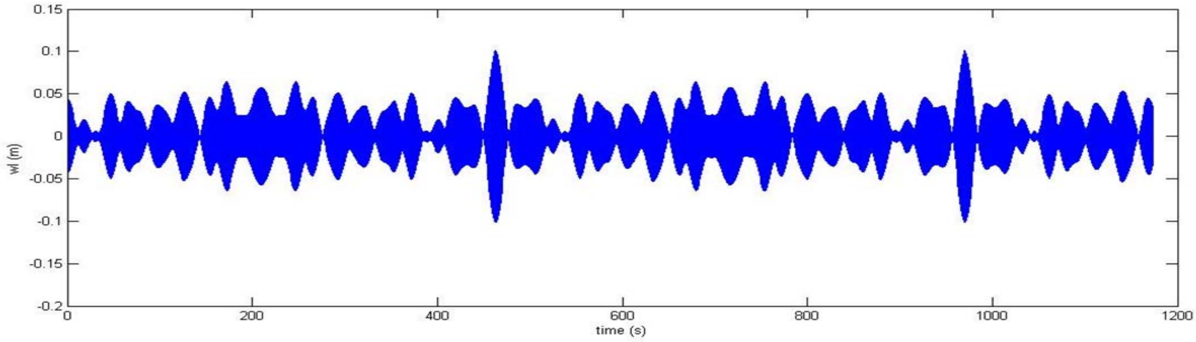

Calculated time series (Matlab)

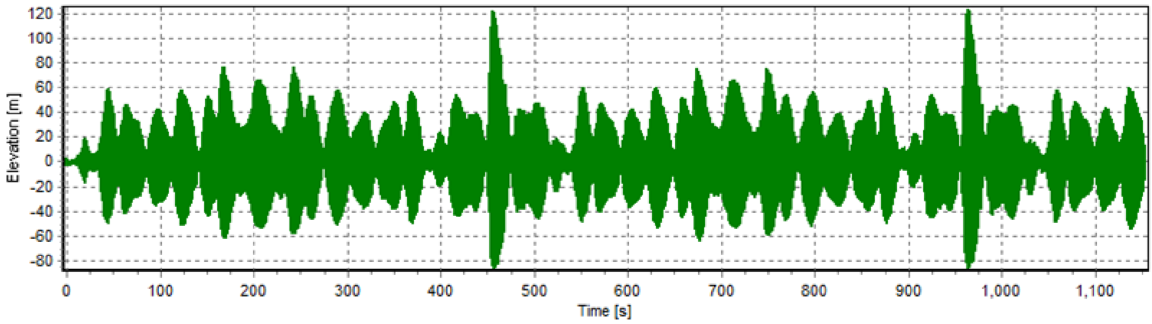

Occurred time series in the flume (Wavelab)

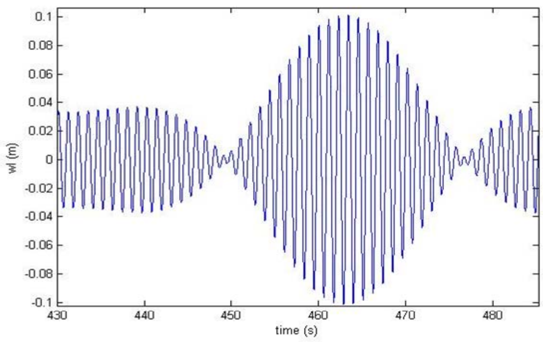

Detail of calculated time series (Matlab)

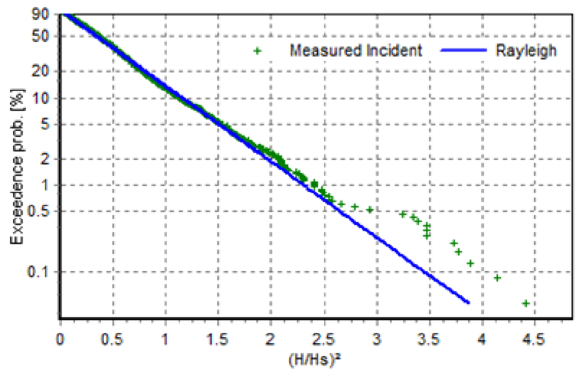

Target wave height distribution (existing model test)

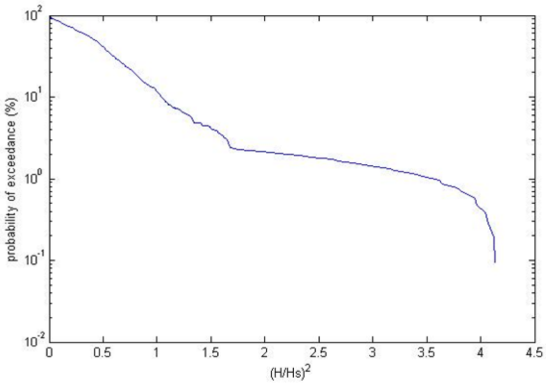

Calculated wave height ditribution (Matlab)

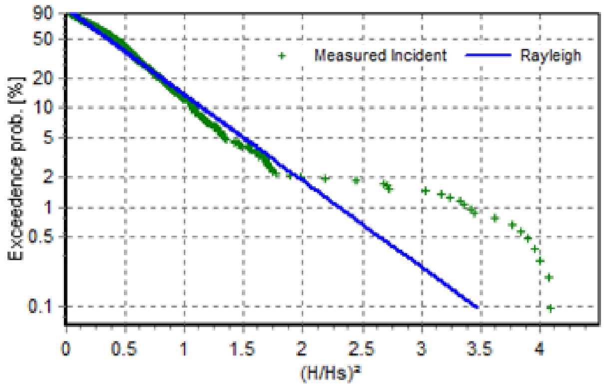

Occurred wave height distribution in the flume (Wavelab)

H2%/Hs = 1.45 ; H0.1%/Hs = 2.03 ; ungrouped ; steepness = 0.03

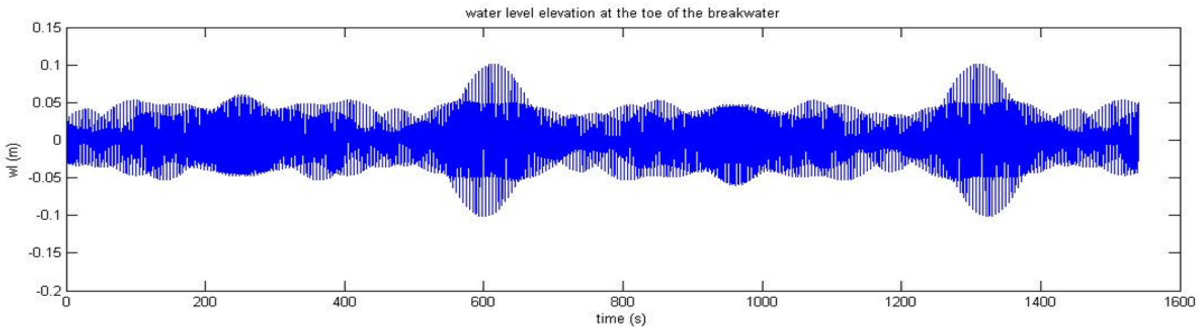

Calculated time series (Matlab)

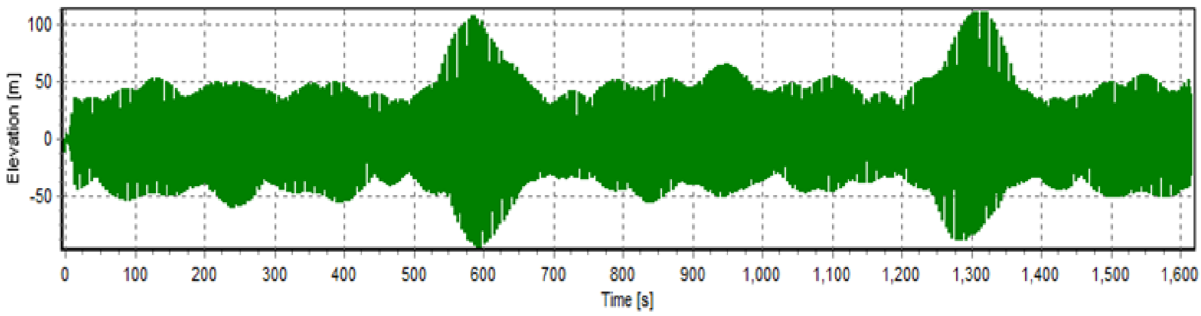

Occurred time series in the flume (Wavelab)

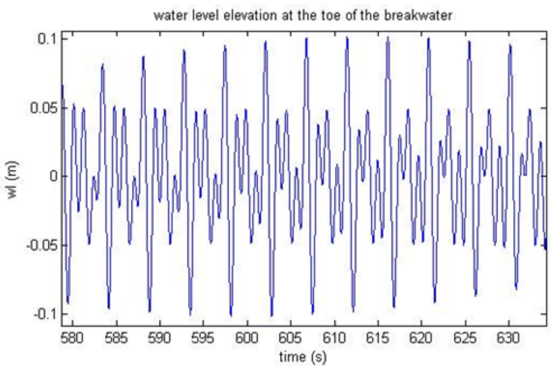

Detail of calculated time series (Matlab)

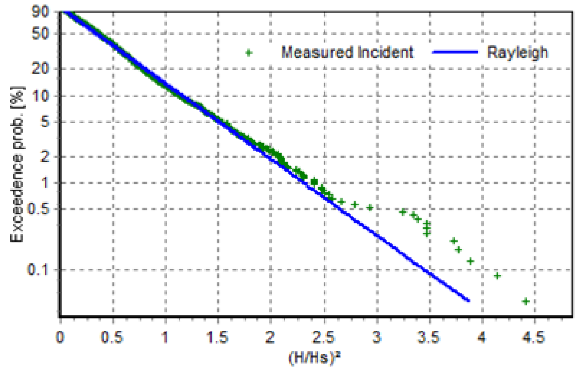

Target wave height distribution (existing model test)

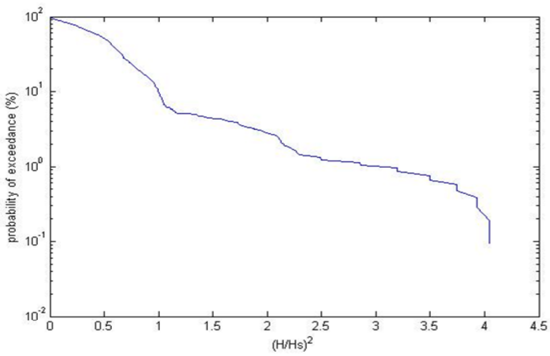

Calculated wave height ditribution (Matlab)

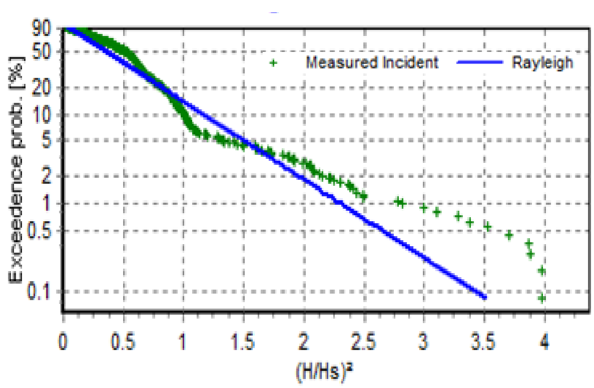

Occurred wave height distribution in the flume (Wavelab)

H2%/Hs = 1.45 ; H0.1%/Hs = 2.03 ; ungrouped ; steepness = 0.05

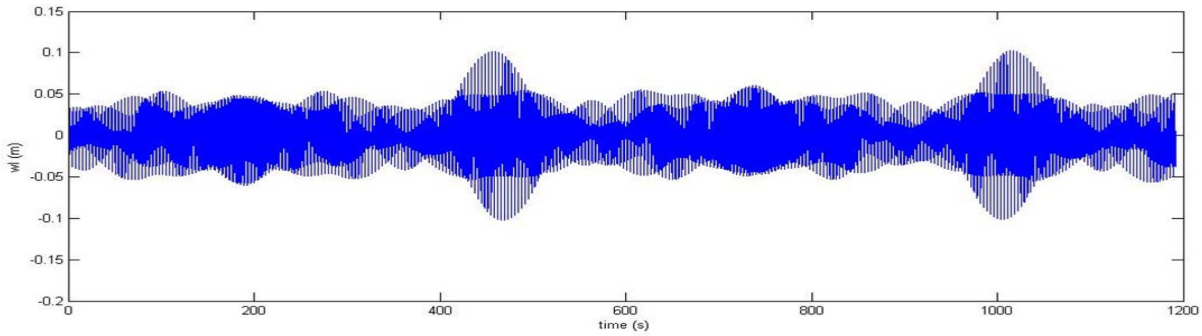

Calculated time series (Matlab)

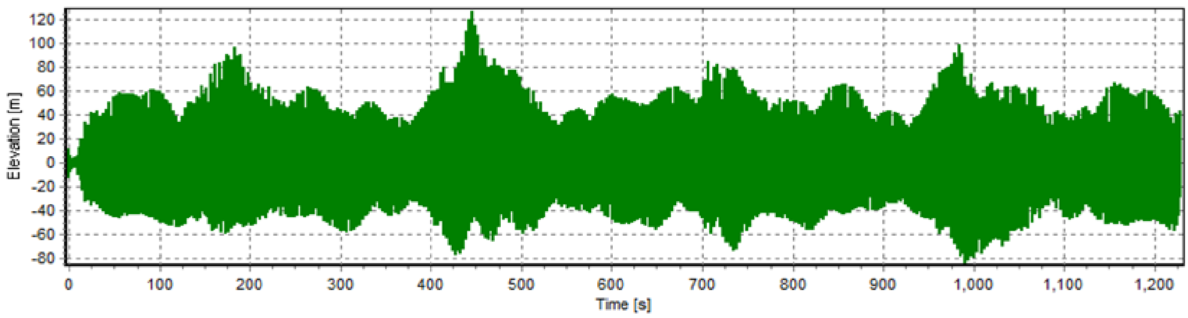

Occurred time series in the flume (Wavelab)

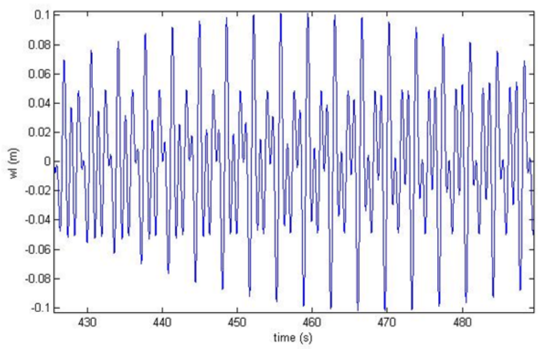

Detail of calculated time series (Matlab)

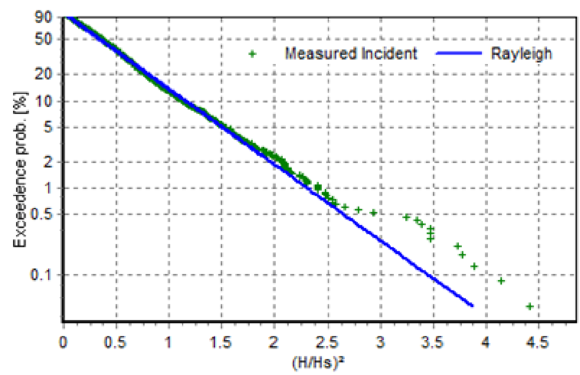

Target wave height distribution (existing model test)

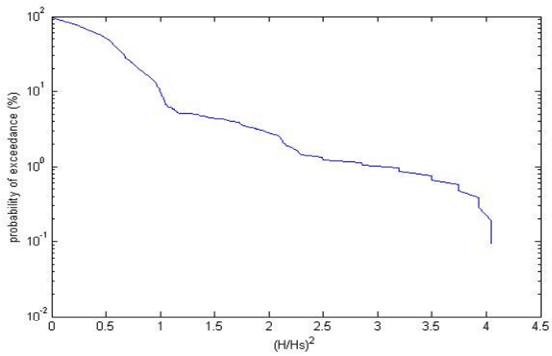

Calculated wave height ditribution (Matlab)

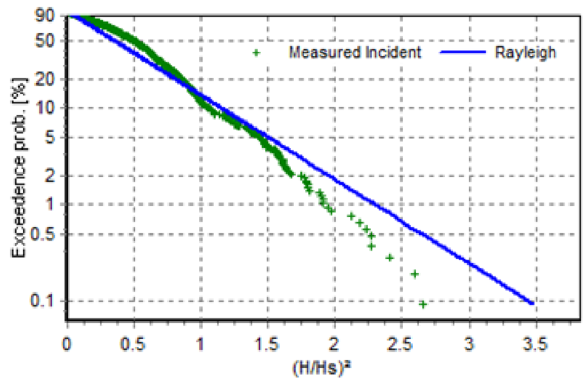

Occurred wave height distribution in the flume (Wavelab)

Appendix F

Rocking during model tests

This appendix gives a summary of the test results. For every repetition of the test series on a replaced armour layer a table is given with the overall results of the test series. The first column shows the name of the test series from which the properties of the wave series can be read as described in section 5.6. The second column shows the sequence of the test series. Thereafter the total number of waves of the wave series and the number of waves which caused rocking of one or more units are given. Thereafter the percentage of waves which caused rocking of one or more units is given. The sixth column shows the number of units which were rocking during one or more of the waves. The total number of visible units of the armour layer was 100, so the number of rocking units is also the percentage of rocking units. The last two columns show the distance between the centre of the units in row 2 from the bottom and the centre of row 18 from the bottom and the corresponding relative packing density after the test. The distance between row 2 and 18 is calculated by measuring and averaging the distance between the individual units of these rows. Because it is quite difficult to estimate the centre of the units and measure the distance accurately, these values should be used with care. It can be used to see the line in settlements, but it should be kept in mind that a decrease in RPD after a test is most likely because of the inaccuracy in measurements than that the RPD is really decreased. Although when the values are rounded to a whole percentage they can be used for analysis.

F.1 Repetition 1

The relative packing density after placement was 97.6%.

Table F.1: Summary of testing results repetition 1

Test series	Test [-]	Waves total [-]	Waves rocking [-]	Rocking [%]	Rocking units [-]	Hight row 2-18 [mm]	RPD [%]
115128ug3	1	1034	284	27.5	1	-	-
115128g3	2	1034	357	34.5	4	-	-
115128ug5	3	910	419	46.0	1	-	-
115128g5	4	911	364	40.0	2	387.5	100.1
115138ug3	5	1040	543	52.2	1	386	100.5
115138g3	6	1032	417	40.4	1	384.5	100.9
115138ug5	7	945	400	42.3	1	384.5	100.9
115138g5	8	923	264	28.6	1	834.5	100.9
135146ug3	9	1009	392	38.9	2	382	101.6
135146g3	10	1042	189	18.1	1	383.5	101.2
135146ug5	11	937	81	8.6	4	383	101.3
135146g5	12	913	266	29.1	2	383	101.3
135185ug3	13	1032	225	21.8	3	383	101.3
135185g3	14	1040	101	9.7	11	382	101.6
135185g5	15	920	101	11.0	6	-	-
145157ug3	16	1118	19	1.7	1	382.5	101.5
145157g3	17	1043	63	6.0	2	382.5	101.5
145157g5	18	922	59	6.4	2	380	102.1
145203ug3	19	1026	20	1.9	9	37.85	102.5
145203g3	20	1045	104	10.0	4	375.5	103.3
145203g5	21	923	99	10.7	7	373	104.0
JONSWAP3	22	1226	22	1.8	6	372	104.3
JONSWAP5	23	952	13	1.4	6	373.5	103.9

F.2 Repetition 2

The relative packing density after placement was 100.1%.

Table F.2: Summary of testing results repetition 2

Test series	Test [-]	Waves total [-]	Waves rocking [-]	Rocking [%]	Rocking units [-]	Hight row 2-18 [mm]	RPD [%]
135146ug3	1	1009	73	7.26	2	38.45	100.9
135146ug5	2	937	0	0.0	0	388	101.3
135146g3	3	1042	0	0.0	0	379.5	102.2
135146g5	4	913	0	0.0	0	381.5	101.7
135185ug3	5	1032	35	3.4	3	380.5	102
135185g3	6	1040	36	3.5	3	381.5	101.7
135185g5	7	-	-	-	1	377.5	102.8
JONSWAP3	8	1226	19	1.5	1	379.5	102.2
JONSWAP5	9	952	71	7.5	2	379.5	102.2
145157ug3	10	1118	0	0.0	0	377.5	102.8
145157g3	11	1043	67	6.4	1	380	102.1
145157g5	12	922	67	7.3	1	378.5	102.5
145203ug3	13	1026	25	2.4	1	377.5	102.8
145203g3	14	1045	47	4.5	1	378.5	102.5
145203g5	15	923	30	3.3	2	378	102.7
115128ug3	16	1034	51	4.9	1	376.5	103.1
115128ug5	17	910	91	10.0	1	378	102.7
115128g3	18	1034	188	18.2	2	377	102.9
115128g5	19	911	322	35.3	1	377.5	102.8
115138ug3	20	1040	503	48.4	1	378.5	102.5
115138ug5	21	945	389	41.2	1	374.5	103.6
115138g3	22	1032	384	37.2	1	379.5	102.3
115138g5	23	923	339	36.7	1	378.5	102.5
145203g5R	24	923	307	33.3	2	376.5	103.1
145203ug3R	25	1026	606	59.1	3	375	103.5

F.3 Repetition 3

The relative packing density after placement was 100.7%.

Table F.3: Summary of testing results repetition 3

Test series	Test [-]	Waves total [-]	Waves rocking [-]	Rocking [%]	Rocking units [-]	Hight row 2-18 [mm]	RPD [%]
135185g5	1	920	115	12.5	10+	-	-
135185g3	2	1040	128	12.3	10	378	103.8
135185ug3	3	1032	51	4.95	8	379	103.5
115138g5	4	923	65	7.0	1	377.5	103.9
115138ug5	5	945	96	10.2	2	380	103.2
115138g3	6	1032	83	8.0	2	380.5	103.1
115138ug3	7	1040	64	6.2	2	379.5	103.3
JONSWAP5	8	952	119	12.5	2	380.5	103.1
145203g5	9	923	96	10.4	5	378	103.8
145203g3	10	1045	202	19.3	6	379	103.5
145203ug3	11	1026	47	4.6	3	378	103.8
JONSWAP3	12	1226	51	4.2	9	379	103.5
135146g5	13	913	36	3.9	2	379	103.5
135146ug5	14	937	127	13.6	2	378.5	103.6
135146g3	15	1042	130	12.5	4	377	104
135146ug3	16	155	10	6.5	3	377.5	103.9
115128g5	17	911	16	1.8	3	378	103.8
115128ug5	18	910	57	6.33	2	378	103.8
115128g3	19	1034	43	4.2	1	377.5	103.9
115128ug3	20	1034	31	3.0	1	377	104
145157g5	21	922	42	4.56	2	377	102
145157g3	22	1043	89	8.5	2	377.5	103.9
145157ug3	23	1118	62	5.5	3	377	104

F.4 Repetition 4

The relative packing density after placement was 100.1%.

Table F.4: Summary of testing results repetition 4

Test series	Test [-]	Waves total [-]	Waves rocking [-]	Rocking [%]	Rocking units [-]	Hight row 2-18 [mm]	RPD [%]
145157g3	1	1043	9	0.9	7	380.5	103.1
145203g3	2	1045	44	4.2	10+	376.5	104.2
115128g3	3	1034	247	23.9	2	380	103.2
115138g3	4	1032	93	9.0	1	378	103.8
135146g3	5	1042	160	15.4	1	378	103.8
135185g3	6	1040	96	9.2	3	379.5	103.3
145157g5	7	922	213	23.1	1	378	103.8
145203g5	8	923	368	39.9	6	378.5	102.6
115128g5	9	911	652	71.66	1	378.5	103.6
115138g5	10	923	521	56.4	1	378	103.8
135146g5	11	913	608	66.6	1	377	104
135185g5	12	920	585	63.65	3	376.5	104.2
JONSWAP5	13	952	570	59.9	2	376.5	104.2
115128ug5	14	910	786	86.4	1	378	103.8
115138ug5	15	945	579	61.3	1	374.5	104.7
135146ug5	16	937	420	44.8	2	377	104
145157ug3	17	1118	417	37.3	2	376	104.3
JONSWAP3	18	1226	736	60.0	1	376.5	104.2
145203ug3	19	1026	661	64.4	2	374.5	104.7
115128ug3	20	1034	707	68.4	1	375.5	104.5
115138ug3	21	1040	640	61.5	1	375	104.6
135146ug3	22	1009	412	40.8	1	374	104.9
135185ug3	23	1032	604	58.5	1	374.5	104.7

Appendix G

Global analysis of dislodged Xblocs

This appendix gives a qualitative analysis of the tests where one or more of the units was dislodged by the waves of one of the previous tests. The influence of the different parameters of the waves are indicated by the rocking relation for the probability of one or more units in the tested armour layer. Analysis in more detail to derive the rocking relation for an individual unit is not performed in this research. The qualitative analysis is done in the same way as in section 7.4.1.

G.1 Dislodged units compared to interlocking units

First the difference in rocking probability between dislodged and interlocking units is showed in figure G.1. It can be seen that dislodged units rock much more than interlocking units.

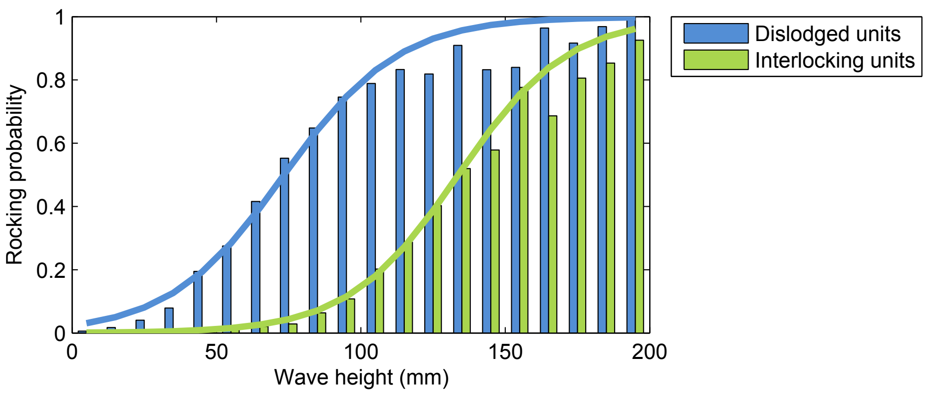

Figure G.1: Rocking probability for dislodged units compared to interlocking units

G.2 Influence of the relative packing density (RPD)

Figure G.2 shows the rocking probability for the tests with a dislodged armour unit divided over three categories of the relative packing density before the start of the test series. Studying this figure it should be kept in mind that the tests with an RPD between 102 and 103 are only tests of repetition 2, the tests with an RPD between 103 and 104 are from both repetition 2 and 4 and the tests with an RPD between 104 and 105 are only of repetition 4. At first sight, the RPD seems of influence. However, since the categories represent a different repetition, the differences in rocking probability are most likely caused by the different repetitions and not the RPD.

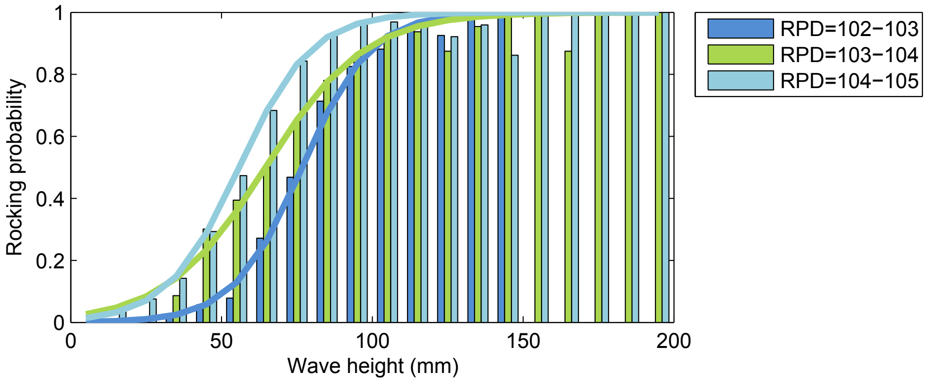

Figure G.2: Rocking probability for different RPD before the test.

G.3 Influence of breaker type of the waves in combination with the location of the dislodged unit

In section 7.4.1 the breaker type appeared to be not of influence on the probability of rocking. Studying figure G.3 and figure G.4 it can be noticed that the probability of rocking for collapsing waves is significantly smaller than the probability of rocking for surging waves, for both repetition 2 and 4.

This can indicate that for dislodged units the breaker type does influence the probability of rocking. However, looking at the location of the rocking unit, it is noticed that the rocking units of the tests of section 7.4.1 are located below the still water line. The dislodged units are located above the still water line. It is likely that the reason for the influence of the breaker type in these tests is dependent on the location of the dislodged units.

G.4 Influence of wave trains

The influence of wave trains on dislodged units is remarkable. Figure G.5 shows the smallest rocking probability for wave series with wave trains and the largest rocking probability for the Jonswap wave series. For the data of the Jonswap

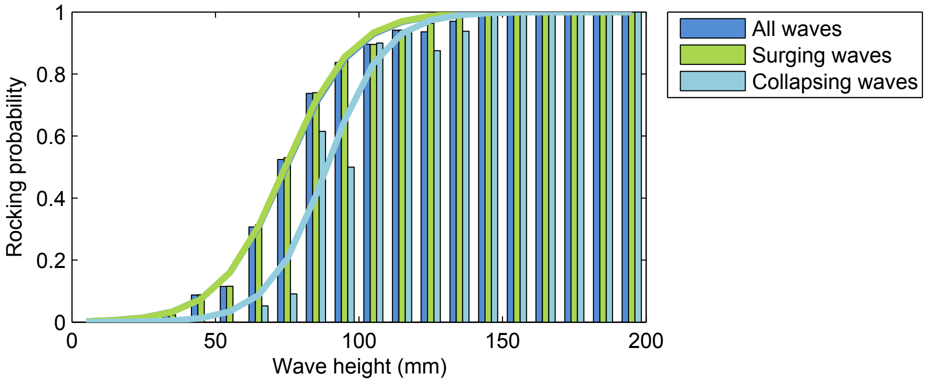

Figure G.3: Probability of rocking for surging and collapsing breaker of the tests with dislodged units of repetition 2.

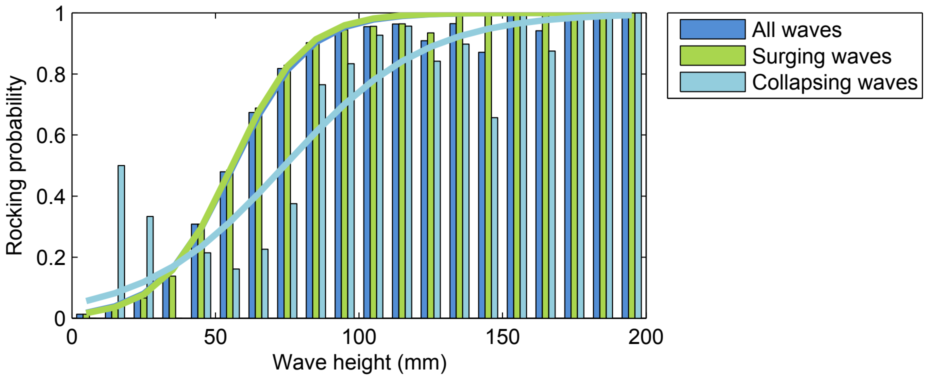

Figure G.4: Probability of rocking for surging and collapsing breaker of the tests with dislodged units of repetition 4.

wave series only repetition 4 was available. As also mentioned in section G.2, repetition 4 showed more rocking than repetition 2. This can be the reason for the large rocking probability for the Jonswap wave series. Why the wave series with wave trains cause less rocking than the wave series without wave trains is unclear. Whether wave trains has a positive effect on the stability of dislodged units or the dataset of the tests with dislodged units is too small for this analysis, should be investigated by further research.

G.5 Influence of wave steepness

Figure G.6 shows the rocking probability for the wave series with a steepness of 0.03 and a steepness of 0.05. It can be seen that the steepness of the waves is of minor influence for dislodged units, like interlocking units.

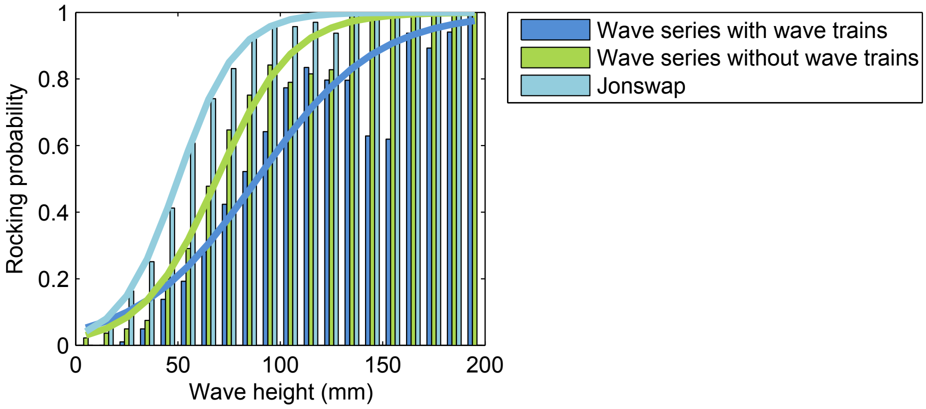

Figure G.5: Probability of rocking for wave series with and without wave trains

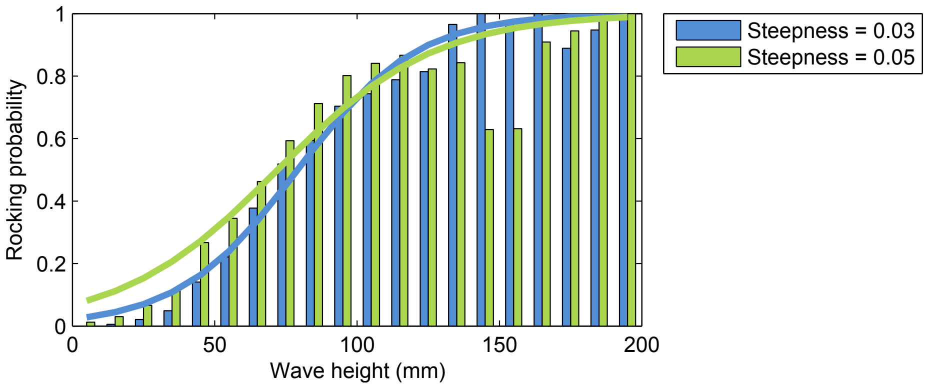

Figure G.6: Probability of rocking for wave series with a different steepness

G.6 Influence wave height distribution

According to figure G.7, the wave height distribution seems of influence on the rocking probability. Although the relation between wave height distribution and rocking probability does not become clear. This figure does not show a relation between, for example, a higher $H_{2\%}$ or $H_{0.1\%}$ and a larger or smaller probability of rocking. For this analysis the data of only 2 to 4 wave series could be used. Therefore the influence of the wave height distribution in G.7 is not very reliable. Based on this analysis, a conclusion for the influence of the wave height distribution can not be made.

G.7 Conclusions

The probability of rocking is larger for dislodged units than for interlocking units. The wave height is the main parameter which determines the rocking probability of a certain wave. The RPD of the armour layer and the steepness of the wave series have not a significant influence on the probability of rocking. Contradictory to the influence of the breaker type on the rocking probability of interlocking units, the breaker type seems of influence for dislodged units. It

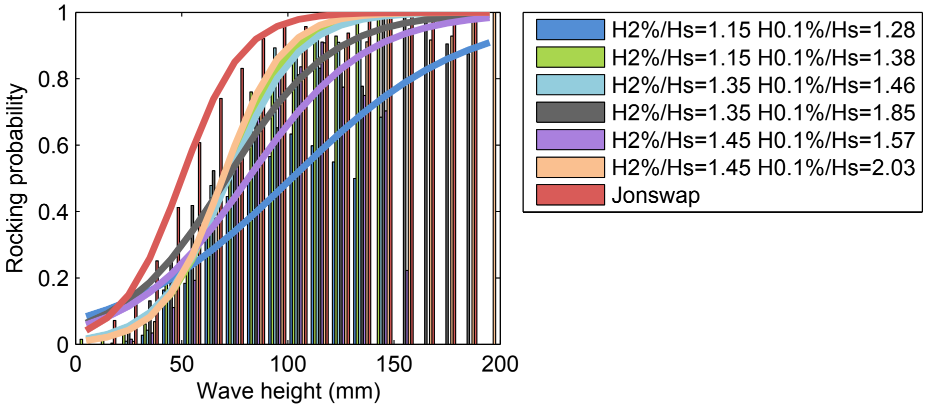

Figure G.7: Probability of rocking for wave series with a different wave height distribution.

is assumed that this is because the dislodged units are located above the still water line. The units which were rocking in the tests of section 7.10 were all located below the still water line. The influence of wave trains and the influence of the wave height distribution is unclear.